

ISTANBUL TECHNICAL UNIVERSITY ★ GRADUATE SCHOOL OF SCIENCE
ENGINEERING AND TECHNOLOGY

**DETERMINING THE EFFECT OF ROUGHNESS
AND CRYSTALLINITY ON PROTEIN ADSORPTION
FOR POLYURETHANE FILMS**

M.Sc. THESIS

Selin Sofi KÜRKÇÜOĞLU

Polymer Science and Technology Department

Polymer Science and Technology Programme

Thesis Advisor: Prof. Dr. F. Seniha GÜNER

Thesis Co-Advisor: Asst. Prof. Dr. F. Ayşe Özge KÜRKÇÜOĞLU LEVİTAS

MAY 2015

ISTANBUL TECHNICAL UNIVERSITY ★ GRADUATE SCHOOL OF SCIENCE
ENGINEERING AND TECHNOLOGY

**DETERMINING THE EFFECT OF ROUGHNESS
AND CRYSTALLINITY ON PROTEIN ADSORPTION
FOR POLYURETHANE FILMS**

M.Sc. THESIS

Selin Sofi KÜRKÇÜOĞLU
(515111027)

Polymer Science and Technology Department

Polymer Science and Technology Programme

Thesis Advisor: Prof. Dr. F. Seniha GÜNER

Thesis Co-Advisor: Asst. Prof. Dr. Ayşe Özge KÜRKÇÜOĞLU LEVİTAS

MAY 2015

İSTANBUL TEKNİK ÜNİVERSİTESİ ★ FEN BİLİMLERİ ENSTİTÜSÜ

**POLİÜRETAN FİLMLERDE YÜZEY PÜRÜZLÜLÜĞÜ VE
KRİSTALİNİTENİN PROTEİN ADSORPSİYONUNA ETKİLERİNİN
İNCELENMESİ**

YÜKSEK LİSANS TEZİ

**Selin Sofi KÜRKÇÜOĞLU
(515111027)**

Polimer Bilim Ve Teknolojisi Anabilim Dalı

Polimer Bilim Ve Teknolojisi Programı

Tez Danışmanı: Prof. Dr. F. Seniha GÜNER

Tez Eş Danışmanı: Yrd. Doç. Dr. Ayşe Özge KÜRKÇÜOĞLU LEVİTAS

MAYIS 2015

Selin Sofi Kürkcüoğlu, a **M.Sc.** student of **ITU Graduate School of Science Engineering and Technology** student ID 515111027, successfully defended the dissertation entitled “**DETERMINING THE EFFECT OF ROUGHNESS AND CRYSTALLINITY ON PROTEIN ADSORPTION FOR POLYURETHANE FILMS**”, which she prepared after fulfilling the requirements specified in the associated legislations, before the jury whose signatures are below.

Thesis Advisor : **Prof. Dr. F. Seniha GÜNER**
İstanbul Technical University

Co-advisor : **Asst. Prof. Dr. Ayşe Özge KÜRKÇÜOĞLU LEVİTAS**
İstanbul Technical University

Jury Members : **Prof. Dr. Metin Hayri ACAR**
İstanbul Technical University

Prof. Dr. Pemra DORUKER TURGUT
Boğaziçi University

Asst. Prof. Dr. Nevra ÖZER
Marmara University

Date of Submission : 15 December 2014

Date of Defense : 5 May 2015

To Arden,

FOREWORD

I would like to thank my dearest advisors Prof. Dr. F. Seniha GÜNER and Assistant Prof. Dr. Ayşe Özge KÜRKÇÜOĞLU LEVITAS who guided me through each step of my journey, enlightened me with their great experiences and their wisdom.

I would like to thank to all my friends in Polymer Research Group; Tuğçe INAN, Nergiz SÖNMEZ, Şeyda Didem YILDIRIM, Berna ÖZTÜRK, Büşra KARAMAN, Dilek DALGAKIRAN and Banu ARABACIOĞLU KOCAAĞA who are always supported and encouraged me. I am so proud of being a part of such an amazing group.

May 2015

Selin Sofi KÜRKÇÜOĞLU

TABLE OF CONTENTS

	<u>Page</u>
FOREWORD	ix
TABLE OF CONTENTS	xi
ABBREVIATIONS	xiii
LIST OF TABLES	xv
LIST OF FIGURES	xvii
SUMMARY	xix
ÖZET	xxii
1. INTRODUCTION	1
2. PROTEIN ADSORPTION PHENOMENA	4
2.1 Factors Effecting Protein Adsorption	4
2.1.1 Protein properties	5
2.1.2 Solution properties	5
2.1.3 Surface properties	6
3. POLYURETHANE IN BIOMEDICAL APPLICATIONS	8
3.1 Polyurethane Structure	8
3.2 Polyurethane as a Biomaterial	9
4. COMPUTATIONAL APPROACHES FOR PROTEIN ADSORPTION	12
4.1 Mathematical Models	12
4.2 Simulation Techniques	14
5. MATERIALS AND METHODS	18
5.1 Experimental Study	18
5.1.1 Chemicals	18
5.1.2 Preparation of polyurethane films	19
5.1.3 Characterization techniques	20
5.1.4 Albumin	22
5.1.5 Protein adsorption on polyurethane films	23
5.2 Computational Study	24
5.2.1 Brownian dynamics	24
5.2.2 CG description of the protein-polyurethane system	25
5.2.3 Simulation details and algorithm	27
6. RESULTS AND DISCUSSION	30
6.1 Experimental Results	30
6.1.1 Polyurethane synthesis	30
6.1.2 Characterization of polyurethane films	31
6.1.3 Protein adsorption results	44
6.2 Computational Results	49
6.2.1 Effect of surface crystallinity on protein adsorption	50
6.2.2 Effect of roughness on protein adsorption	53
7. CONCLUSION	56

REFERENCES	58
APPENDICES	64
CURRICULUM VITAE	82

ABBREVIATIONS

AFM	: Atomic Force Microscopy
BD	: Brownian Dynamics
BSA	: Bovine Serum Albumin
CO	: Castor Oil
DMA	:Dynamic Mechanical Analysis
DMAc	:Dimethylacetamide
DSC	: Differential Scanning Calorimeter
FT-IR	: Fourier Transform Infrared Spectroscopy
PBS	: Phosphate Buffer Solution
PEG	: Poly(ethylene) glycol
PU	: Polyurethane
THF	:Tetrahydrofuran
TGA	: Thermal Gravimetric Analysis
XRD	: X-Ray Diffraction

LIST OF TABLES

	<u>Page</u>
Table 5.1 : Properties of used chemicals	19
Table 5.2 : Codes of polymers	20
Table 6.1 : Glass transition and melting temperatures of polymers.....	32
Table 6.2 : TGA results	33
Table 6.3 : DMA results	34
Table 6.4 : Crystallinity percentage	40
Table 6.5 : Surface roughness	41
Table 6.6 : Contact angle and surface free energy	43
Table 6.7 : Crystallinity percentage, roughness, hydrophilicity and rate of protein adsorption.	45

LIST OF FIGURES

	<u>Page</u>
Figure 2.1: Representation of reversible protein adsorption.....	4
Figure 3.1: Reaction of diisocyanate with hydroxy compound.	8
Figure 4.1: Mathematical models for protein adsorption.....	13
Figure 4.2: HSA representations.	16
Figure 5.1: Chemical structure of CO, PEG, HDI and BDO	18
Figure 5.2: Calculation of crystallinity from XRD	21
Figure 5.3: Crystal structure of HSA	23
Figure 5.4: Lattice polymer surface models with different topology	27
Figure 5.5: The algorithm of BD simulations.	29
Figure 6.1: PU synthesis.	30
Figure 6.2: FT-IR spectrum of PU100.	31
Figure 6.3: TGA thermogram of samples.	33
Figure 6.4: Storage modulus, loss modulus and $\tan\delta$	35
Figure 6.5: XRD patterns.	37
Figure 6.6: Topography images.	40
Figure 6.7: Phase images.	42
Figure 6.8: BSA adsorption.	44
Figure 6.9: Surface properties of albumin protein.	46
Figure 6.10: The effect of each parameter on protein adsorption.....	47
Figure 6.11: Percentage variance of each parameter.	48
Figure 6.12: Protein adsorption on smooth and rough surfaces.....	49
Figure 6.13: Protein adsorption on flat surface.....	51
Figure 6.14: Protein adsorption on rough surface.....	52
Figure 6.15: Effect of roughness on protein adsorption.....	53
Figure 6.16: Macromolecular crowding effect.	54

DETERMINING THE EFFECT OF ROUGHNESS AND CRYSTALLINITY ON PROTEIN ADSORPTION FOR POLYURETHANE FILMS

SUMMARY

Accelerating developments for human health care necessitate need for biocompatible devices to be used inside the body and for outside applications. There has been an increasing trend to use biocompatible polymeric materials in biomedical field. Among biopolymers, polyurethanes are widely used in many fields such as prosthesis, implants and in controlled drug delivery systems due to their excellent chemical and mechanical properties.

The most important factor in determining and developing a biomaterial is to examine the relationship between polymeric structures with blood proteins. Thus, a clear understanding of protein adsorption is crucial to design new biomaterials. It is known that protein structure, protein solution and surface properties are major components that determine adsorption kinetics. In this point of view, important surface properties such as crystallinity, hydrophilicity and roughness were investigated in the context of this study using both experimental and computational approaches.

When analyzing protein-polymer surface interactions in a solution, chemical and physical properties of each component should be investigated. Experimental methods provide valuable information on system level. However, they cannot monitor molecular details of protein adsorption at nanoscale, which occurs at microsecond-millisecond level. Molecular simulation approaches at various levels, help to monitor molecular dynamics during the adsorption of a protein on a polymeric surface, whereas mathematical models describe the kinetics of the phenomena in certain conditions specific to the protein-polymer-solution system studied. Recently, in many significant studies, simulation approaches have been employed to design experimental studies.

In this study, six different polyurethane films were synthesized by using castor oil (CO), hexamethylene diisocyanate (HDI) and 1,4-butanediol (BDO). Among these polyurethanes, poly(ethylene glycol) (PEG) was also used as polyol in the synthesis of three polyurethane samples. Polymers were synthesized at different CO/PEG weight ratios (50/50, 60/40, 70/30, 100/0) by bulk polymerization. In order to obtain chemically identical surfaces with different roughness, tetra hydrofuran (THF) or dimethylacetamide (DMAc) were used during the polymer synthesis for two PEG free samples. Structural characterization of films was carried by Fourier transform spectroscopy (FT-IR). Thermal and mechanical characterization were performed by thermal gravimetric analyses (TGA), differential scanning calorimeter (DSC) and dynamic mechanical analyses (DMA). Crystallinity of films was determined by x-ray diffraction (XRD), hydrophilicity of films was calculated by contact angle

measurements and surface properties were analyzed by atomic force microscopy (AFM).

According to XRD data, crystallinity of samples increases while increasing PEG content in the sample. Contact angle measurements demonstrated that hydrophilicity of samples decreases while decreasing PEG content in the sample. According to AFM topology images, increasing PEG content in polymer structure increases surface roughness as expected. For PEG free samples, addition of solvent in the reaction medium increases surface roughness in various degrees due to the difference in boiling point of solvents. Interestingly, the highest protein adsorption rate was obtained for the most hydrophilic sample. This can be explained by the effectiveness of crystallinity and roughness on protein adsorption for polyurethane films and also by the hydrophilic nature of the albumin. Experimental results suggest that crystallinity is a more effective parameter on protein adsorption than roughness and hydrophilicity.

Effect of each surface property on protein adsorption kinetics was investigated using Brownian dynamics simulations for albumin-polyurethane system. Brownian dynamics enabled the simulation of the coarse-grained polymer-protein system in three-dimension comparable with experimental findings. For this purpose, polymeric film was modeled as lattice surface with protein binding regions predetermined according to the experimental results on crystallinity. Furthermore, the polymeric film was modeled as a flat or rough surface, which actually depended on the solvent evaporation rate employed in the experiments. Bovine serum albumin proteins were described as uniform spheres interacting with the polymeric surface. Various protein concentrations were considered in order to reveal the effect of macromolecular crowding on protein adsorption rate. The model system represented quarter of one-micrometer square polymer film interacting with proteins at real molar levels, which provided an effective comparison with experimental observations.

Considering the effect of surface roughness, hydrophilicity, crystallinity and protein adsorption results together, computational results indicated that the molecular crowding, i.e. high concentrations had the biggest impact on protein adsorption, then degree of surface crystallinity and finally roughness. Observation from simulations suggested the roughness had an implicit effect on protein adsorption by providing higher surface area compared to smooth surfaces. In other words, if high surface area revealed more crystalline regions, more proteins adsorbed on the surface. In contrary, if high surface area revealed more amorphous regions, protein adsorption rate diminished.

POLİÜRETAN FİLMLERDE YÜZEY PÜRÜZLÜLÜĞÜ VE KRİSTALİNİTENİN PROTEİN ADSORPSİYONUNA ETKİLERİNİN BELİRLENMESİ

ÖZET

İnsan sağlığının korunmasının gelecekteki gelişimi biyo uyumlu malzemelere olan ihtiyacın artmasına neden olmaktadır. Bu amaçla yapılan çalışmaların ve araştırmaların sonuçlarına bakıldığında, son zamanlarda en çok kullanılan biyomedikal malzemelerin polimerik malzemelerden elde edildiği görülmektedir. Polimerler çok geniş bir çeşitlilik aralığında sentezlenebildikleri, amaca yönelik olarak morfolojik ve yüzeysel değişikliklere yatkın oldukları ve bir takım yöntemler uygulanarak bir çok farklı özelliğe sahip olabildikleri için biyomedikal alanda kullanımları son zamanlarda artmıştır. Biyopolimerler içerisinde polüüretanlar yüksek mekanik ve fiziksel özellikleri ile sıklıkla tercih edilmektedirler. Polüüretanların kullanım alanları içerisinde protezler, implantlar ve kontrollü ilaç salınım sistemleri sayılabilir. Polimerik yüzey ile kan proteinleri arasındaki etkileşimin biyomalzeme geliştirilmesinde önemli bir yere sahip olduğu pek çok araştırmacı tarafından açıklanmıştır. Böylelikle protein adsorpsiyon çalışmalarının önemi ortaya çıkmaktadır. Protein yapısının ve polimerik filmin yüzey özelliklerinin adsorpsiyona etkisinin önemi pek çok araştırmacı tarafından belirtilmiştir. Bu tez kapsamında, yüzey pürüzlülüğü ve hidrofilitenin adsorpsiyona olan etkisi incelenmiştir.

Çözelti içerisindeki protein-polimer yüzey etkileşimleri incelendiğinde, her bir bileşenin fiziksel ve kimyasal özellikleri ayrı ayrı göz önünde bulundurulmalıdır. Bu kapsamda, deneysel çalışmalar sistem seviyesinde bilgiler sunarken, mikrosaniye-milisaniye mertebesinde gerçekleşen protein adsorpsiyonu hakkında moleküler detayda bilgi sağlayamaz. Farklı ölçeklerde uygulanabilen moleküler simülasyon yaklaşımları, proteinin polimerik yüzeye adsorblandığı sırada meydana gelen dinamiği moleküler seviyede açıklarken, matematiksel modeller belirli koşullar altında protein-polimer-çözelti sisteminin kinetiği hakkında bilgi verir. Ayrıca yakın zamanda yapılan önemli çalışmalarda simülasyonlar, deneysel çalışmaları tasarlamak için kullanılmıştır.

Bu çalışmada altı farklı poliüretan, polietilen glikol (PEG), hint yağı (HY), hegzameten diizosiyanat (HDI) ve 1,4-bütandiol (BDO) kullanılarak sentezlenmiştir. Sentezlenen polimerlerden üç tanesinde poliöl kaynağı olarak PEG kullanılmıştır. Kütle polimerizasyonu ile sentezlenen poliüretan filmlerin kristalinite dereceleri HY/PEG ağırlık oranının (50/50, 60/40, 70/30, 100/0) değiştirilmesi ile elde edilmiştir. Diğer taraftan, kimyasal olarak eş ancak farklı pürüzlülük derecelerine sahip poliüretanlar elde etmek için tetrahidrofuran ve dimetilasetamid kullanılmıştır. Fourier transform infrared spektroskopisi ile numunelerin yapısal karakterizasyonu, ısı ve mekanik karakterizasyon termal gravimetrik analiz, diferansiyel taramalı kalorimetre ve dinamik mekanik analiz ile gerçekleştirilmiştir. X-ışını kırılımı (XRD) yöntemi ile polimerlerin kristaliniteleri, temas açısı ölçümü ile hidrofilite ve atomik kuvvet mikroskobu ile (AFM) yüzey özellikleri belirlenmiştir.

XRD verilerine göre, polimer yapısındaki PEG miktarı arttıkça polimerin kristalinitesi de artmaktadır. Temas açısı ölçümleri, polimer yapısındaki PEG miktarı azaldıkça polimerin hidrofilitesinin de azaldığını göstermektedir. AFM topoloji görüntülerine göre, polimer yapısındaki PEG miktarının artması beklenildiği gibi yüzey pürüzlülüğünü arttırmıştır. PEG kullanılmadan sentezlenen poliüretanlarda, reaksiyon ortamına farklı çözücülerin eklenmesi çeşitli pürüzlülük derecelerine sahip polimer filmler elde edilmesini sağlamıştır.

Çalışmada, hidrofilitesi en yüksek olan örnek daha fazla protein adsorplamıştır. Bu durum kristalinitenin ve yüzey pürüzlülüğünün poliüretan filmler için hidrofiliteye göre daha etkin olması ile açıklanabilir. Ayrıca albüminin hidrofilik dış yapısının hidrofilik yüzeylere bağlanmasını teşvik ettiği düşünülmektedir. Elde edilen deneysel veriler doğrultusunda, kristalinitenin protein adsorpsiyonuna olan etkisinin, pürüzlülük ve hidrofiliteye oranla daha fazla olduğu söylenebilir.

Albümin-poliüretan sisteminde her bir parametrenin protein adsorpsiyon kinetiğine olan etkileri Brownian dinamiği simülasyonları kullanılarak araştırılmıştır. Brownian dinamiği kullanılarak elde edilen polimer-protein sisteminin kaba ölçekte 3 boyutlu simülasyonu, deneysel veriler ile karşılaştırılabilir sonuçlar sağlar. Bu amaç doğrultusunda, polimerik film latis yüzey şeklinde modellenmiş, protein bağlantı bölgeleri ise deneysel sonuçlar ile elde edilen veriler doğrultusunda belirlenmiştir. Deneysel çalışmada çözücü kullanılarak elde edilen pürüzlü yüzeylerin protein adsorpsiyonuna olan etkisi, polimerik filmin düz ve pürüzlü yüzey olarak modellenmesi ile araştırılmıştır. Polimerik yüzey ile etkileşime giren sığır serum albümini (BSA) tekdüze küreler ile ifade edilmiştir. Makromoleküler kalabalık etkisinin protein adsorpsiyonuna olan etkileri, farklı protein konsantrasyonları kullanılarak incelenmiştir. Deneysel sonuçlar ile etkili karşılaştırma yapılabilmesi için sistem, gerçek molar düzeyde proteinler ile bir-mikrometre kare polimer filmin dörtte birinin etkileşimi ile modellenmiştir.

Yüzey pürüzlülüğü, hidrofilite ve kristalinitenin etkileri ile protein adsorpsiyon sonuçları değerlendirildiğinde, moleküler kalabalığın (yüksek konsantrasyon) protein adsorpsiyonunu en fazla etkileyen parametre olduğu, sonrasında ise kristalinite ve pürüzlülüğün geldiği gözlemlenmiştir. Simülasyon sonuçları değerlendirildiğinde, pürüzlü yüzeylerin (yüzey alanını artması sonucu) pürüzsüz yüzeylere kıyasla da fazla protein adsorbladığı belirlenmiştir. Diğer bir deyişle, eğer yüksek yüzey alanı

daha fazla kristalin bölge içerirse, yüzey üzerine daha çok protein adsorblanacaktır. Eğer yüksek yüzey alanı tam tersi şekilde daha fazla amorf bölgelerden oluşursa, buna bağlı olarak protein adsorbsiyonu azalacaktır.

1. INTRODUCTION

Biomaterials are engineered substances or combination of substances in the form of implants and medical devices used in living systems for therapeutic purposes or diagnosis. Biomaterials are most commonly produced from metals, ceramics, composites and polymers, while the latter source is widely used in prosthesis, implants and in controlled drug delivery systems [1,2]. Although there seems to exist a wide range of materials to produce biomaterials, there are certain limitations in their usage in contact with a body tissue; a biomaterial should be biocompatible i.e. nontoxic, inert, chemically stable and mechanically strong. In this line, the most important factor to consider when developing a biomaterial that would be in contact with blood is its interactions with blood proteins in molecular level, in order to ensure its long-time usage without body rejection. When proteins face a synthetic substance, they tend to adsorb on the surface due to the presence of electrostatic and hydrophobic forces, which mainly control protein adsorption and desorption kinetics [3]. Therefore, the effectiveness of an equipment used for a distinct application depends on the degree of surface-protein interactions, which also classifies biomaterials as inert and resorbable [1]. For example, cardiovascular applications require minimal protein adsorption on the biomaterial to achieve minimal fouling, i.e. an inert polymer [4]. On the other hand, in wound healing, protein adsorption on the polymer surface is preferred because platelet adhesion and activation are required, i.e. a resorbable polymer [5].

When analyzing protein-polymer surface interactions in a solution, chemical and physical properties of each component should be investigated separately, this will further allow the control of these properties. As will be elaborated in this thesis, major surface properties of a polymer can be classified as hydrophilicity, roughness, and microphase separation and distribution. On the other hand, proteins are flexible macromolecules with distinct shapes and surface charge distributions, which coordinate their response to an interaction with an environment. For the solution properties, pH, ionic strength and temperature are major parameters affecting protein

adsorption. Due to these numerous properties of polymers that may change together or depending on polymer synthesis methods, as well as complex motions of proteins in a solution, controlling protein adsorption behavior on a polymeric surface and its biocompatibility is a challenging task [6-8].

In order to understand critical properties of polymer-protein-solution systems affecting protein adsorption, various experimental techniques may be employed. For example, electron microscopy technique reveals the topology of the polymeric surface, whether rough or flat, and the distribution of adsorbed proteins on the surface. Contact angle measurements give some information on hydrophilicity of the surface as described in many studies [9,10]. When a gas and liquid are exposed to a solid surface, a phase called 'common line' is obtained. The contact angle θ is the angle between the liquid-solid and liquid-gas interfaces measured within liquid. If the contact angle is less than 90° , the liquid is considered to wet the solid otherwise the liquid is non-wetting. Polyurethane prepared from a high molecular weight polyol, a diisocyanate and a chain extender contains soft and hard segments. The microphase separation is the result of the arrangement of the hard segments into continuous soft segment matrix due to the hydrogen bonding between the urethane hard segments [11,12]. Morphological properties of polyurethanes have been investigated by applying small angle X-ray scattering (SAXS), thermal characterization techniques and transmission electron microscopy (TEM). Recently, atomic force microscopy (AFM) has been viewed as an important tool to enlighten these structures at nanoscale levels [12,13]. On the other hand, change of the concentration of proteins in solution gives information about the adsorption kinetics. While experimental methods provide valuable information on system level, they cannot monitor molecular details of protein adsorption at nanoscale, which occurs at microsecond-millisecond level. Molecular simulation approaches at various levels, i.e. atomistic or coarse-grained, help to monitor molecular dynamics during the adsorption of a protein on a polymeric surface, whereas mathematical models describe the kinetics of the phenomena in certain conditions specific to the protein-polymer-solution system studied [14]. Recently, in many significant studies, simulation approaches have been employed to design experimental studies [15].

In this thesis, bovine serum albumin adsorption on polyurethane surfaces was studied using experimental and computational approaches. Polyurethanes have been widely

investigated as biomaterials due to their flexibility in their physical and chemical properties that may be tuned according to the application, as well as their mechanical strengths [8]. Here, the effect of roughness, crystallinity and microphase separation in polyurethane films on bovine serum albumin adsorption was investigated. Polyurethanes were synthesized by using poly(ethylene glycol) (PEG), castor oil (CO), hexamethylene diisocyanate (HDI) and 1,4-butanediol (BDO) at various stoichiometric ratios using different solvents. Structural characterization of polyurethane films was analyzed by Fourier transform spectroscopy (FT-IR). Thermal and mechanical characterization of the polymeric films was performed by thermal gravimetric analysis (TGA), differential scanning calorimeter (DSC) and dynamic mechanical analysis (DMA). Crystallinity of films was determined by X-ray diffraction (XRD), hydrophilicity was calculated by contact angle measurements and surface topology was analyzed by AFM. Characterization and determination of polymer properties were discussed in detail in the Methods section.

Effect of each surface property on protein adsorption kinetics was investigated using Brownian dynamics simulations [16], specifically developed for the studied albumin-polyurethane system. Brownian dynamics enabled the simulation of the coarse-grained polymer-protein system in three-dimension comparable with experimental findings. For this purpose, polymeric film was modeled as lattice surface with protein binding regions predetermined according to the experimental results on crystallinity. Furthermore, the polymeric film was modeled as a flat or rough surface, which actually depended on the solvent evaporation rate employed in the experiments. Bovine serum albumin proteins were described as uniform spheres interacting with the polymeric surface. Various protein concentrations were considered in order to reveal the effect of macromolecular crowding on protein adsorption rate. The model system represented quarter of one-micrometer square polymer film interacting with proteins at real molar levels, which provided an effective comparison with experimental observations. Modeling of molecular forces, polymeric surface and proteins, algorithm of the simulation were elaborated in Methods section. Finally, experimental findings and simulation results were compared in the Results and Discussion section in order to discuss the sensitivity of protein adsorption on polyurethane surfaces to polymer surface properties investigated in this study. Future studies were discussed in Conclusions section.

2. PROTEIN ADSORPTION PHENOMENA

2.1 Factors Effecting Protein Adsorption

Generally, protein adsorption is considered as multiple variable-dependent and complicated processes [7]. In the first step of protein adsorption, all protein molecules diffuse rapidly from bulk near the interface by convection, external forces and diffusion (Figure 2.1, step 1). The rate of particle diffusion increases by increasing temperature or decreasing particle size. Then, proteins create a layer over the interface (step 2). Due to electrostatic and hydrophobic interactions both with surface and other proteins, they adsorb on the surface (step 3) and pack into a more organized interface (step 4), while they may undergo small or large conformational changes according to the stability of the protein structure. Later, adsorbed proteins transport away from interface to bulk fluid (steps 5 and 6). Figure 2.1 shows simple schematic representation of protein adsorption phenomena.

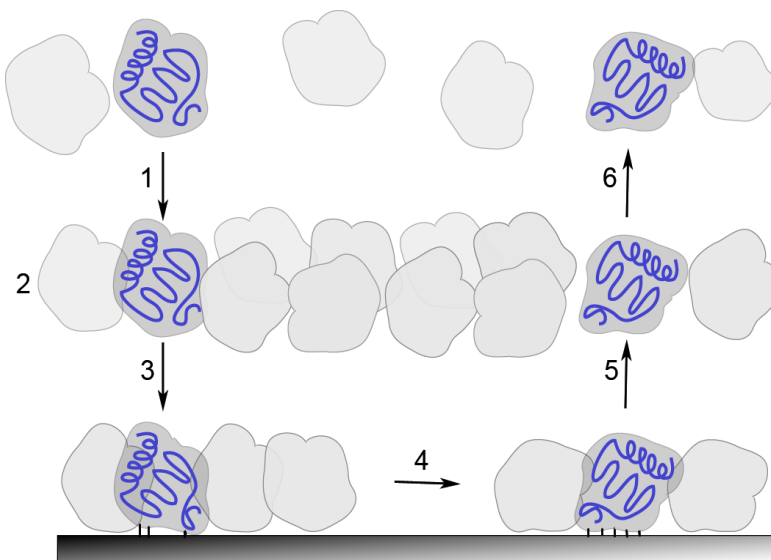


Figure 2.1:Representation of reversible protein adsorption [8].

In an adsorption process, change in Gibbs energy of the system is negative, which is due to electrostatic forces, dehydration processes and conformational rearrangements of macromolecules leading to an increased entropy. Consequently, protein structure, properties of protein solution and the surface properties of polyurethane are major components that determine protein adsorption on all types of surfaces, including polyurethanes. Therefore, a clear understanding of those parameters and their level of impact on protein adsorption will enlighten the process.

2.1.1 Protein properties

Proteins are complex biopolymers composed of 20 natural amino acids with additional chains like phosphates and oligosaccharides. Properties like size, structural stability and composition of each protein enables to classify them with respect to their interfacial behavior. For example, small and rigid proteins like lysozyme, β -lactoglobulin and α -chymotrypsin are considered as 'hard' proteins with low tendency for structural alterations after surface adsorption [17-19]. Intermediate size proteins like serum proteins such as albumin, transferrin, immunoglobulins usually perform conformational reorientations after surface contact under the influence of electrostatic forces [20]. High molecular weight proteins may contain lipids or glycans, which alter the adsorption behavior of the protein; lipoproteins show a strong affinity to hydrophobic surfaces with conformational reorientation, on the other hand glycoproteins prefer hydrophilic surfaces due to a high content of hydrophilic glycans [21]. Therefore, it is possible to classify protein structures as hard/soft according to their structural stability, and hydrophilic/hydrophobic, polar/non-polar or charged/uncharged according to their surface properties [14].

2.1.2 Solution properties

Temperature, pH, ionic strength and buffer composition are the parameters that highly influence protein adsorption. Temperature affects both the equilibrium state and the kinetics of adsorption. The amount of adsorbed proteins are expected to increase by increasing the temperature, as diffusion motion of particles are stimulated [22]. The pH determines the electrostatic state of proteins. Adsorption rate increases when protein and surface have opposite charge. When solution pH is smaller than isoelectric point (pI) of a protein then proteins are positively charged.

By contrast, if solution pH is greater than pI, proteins are charged negatively [23]. Therefore, controlling pH of a solution can facilitate the control of protein adsorption on a solid surface or its protein repellency [24]. On the other hand, higher ionic strength depending on the concentration of dissolved ions suppresses electrostatic interactions between the charged particles located on protein and solid surfaces. Therefore, the adsorption of charged proteins on the oppositely charged surface may be hindered, while adsorption of a protein on similarly charged surface may be enhanced [24]. In high salt concentrations of solutions, salt ions interact with water molecules leading to dehydration of proteins, which further expose their hydrophilic regions to interact with a hydrophilic surface, whether on a solid substance or a protein structure. Furthermore, different ions have different degrees of affinity for water; ‘Hofmeister series’, which are the series of salt ions (Mg^{2+} , Ca^{2+} , F^-) that promote protein precipitation, result into a more complicated adsorption process [25].

2.1.3 Surface properties

Generally, hydrophilic surfaces are more resistant to protein adsorption than hydrophobic surfaces, due to a water shield formed above the hydrophilic surface. Hence, PEG based polymers, which are hydrophilic, are widely used as protein repellent materials [5]. A common explanation about this property is that PEG chains undergo extensive hydration in aqueous medium. Together with high conformational flexibility and chain mobility, hydrated PEG chains sterically hinder protein adsorption [18]. As polyurethanes can be synthesized using PEG, the role of hydrophilicity of polyurethane surfaces on protein adsorption has been widely studied [26,27]. The role of hydrophilicity/hydrophobicity of polyurethane surfaces in fibrinogen adsorption followed by platelet adhesion was investigated using a series of polyurethanes synthesized from different monomers resulting into different degrees of hydrophilicity [28]. Depending on the monomer used, polyurethanes with a range of water contact angle changing between 50 and 110° were obtained. Among them, PEG-based polyurethanes were more hydrophilic with contact angle of about 50° - 60° and showed very low fibrinogen adsorption therefore low platelet adhesion. On the other hand, polyurethanes that were synthesized without PEG had water contact angle between 70° - 110° and showed relatively higher fibrinogen adsorption.

In high water wettability characterized by contact angle lower than 65° , the energetic cost to dehydrate the solid surface is high for water molecules form a strong hydrogen-bonding network at the solid interface. Consequently, protein adsorption is hindered [7].

Surface topology and roughness are other key parameters in determining the response of proteins and cells to a biomaterial, especially when biocompatibility is desired. Rough surfaces can alter contact guidance in which the direction of cell movement is affected by the morphology of the substrate [29]. Clarotti *et al.* [30] reported that surface roughness influences thrombogenicity and consequently the biocompatibility more than the other surface properties of polysulphone and poly(hydroxybutyrate) membranes. Campbell and von Recum showed that implant surfaces with pore sizes between 1-3 μm allow fibroblast attachment that eventually diminishes the presence of inflammatory cells at the implant-tissue interface *in vivo* [31]. In another study, to investigate the effect surface topology on protein adsorption, polyurethane surfaces were prepared in lotus-leaf like shapes [26]. Compared with polyurethanes having smooth surfaces, both fibrinogen and bovine serum albumin adsorption were increased for leaf-like polyurethane surface due to a larger surface area. On the other hand, a blend of polyurethane and PEO/PPG/PEO triblock copolymer forming a rough surface exhibited low protein adsorption due to the presence of hydrophilic PEO extending to the surface. For the latter case, the protein adsorption was reduced by 94.5%, compared with the polyurethanesmooth surface. In another study [32], the biocompatibility of poly(hydroxyethylmethacrylate) hydrogels was increased with increasing porosity of the artificial implant for bone tissue.

3. POLYURETHANE IN BIOMEDICAL APPLICATIONS

3.1 Polyurethane Structure

Polyurethanes (PUs) are prepared from a high molecular weight polyol, a diisocyanate and a chain extender and contain soft and hard segments. The soft segments are usually diols of long-chain molecules of polyether, polyesters, polysiloxane, polycarbonate that impart flexibility. Hard segments are usually the combination of diisocyanates and the chain extender, in which chain extender also acts as a cross-linker. By varying the ratio of these segments, PUs with required chemical and mechanical properties can be obtained with their hydrophilicity/hydrophobicity and hardness/softness can be adjusted. Figure 3.1 shows PU reaction.

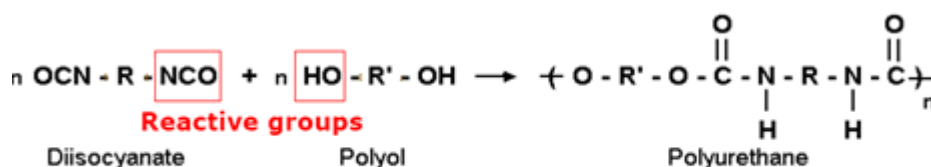


Figure 3.1: Reaction of diisocyanate with di or polyhydroxy compound.

PU is considered as one of the most biocompatible materials. It has been used in biomedical area for various applications due to their excellent properties such as processability, toughness, durability, surface functionality, flexibility, biocompatibility and biostability. It has been first obtained for biomedical applications in the late 1950s. In 1958, Pangman obtained composite breast prostheses covered with polyurethane [33]. Since then it has been used in the preparation of all kinds of medical devices including wound dressing, artificial organs, vascular stents etc.

Biocompatibility is one of the most important characteristic of a biomedical polymer. At this point, surface of the material is a critical parameter, since it interacts with a biological system. Proteins are viewed as the one of the most important actor in polymer- biological system interactions. Protein adsorption is the initial event when a foreign material meets a biological environment. In this line, understanding the adsorption phenomenon in detail, both from protein and polymeric surfaceperspective will enable us to design biocompatible materials with desired chemical and mechanical properties.

3.2 Polyurethane as a Biomaterial

There are many studies about biocompatibility of PU. In order to investigate the effect of hydrophilic and hydrophobic soft segments on protein resistance of PU surfaces, Ma *et al.* synthesized a series of PUs by using poly (propylene glycol) (PPG) and poly (tetra methylene oxide) (PTMO), which have similar structure as poly (ethylene glycol) PEG [23]. PPG-based PU could be changed from hydrophilic to hydrophobic with increasing temperature, on the other hand, PTMO-based polyurethane remained hydrophobic in the range between 15-30°C. They concluded that hydrophilic surface could prevent protein adsorption.

Yang *et al.* [34] synthesized a series of PU by using PEG with various molecular weight (between 200-4600) and they investigated their protein (fibrinogen, lysozyme and bovine serum albumin) adsorption. For high molecular weight of PEG (PEG1000-4600), ultra-low fouling polymer surfaces with contact angle higher than 55° were obtained for biomedical applications.

In another study, Nagaoka *et al.* [35] showed that, increasing molecular weight of PEG in PU reduced protein adsorption. They found that surfaces coated with PEG with a molecular weight of 5000 performed lower protein adsorption and platelet adhesion.

Zheng *et al.* [26] prepared PU surfaces in lotus leaf-like topology to investigate the effect of surface topology on protein adsorption. Compared with smooth surfaces, adsorption of fibrinogen and bovine serum were increased due to increasing surface area. A blend of PU and poly (ethylene oxide) PEO/PPG/PEG triblock copolymer

exhibited low protein adsorption. After fabrication of this surface as lotus leaf-like topology, the protein adsorption of the blend was reduced by 94.5% compared to smooth surface.

In order to compare the effect of surface roughness, wettability and swelling of the polymer on protein adsorption, Akkas *et al.* [36] prepared PUs with different PEG/castor oil ratio to maintain hydrophilicity. Since wettability and roughness of the films were not at the same level, they coated PU surfaces with poly (acrylic acid) (PAA) by plasma polymerization and they obtained same wettability with different roughness values. According to their results, they concluded that surface roughness and swelling of the polymer are important parameters in protein adsorption, like hydrophilicity of surfaces.

Simulation studies on protein adsorption on PU surfaces are limited. Panos *et al.* [37] analyzed adsorption characteristics of fibronectin type I module on crystalline, amorphous and rough PU surfaces with molecular dynamic (MD) simulations. MD simulations in explicit water were performed to study the effects of crystalline/hydrophilic PEG-based surface and amorphous/hydrophobic castor oil-based surface on protein adsorption. They concluded that, fibronectin-water competition in hydrophilic PEG-based surface hindered fibronectin adsorption. On the other hand, roughness and hydrophobicity are considered as two important properties favoring protein adsorption [38,39]. However, MD simulations indicated that rough hydrophobic amorphous surface entrapped water molecules, which resulted in less protein affinity than expected. This observation suggested that surface roughness, protein size and anisotropy affect protein adsorption simultaneously [38].

On the other hand, there exist many computational studies investigating the interaction between PEG and proteins, since PEG has been considered as a protein-repelling material due to its high hydrophilicity. By increasing molecular weight of PEG chains, bigger crystalline regions may occur on PU surfaces. Therefore, various simulation approach for protein adsorption on PEG surfaces [40-43], provide useful information to understand the protein adsorption mechanism on PU surfaces synthesized by using PEG.

In this thesis, the effect of surface roughness and crystallinity on protein adsorption was investigated both experimentally and computationally by studying PU films prepared by PEG and castor oil in various roughness, crystallinity and hydrophilicity. In order to compare experimental observations with computational results, Brownian dynamics simulations, which is a coarse-grained simulation technique, were performed as will be discussed in detail in Methods section.

4. COMPUTATIONAL APPROACHES FOR PROTEIN ADSORPTION

4.1 Mathematical Models

Mathematical models or kinetic models are developed to explain possible mechanisms in protein adsorption phenomena by examining adsorption isotherms considering simple models of protein-surface systems [14]. Adsorption isotherms show the change in concentration of adsorbed proteins with respect to time, at constant temperature. In this context, the first model proposed to explain the adsorption mechanism of rigid molecules was Langmuir adsorption model assuming distinct surface sites for adsorption and desorption of particles (figure 4.1) [44]. With the efforts for modelling protein adsorption and improvements to Langmuir model, random sequential model [45-47] was proposed. In this technique, proteins are modeled as two-dimensional shapes that are placed to the surface randomly and subsequently without overlapping, following a Monte-Carlo scheme. The coverage fraction of the forming monolayer by the adsorption, approaches a ‘jamming limit’, where no more particles can adsorb on the surface, and the kinetics of the system is obtained. This approach has been usually used to explain irreversible adsorption without lateral diffusion and desorption [44]. Later, lateral diffusion, particle desorption, particle anisotropy and surface topology were added to random sequential adsorption model [14].

Internal stabilities and electrostatic properties of proteins are dominant parameters that influence their adsorption characteristics. From that point of view, models that are more realistic have been developed to take into account reversible and irreversible states of proteins on a surface, which can be referred as ‘two state model’ [48,49].

Rabe *et al.* [14] proposed a comprehensive model based on experimental findings on β -lactoglobulin on a hydrophilic glass surface. This model, referred as ‘three state model’, contains three different adsorbed states, an irreversible initial state, a

reversible intermediate state, and an irreversible final state. Accordingly, in the first step, bulk proteins are adsorbed on the surface. Lateral protein-protein interactions and critical surface coverage occur in the intermediate step. Proteins in the intermediate stage are assumed to undergo conformational changes in the final step.

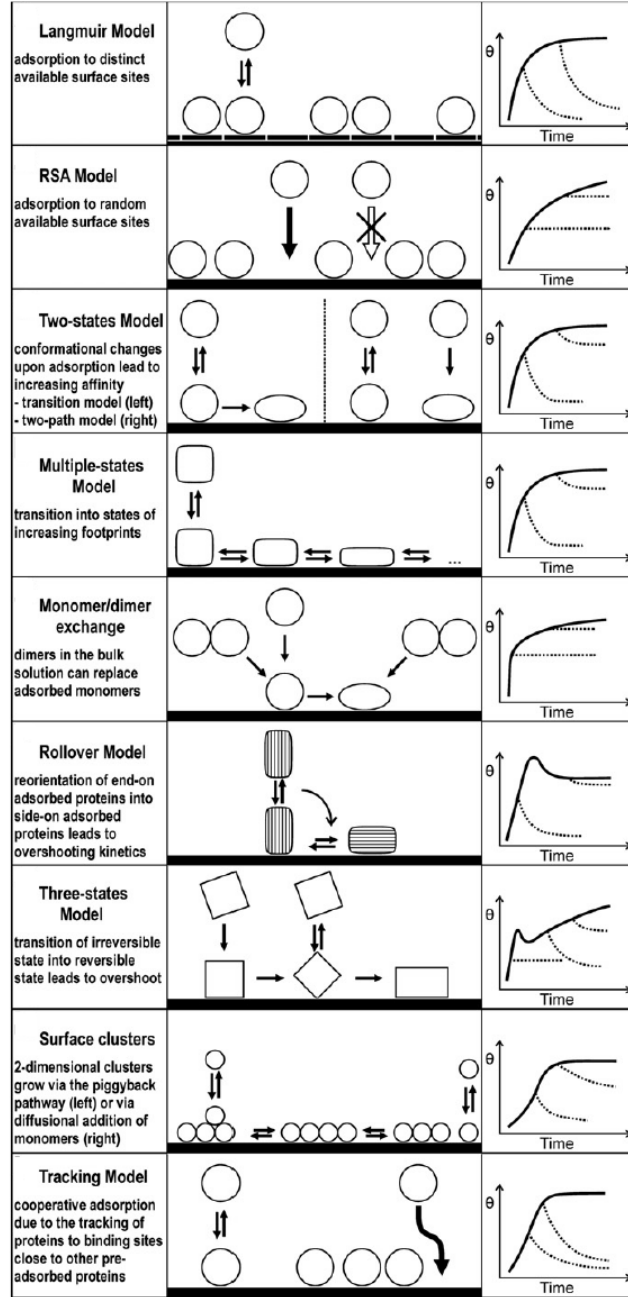


Figure 4.1: Mathematical models used to describe protein adsorption[14].

Chemical and physical properties of proteins coordinate their adsorption behavior, as discussed earlier. This was clearly observed for β -lactoglobulin A and B adsorption on methylated silica surfaces [50]. A mathematical model, called ‘monomer/dimer exchange mechanism’, was proposed based on different desorption resistances of two monomer types of β -lactoglobulin. Here, adsorption of dimers could displace pre-adsorbed monomers from the surface. Another protein adsorption behavior was explained by ‘displacement and rollover model’, where a protein rapidly but weakly adsorbs from its end-on orientation, and slowly but tightly adsorbs from its side-on orientation [51]. This model can explain the ‘overshooting’ effect frequently occurring in protein adsorption kinetics; a high peak observed in the isotherm and a decrease in protein concentration over the surface. Another protein adsorption behavior is forming protein layers over the surface due to protein-protein interactions. Growth of two-dimensional protein layers and forming of protein clusters was proposed by Minton [52].

As seen from all these kinetic models, the adsorption behavior of proteins depends on their structural and chemical features. It is therefore necessary to study proteins and their interacting surfaces in three-dimension by using simulation techniques.

4.2 Simulation Techniques

An increasingly important number of molecular modeling and molecular dynamics (MD) simulations of protein adsorption over solid surfaces have been performed by various computational approaches [see 14 for review]. The adsorption of one or several proteins to a specific surface can be simulated at different molecular levels developed based on physical laws. There exist constraints related to degrees of freedom due to limitations in computational sources, which limits the system size; nonetheless, computational approaches do not depend on physical or technical constraints of experimental conditions that may be difficult to control. Thus, computational approaches allow us to see the dynamics and/or interactions of every atom and protein in the system and provide important clues about the adsorption process at nanoscale.

Quantum mechanical (QM) simulations represent the highest level of precision; they can be performed on single amino acids or small peptides adsorbing on a solid surface. Due to the high computational costs, it finds its usage in small systems,

consisting of one or few amino acids with a restricted surface at picoseconds, which is too short to reach the system in equilibrium state. [53-55].

In order to simulate larger systems in longer time scales, all-atom empirical force field methods such as MD simulations and Monte Carlo (MC) simulations are applied. In these models, the choice of the appropriate force field is the key factor [56]. Detailed potential energy functions (covalent bond stretching, bond bending, bond torsional rotation, and non-bonded forces due to electrostatic and van der Waals forces) are used to calculate the net force on each particle. Then, forces are used to obtain the movement of all components of the system by numerical integration of Newton's equation of motion $F=ma$ over time. [57-59]

Generally, accurate forces increase computational cost. Therefore, treating solvent molecules implicitly with an effective dielectric medium is a common approach to reduce the computational cost [18].

A drawback for these models is that simulated time is often too short to make an accurate sampling of the configurational and conformational spaces.

Limitation in computational resources is the primary obstacle to model the system in molecular detail with respect to time and space. Therefore, some approximations in macromolecular structure and molecular interactions can be considered in each simulation approach, resulting into simple coarse-grained scales. Larger systems and more realistic time scales at milliseconds-minutes can be attained based on coarse-grained models in which structural information is simplified. There exist different representations of a macromolecule such as a protein or a solid surface. To maintain anisotropic shape of proteins, it is common to model them as a bundle of coarse-grained beads or as a hard spherical particle, while an interface can be represented by a lattice surface. Brownian dynamics (BD) simulations can follow coarse-grained approaches. For example, Ravichandran and Talbot [60] modeled lysozyme adsorption by using BD. A protein molecule was represented as a uniformly charged sphere interacting with other molecules through electrostatic, van der Waals and repulsive forces, where the effect of ionic strength and protein concentration taken into account in this coarse-grained scheme. Figure 4.2 demonstrates hierarchical representations of human serum albumin, namely all atom, one-node-per-residue and one bead-per-protein. In order to provide a balance between

atomistic and coarse-grained models for protein adsorption, multi-scale molecular simulation methods are needed to be improved. For example, active site of a biomolecule can be modeled at atomistic level and everything else would be coarse-grained. In this manner, the computational efficiency could be increased [60].

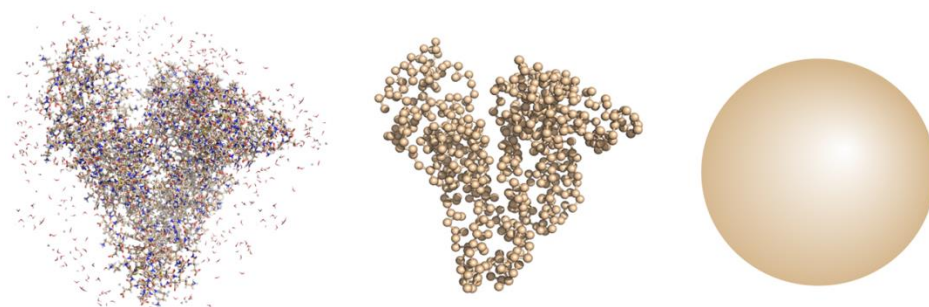


Figure 4.2:Human serum albumin representations. From left to right, all atom model with explicit water molecules, coarse-grained model i.e. Ca atoms represents amino acids, high coarse-grained one bead model.

5. MATERIALS AND METHODS

5.1 Experimental Study

5.1.1 Chemicals

Polyurethanes (PUs) were synthesized by using Sigma-Aldrich brand polyethylene glycol (PEG) and castor oil (CO) as a polyol source and crosslinker. 1,4-butanediol (BDO) was used as chain extender (Figure 5.1(d)) and hexamethylene diisocyanate used as an isocyanate source. Their chemical structures are given in Figure 5.1. Sigma-Aldrich brand tetrahydrofuran (THF) and dimethylacetamide (DMAc) were used to prepare rougher PU surfaces. Properties of chemicals that were used in PU synthesis are given in Table 5.1.

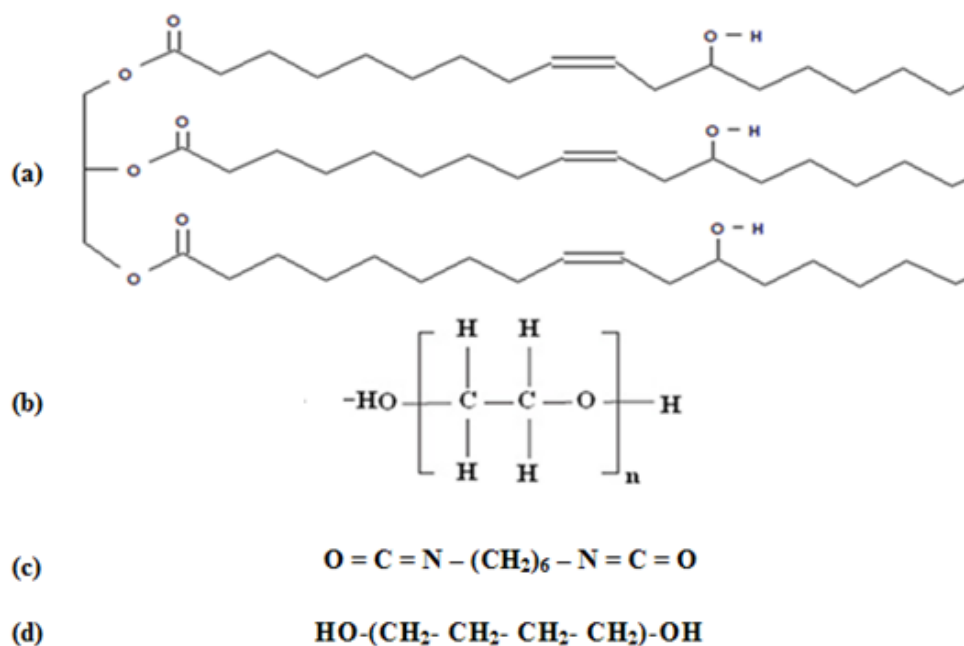


Figure 5.1:Chemical structure of (a) CO, (b) PEG, (c) HDI and (d) BDO

Table 5.1: Properties of chemicals used in PU synthesis.

Name	Properties	Value
PEG	Molecular weight, g/mol	3000
	Density, g/cm ³	1.21
CO	Hydroxyl value, mgKOH/g sample	161.01
	Acid number, mgKOH/g sample	1.47
HDI	Molecular weight, g/mol	168.19
	Density, g/ml(20 °C)	1.047
	Boiling point, °C	82-85
	Melting point, °C	- 67
THF	Molecular weight, g/mol	72.11
	Density, g/ml	0.889
	Boiling point, °C	65-67
	Melting point, °C	- 108
DMAc	Molecular weight, g/mol	87.12
	Density, g/ml	0.9366
	Boiling point, °C	164.5-166
	Melting point, °C	- 20

5.1.2 Preparation of polyurethane films

PU was synthesized by one-step bulk polymerization method with or without solvent [36]. To eliminate the moisture within the monomers, PEG was kept in rotary evaporator for 6 hours at 90-95°C under vacuum. CO was left in vacuum oven at 80°C for 24 hours. BDO was kept also in vacuum oven at 50°C for 24 hours. In order to obtain a homogenous mixture, CO and PEG were stirred in rotary evaporator at 90-95°C for 30 minutes. Then, BDO with an equal amount of hydroxyl value of PEG and CO, was added into the mixture of CO and PEG which was continuously stirred for 30 minutes.

The reaction mixture of PEG, CO and BDO was poured into the reaction flask with nitrogen gas feed. Then the flask was immersed into an oil bath at 50°C. By keeping the temperature constant, HDI with equal hydroxyl number of the reaction mixture was added slowly into the reaction flask.

Six different PU films were synthesized by using CO, HDI, BDO, where poly(ethylene glycol) PEG was used as polyol in the synthesis of three PU samples. Polymers were synthesized at different CO/PEG weight ratios (50/50, 60/40, 70/30, 100/0) by bulk polymerization. In order to obtain chemically identical surfaces with different roughness, tetra hydrofuran (THF) and dimethylacetamide (DMAc) were used. Solvent was added to the reaction flask by weight equivalent of the reactant. The reaction was carried out with stirring speed of 300 r.p.m about 5 minutes. Then, the mixture was poured into the petri dishes and it was left in the 80°C oven for 20-24 hours to complete the polymerization reaction. Table 5.2 shows codes of each polymer synthesized in this thesis. The reaction was monitored by Fourier transform infrared (FT-IR) spectroscopy. Disappearance of the absorption peak at 2270 cm⁻¹ assigned to the free isocyanate group, was used to confirm that all the diisocyanates were consumed in the reaction.

Table 5.2: Codes of polymers.

Code	Solvent	HY/PEG (by weight)
PU50	-	50/50
PU60	-	60/40
PU70	-	70/30
PU100	-	100/0
PU100-THF	THF	100/0
PU100-DMAc	DMAc	100/0

5.1.3 Characterization techniques

Fourier Transform Infrared Spectroscopy

FTIR spectroscopy analysis was carried out on a Perkin Elmer spectrometer spectrum one model between 650-4000 cm⁻¹ by using ATR mode.

Differential Scanning Calorimeter

Thermal properties of the polymers were determined by Perkin Elmer 4000 differential scanning calorimeter (DSC) brand device under nitrogen atmosphere. Analyses were done between -50°C to 150°C with $10^{\circ}\text{C}/\text{minute}$ scanning rate.

Thermal Gravimetric Analysis

Thermal behavior of polymers was analyzed by Perkin Elmer 4000 thermal gravimetric analyzer (TGA). The experiments were carried under nitrogen atmosphere at 550°C with 20°C minute heating rate.

Dynamic Mechanical Analysis

The viscoelastic properties of polymers were analyzed by Perkin Elmer Diamond dynamic mechanical analyzer (DMA) under nitrogen atmosphere between -50°C and 150°C with $3^{\circ}\text{C}/\text{minute}$ heating rate at 1 Hz frequency for scanning.

Atomic Force Microscopy

To investigate the surface of polymers, Nanomagnetics Instruments – ezAFM brand AFM was used with tapping mode for $10 \times 10 \mu\text{m}^2$ surface area.

X-Ray Diffraction

X-ray diffraction (XRD) patterns were obtained from PANalytical brand device. Crystallinity percentage of polymers was calculated using the area under the XRD peak as shown in the Figure 5.2 by using the equation 5.1.

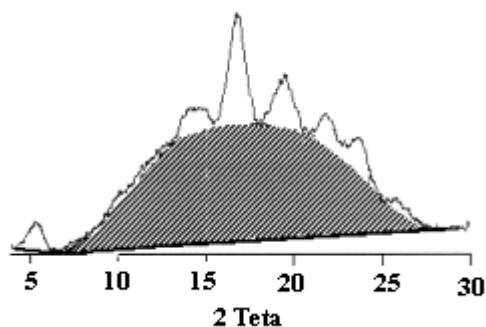


Figure 5.2: Calculation of crystallinity from XRD data. Grey regions under the peak refer to amorphous and white regions refer to crystalline parts.

$$\text{Crystallinity (\%)} = \frac{\text{Area of crystalline}}{\text{Area of amorphous} + \text{area of crystalline}} \times 100 \quad (5.1)$$

Contact Angle Measurements

Water contact angle of the PU films was measured in room temperature by the KSV CAM200 brand contact angle measurement device using sessile drop method and surface free energy was calculated for each film.

5.1.4 Albumin

Protein source for the protein adsorption on polyurethane films experiments is bovine serum albumin. Albumin is the most abundant protein in plasma, constituting approximately 50% of the total protein content (3.5-5 g/gl) [61]. It is a globular, 'all α -helical' protein made up of 585 amino acid residues and weighting 66.5 kDa. In its native form, albumin is elongated, flexible with a stable structure. It consists of single chain of amino acids that develops through nine loops, which are then organized into three domains (I-II-III) each containing two sub-domains (A-B). There are 35 cysteine residues in the molecular structure of albumin. 34 of them are involved in internal disulfide bonds which stabilize the conformation of the molecule while the cysteine at position 34 (Cys-34) remains free as shown in Figure 5.3. Different domains are capable of folding into hydrophobic pockets, which can open and close [61].

Albumin is the main modulator of fluid distribution of the body. About 70-75% of the oncotic pressure, which tends to pull water into circulatory system, of the plasma is determined by its osmotic property. Albumin binds and carries many hydrophobic molecules like metals, fatty acids, metabolites and drugs, it explicitly plays role in solubilization, transportation and metabolism of many endogenous and exogenous substances. Furthermore, through the binding with albumin, many potentially toxic ligand are neutralized with the protein degradation. Moreover, it constitutes the main circulating antioxidant system in the body, where its sulfhydryl groups (-SH) act as scavengers of reactive oxygen species. Due to its high concentration, it is the prime protein that reaches the implanted surface. Therefore, it plays a key role in adsorption process regarding biomaterials in contact with living tissues.

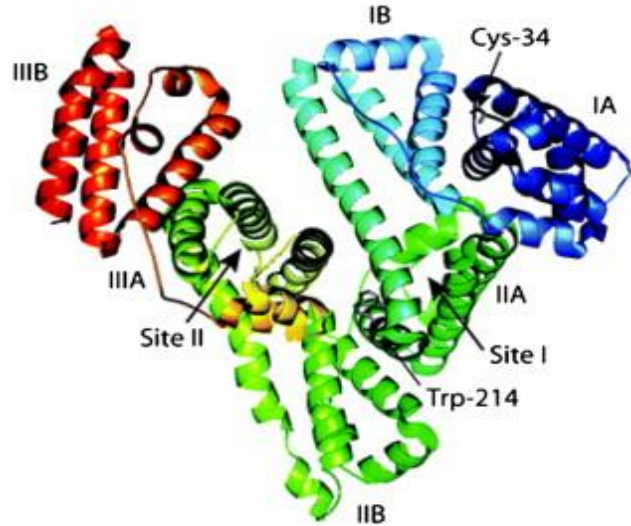


Figure 5.3:Crystal structure of human serum albumin (HSA) from protein data bank (1ha2) [61].

5.1.5 Protein adsorption on polyurethane films

Sigma-Aldrich brand bovine serum albumin (BSA) was used as a protein source. Protein solution was prepared with an initial concentration of 1 mg protein/ ml phosphate buffer solution (PBS). Each polyurethane film (1x1 cm²) was immersed into the protein solution of 60 ml. Protein adsorption was calculated from each protein solution by Perkin Elmer Lambda 35 brand UV Spectrophotometer at 280 nm wavelength by using calibration curve of protein solutions with different concentrations (0 g/ml, 0.50 g/ml, 0.80 g/ml, 0.90 g/ml, 1.0 g/ml). All experiments were carried at 36 °C. The amount of adsorbed proteins was calculated by using Equation 5.2 [36]. Calibration curve that was used to calculate the amount of adsorbed proteins is given in the Appendix F.

$$q = \left(\frac{C_o - C_A}{A} \right) V \quad (5.2)$$

q : Amount of adsorbed proteins(mg/cm²)

C_o : Initial concentration (mg/ml)

C_A : Solution concentration at measurement(mg/ml)

V : Volume of the solution (ml)

A : Area of the film(cm²)

5.2 Computational Study

5.2.1 Brownian dynamics

Brownian dynamics (BD) is a stochastic technique, where rigid particles obey Langevin equation following a continuum time and space. In this mesoscopic approach, coarse-grained (CG) description of molecules and their simplified molecular interactions as well as exclusion of explicit solvent molecules enables to monitor the behavior of especially complex systems, such as colloidal solutions, polymers and biomolecules in larger time scales when compared to full-atom simulation methods such as molecular dynamics [62,63]. In BD simulations, inertia is often ignored because of the small mass m_i of particles; this means the total force applied on each particle i is approximately zero $F_i^{total} = m_i a_i$. The total force acting on i^{th} particle includes drag force F_i^d (due to solvent), Brownian force F_i^B (due to the random collisions) and all non-hydrodynamic forces F_i^{nh} (includes external body forces, spring forces, and excluded volume interactions) [16]

$$\mathbf{F}_i^{total} = \mathbf{F}_i^d + \mathbf{F}_i^B + \mathbf{F}_i^{nh} \cong \mathbf{0} \quad (5.3)$$

$$\mathbf{F}_i^d = -\zeta \left(\frac{d\mathbf{r}_i}{dt} - \mathbf{u}^\infty(\mathbf{r}_i) \right) \quad (5.4)$$

where, ζ is the drag coefficient and $u^\infty(r_i)$ is the unperturbed velocity of the solvent obtained from the position of the particle. Then, the equation of motion becomes:

$$\frac{dr_i}{dt} = u^\infty(r_i) + \frac{1}{\zeta} (F_i^{nh}\{r_j\} + F_i^B(t)) \quad (5.5)$$

where $\{r_j\}$ is the set of particle positions.

Expectation values of the Brownian force are:

$$\langle F_i^B(t) \rangle = 0 \quad (5.6a)$$

$$\langle F_i^B(t) F_j^B(t)' \rangle = 2k_B T \zeta \delta_{ij} \delta(t - t') \quad (5.6b)$$

Here, k_B is the Boltzman constant, T absolute temperature, δ_{ij} is Kronecker delta, $\delta(t - t')$ is Dirac delta function and δ is unit second-order tensor.

BD simulations have been successfully employed to study spatial behavior of various systems with respect to time. Several examples using CG to full-atom approaches include polymer dynamics in flow, where polymers we modeled as bead and rods [16], protein-protein interactions in a crowded environment [64], behavior and dynamics of protein solutions [65].

5.2.2 CG description of the protein-polyurethane system

In order to model dynamics of molecular systems in higher temporal and spatial scales, CG models of macromolecules and their interactions are useful in various computational approaches, such as in BD [66], molecular dynamics [62], elastic network models [67] and Monte Carlo simulations [68]. The interest on CG modeling is not new. The first effort on simplified representation of polymers was carried by Flory in the 1950s [69]. Since then, there has been an increasing concern in CG modeling. The aim is to create a simplified, lower resolution model of the system by grouping clusters of atoms into CG beads. The level of coarse-graining relates to the number of atoms represented by a CG bead. Increasing the atom to bead ratio lowers the total number of degrees of freedom represented in the system, which therefore leads to a more computationally efficient potential with the expense of molecular details.

As the macromolecular structures are simplified, bonded and non-bonded interactions between molecules should be adjusted as well for a correct behavior of the system studied. There are different approaches in CG molecular interactions; these are energy-based, force-matching and structure-based models. In energy-based models, the interaction potentials of CG beads are parametrized so that the free energies of the all-atom (AA) system is obtained [70]. In the force-matching model, the sum of the atomistic forces is mapped onto the corresponding CG beads [71]. Finally, structure-based CG method is generated from an AA model of the protein (i.e. crystal structure) which bonded interactions are described by harmonic interactions [72]. In addition, mixed AA-CG systems also take attention from researchers while one part retain the AA detail but the remainder of the system retains CG [63].

In this study, the aim was to understand the role of polyurethane surface properties, crystallinity percentage and degree of surface roughness, in serum protein albumin adsorption at molecular level. If the effect of each parameter can be understood, it would be possible to develop new polymeric surfaces where the protein adsorption can be controllable in biomedical applications. In order to compare computational results with experimental observations, protein structures, polymer surface topology and intermolecular forces were represented by simple rigid body interactions, allowing to study protein adsorption on large polymer surfaces in micron level.

Albumin proteins were described as uniform spherical particles having radius equal to unity (dimensionless) as a basis, where 1 unit was equal to 35Å. Total number of $N = 1000$ and 2000 particles were modeled in the system in order to study the effect of crowding on protein adsorption kinetics. Polyurethane film was modelled as a square lattice surface, with smooth or rough topology (Figure 5.4 top panel), in order to study the effect of surface roughness on protein adsorption. Side length of one tile was taken as 2.2 in the smooth lattice, slightly larger than the diameter of protein particles; as a result, the largest smooth surface lattice studied was a flat plane with $0 \leq x, y \leq 134$ and $z=0$. These values corresponded to a surface of 0.5µm by 0.5µm. Side lengths of tiles were much larger in the rough surface lattice, within a range of 2.2 - 5.5 due to the cosine function employed to distort the flat plane $z=0$ into a curved plane with dimensions of $0 \leq x, y \leq 134$ and $z = 65\cos 100x + 35\sin 100y$.

Our experimental observations indicated that albumin proteins adsorbed on crystalline regions, rather than amorphous regions [36]. Therefore, degree of crystallinity on the polyurethane surface was considered as another parameter in protein adsorption, and both rough and smooth polymeric surfaces were described with different crystallinities, i.e. low and high crystallinity (Figure 5.4 bottom panel). Low crystallinity was represented by a lower number of binding regions. Therefore, 800 binding regions over a total of 3721 sites corresponded to low crystallinity, and 1300 sites over 3721 sites corresponded to high crystallinity for the smooth surface. Similarly, for the rough surface, 1300 sites over 3721 sites represented low crystallinity and 1600 binding sites over 3721 sites represented high crystallinity.

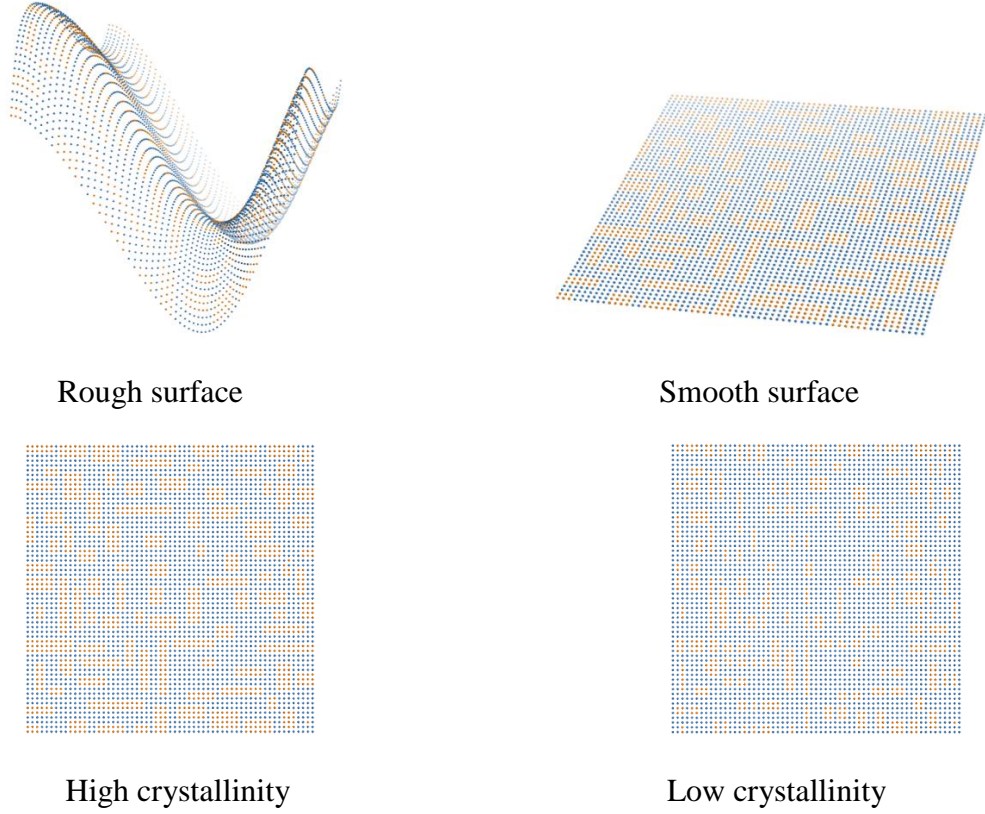


Figure 5.4: Lattice polymer surface models with different topologies. Blue and orange regions display amorphous (not protein binding) and crystalline (protein binding) regions, respectively.

5.2.3 Simulation details and algorithm

Total force acting on each protein particle i , at time t was calculated as,

$$F_i^{total}(t) = F_i^B(t) + F_i(t) \quad (5.7)$$

where $F_i^B(t)$ is the Brownian force and $F_i(t)$ is attractive and repulsive forces acting on i^{th} particle at time t . The latter force included excluded volume term that prevents rigid particles passing through each other and a simple attractive force between the i^{th} particle and the vacant binding region placed at intersection points along the lattice, which was effective within a cutoff distance of $R_{cut}=1.1$. Major assumption in calculations was that particles were irreversibly adsorbed on the static surface, even though this may not be the case with a small dissociation constant for albumin.

Midpoint algorithm was used for numerical integration to calculate the coordinates of each particle R_i at two time steps δt (1/2 and 1) as shown in the Equation 5.8. Here, F_i^{film} is binding force of the particle to the lattice surface and $F_i^{excl_vol}$ is the excluded volume effect.

$$\begin{aligned} R_i|_{1/2} &= R_i|_0 + \frac{\delta t}{2} (F_i^{Brownian}|_0 + F_i^{film}|_0 + F_i^{excl_vol}|_0) \\ R_i|_1 &= R_i|_0 + \delta t (F_i^{Brownian}|_0 + F_i^{film}|_{1/2} + F_i^{excl_vol}|_{1/2}) \end{aligned} \quad (5.8)$$

Periodic boundary conditions were employed to allow particles to diffuse over an extended polymeric surface.

In the simulation, first random positions of protein particles were generated over the lattice surface. Then, all forces (Brownian, excluded-volume and film) were calculated for each particle. The movement of particle i at the middle of time step $\delta t/2$ was generated. Again forces were calculated and the movement of particle at time step δt was obtained, as given in Equation 5.8. If a spherical particle center was close to a vacant binding site on the surface within a cutoff distance of 1.1, particle bound to the surface irreversibly. Positions of other freely diffusing particles were checked for boundary conditions. Finally, new positions for particles, adsorbed or not, and status of binding sites, vacant or not were updated at the end of time step. Figure 5.5 shows simplified diagram of the algorithm.

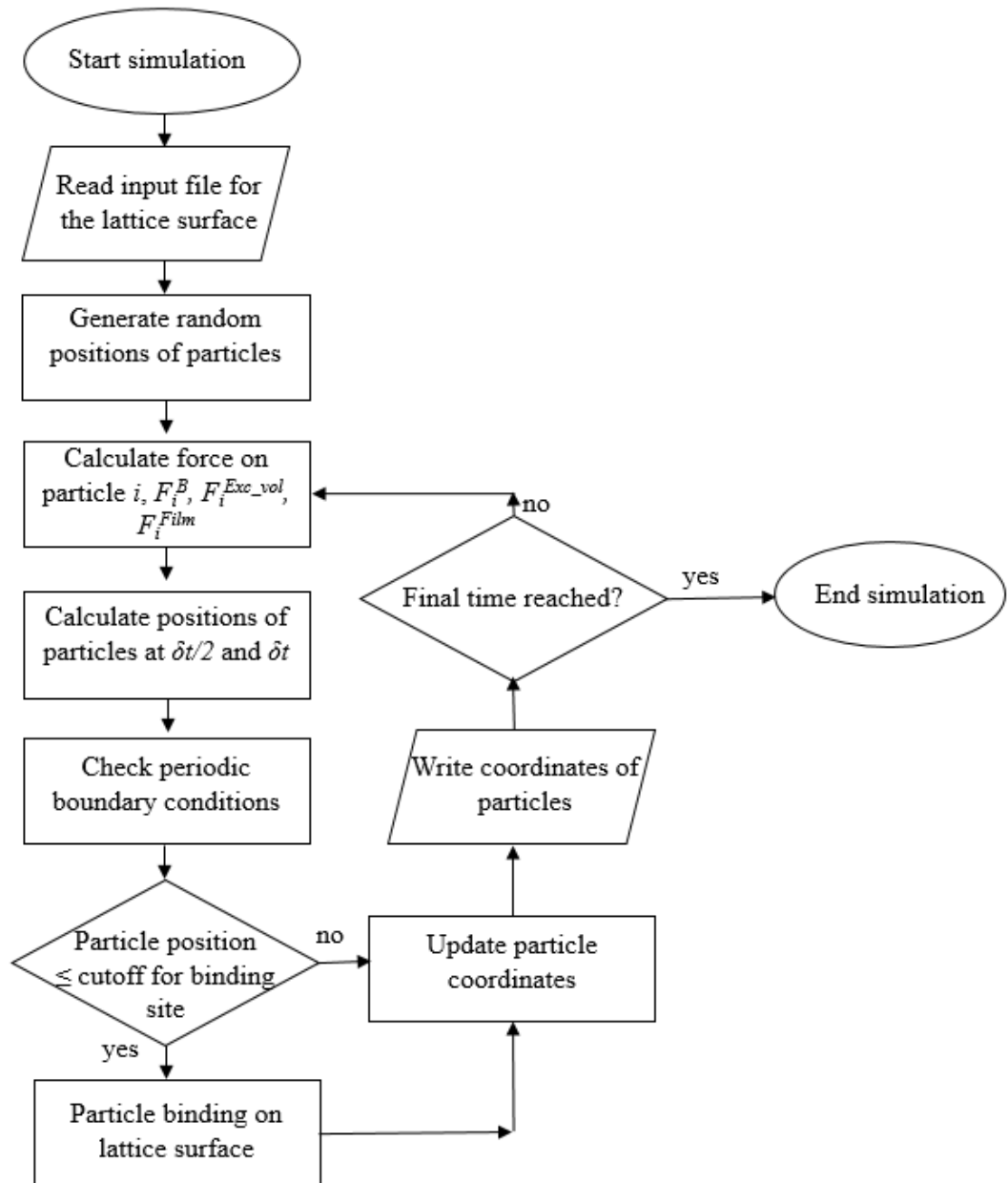


Figure 5.5: The algorithm of the BD simulation for protein adsorption.

6. RESULTS AND DISCUSSION

6.1 Experimental Results

6.1.1 Polyurethane synthesis

PU synthesis reactions with two different CO:PEG ratios (0:100 and 100:0 by weight) are shown in Figure 6.1. The similar reactions can be written for the synthesis of PU prepared from the mixture of PEG and CO where, PEG and CO molecules are randomly arranged in the polymer chain.

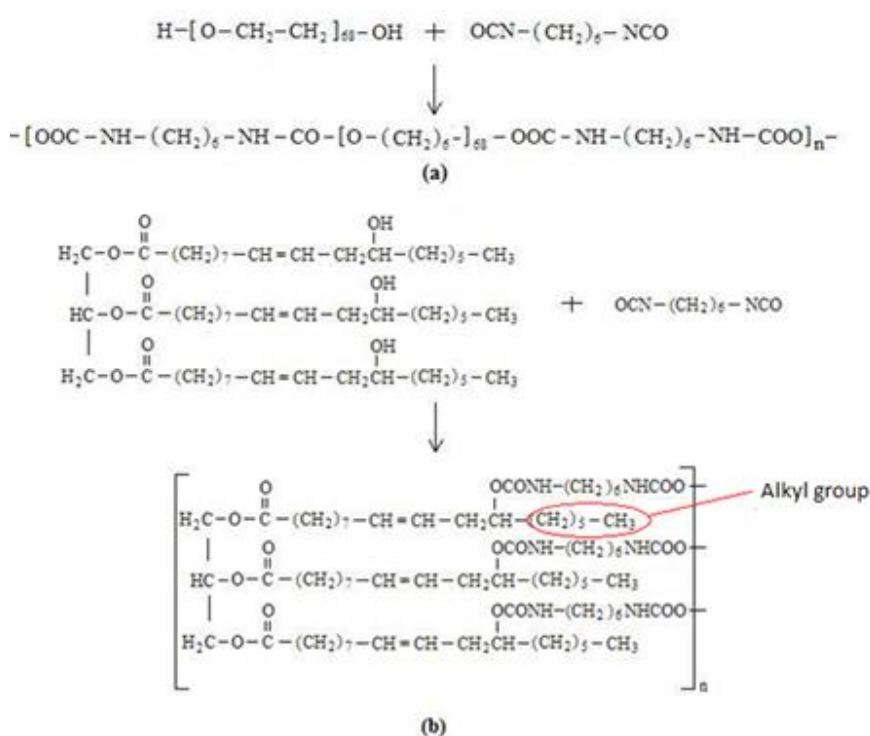


Figure 6.1: PU synthesis with; (a) PEG and (b) CO.

6.1.2 Characterization of polyurethane films

Fourier Transform Infrared Spectroscopy

In order to monitor the polymerization reaction and characterize the structure of PU films, Fourier transform infrared (FT-IR) spectroscopy was used. Figure 6.2 shows FT-IR spectrum of the sample PU100 in the beginning of reaction and after synthesis.

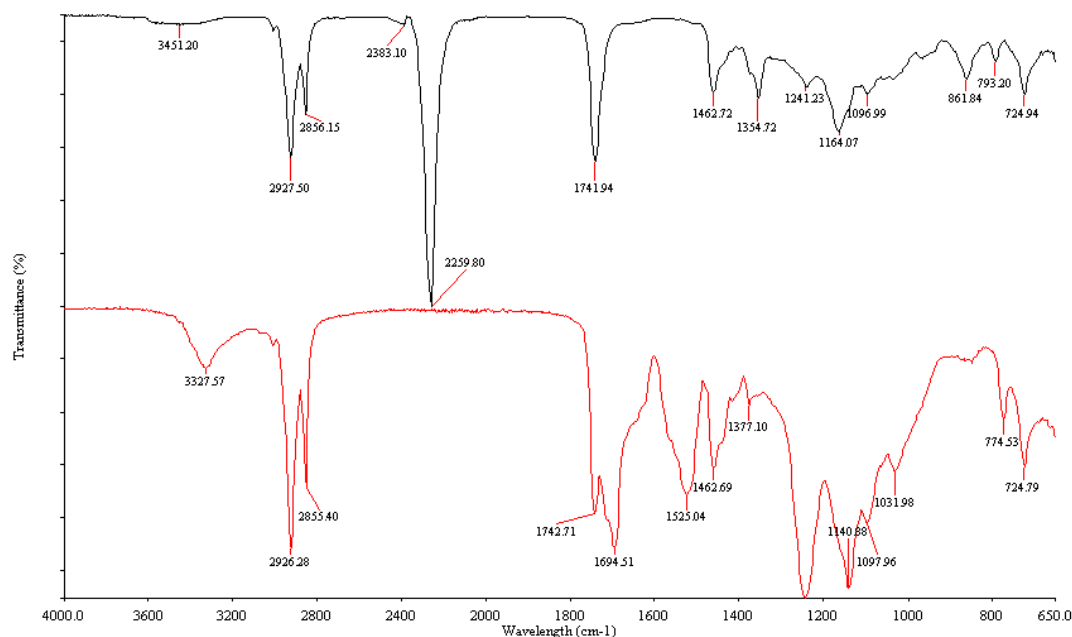


Figure 6.2:FT-IR spectrum of sample coded PU100 at the beginning and after the reaction.

In the beginning of the reaction, -OH peaks around 3351 cm^{-1} and the free isocyanate peak at around 2260 cm^{-1} we observed. After the reaction, the free isocyanate peak was disappeared and characteristic urethane peak was formed at 3327 cm^{-1} . Also C=O of urethane at 1694 cm^{-1} and C-N bending at 1525 cm^{-1} were detected. The peak at around 1741 cm^{-1} is attributed to the C=O stretching of the ester group. All FT-IR spectrums are shown in the Appendix-A.

Differential Scanning Calorimeter

The glass transition temperatures (T_g) and melting temperatures (T_m) of the polymers were determined by differential scanning calorimeter (DSC). T_g and T_m values of PUs are given in Table 6.1. All DSC thermograms were given in the Appendix-B.

Table 6.1: Glass transition and melting temperatures of polymers.

Code	CO/PEG Ratio	T_g ($^{\circ}\text{C}$)	T_m ($^{\circ}\text{C}$)
PU50	50/50	-44.09	38.64
PU60	60/40	-44.72	34.12
PU70	70/30	-46.23	24.60
PU100	100/0	-23.66	-
PU100-THF	100/0	-23.25	-
PU100-DMAc	100/0	-24.82	-

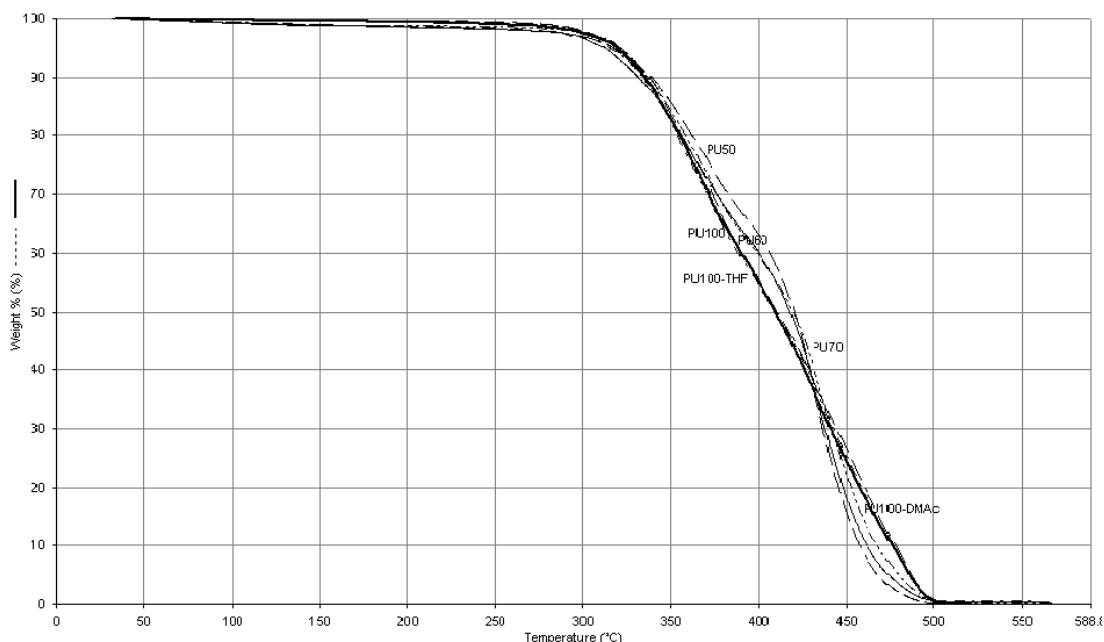
Increase in CO/PEG ratio increases T_g of polymers. T_g values of samples that did not contain PEG (PU100, PU100-THF and PU100-DMA) were significantly higher. Since functionality of CO is greater than 2, it causes crosslinks in the polymer structure. Linear structure of PEG provides easier movement of the polymer chain (for PU50, PU60 and PU 70). Decrease of PEG content in polymer structure led to an increase in the polymer melting temperature. Polymers synthesized without PEG do not have melting temperature because polymer crystallinity in low temperatures is gained due to the crystalline properties of PEG.

Thermal Gravimetric Analysis

Thermal behaviour of the samples was investigated by thermal gravimetric analyser (TGA) and the results are given in Table 6.2 for 10% and 50% weight losses. TGA thermogram of all samples is shown together in the Figure 6.3. TGA thermograms of each sample are given separately in Appendix -C.

Table 6.2: TGA results

CODE	Decomposition Temperature (°C)	
	10% Weight Loss	50% Weight Loss
PU50	342	422
PU60	331	418
PU70	334	419
PU100	335	411
PU100-THF	339	408
PU100-DMAc	336	408

**Figure 6.3:** TGA thermogram of all samples.

Since catalyst or any other additive was not used in PU synthesis, weight loss between 100-300°C was not observed for all samples. Thermal stability of PEG-free polymers was about the same values for 50% weight loss. The thermal decomposition of all samples was characterized with two distinctive steps, which corresponded to the degradation of hard and soft segments in PU structure. All TGA curves intersected approximately at 430°C. Below that temperature, samples prepared without PEG (PU100, PU100-THF, PU100-DMAc) show the lowest

thermal stability. On the other hand, they showed highest thermal stability above 430°C. As expected, at 500°C weight loss for all polyurethanes was 100%.

Dynamic Mechanical Analysis

Polymers perform both elastic properties like solid and viscous properties as liquid. Therefore, they are viscoelastic. Dynamic mechanical analysis (DMA) measures viscoelastic properties of materials. DMA graphs comprises storage modulus (E'), loss modulus (E'') and $\tan\delta$. While, storage modulus gives some information about material elasticity, loss modulus indicates viscous properties of materials. $\tan\delta$ is the ratio of E''/E' . The maximum point of $\tan\delta$ indicates the T_g of the sample. Table 6.4 shows the T_g and height of $\tan\delta$ peak obtained from DMA results for all samples and Figure 6.4 shows storage modulus, loss modulus and $\tan\delta$ curves of all samples. DMA curves of each sample are given separately in Appendix-D.

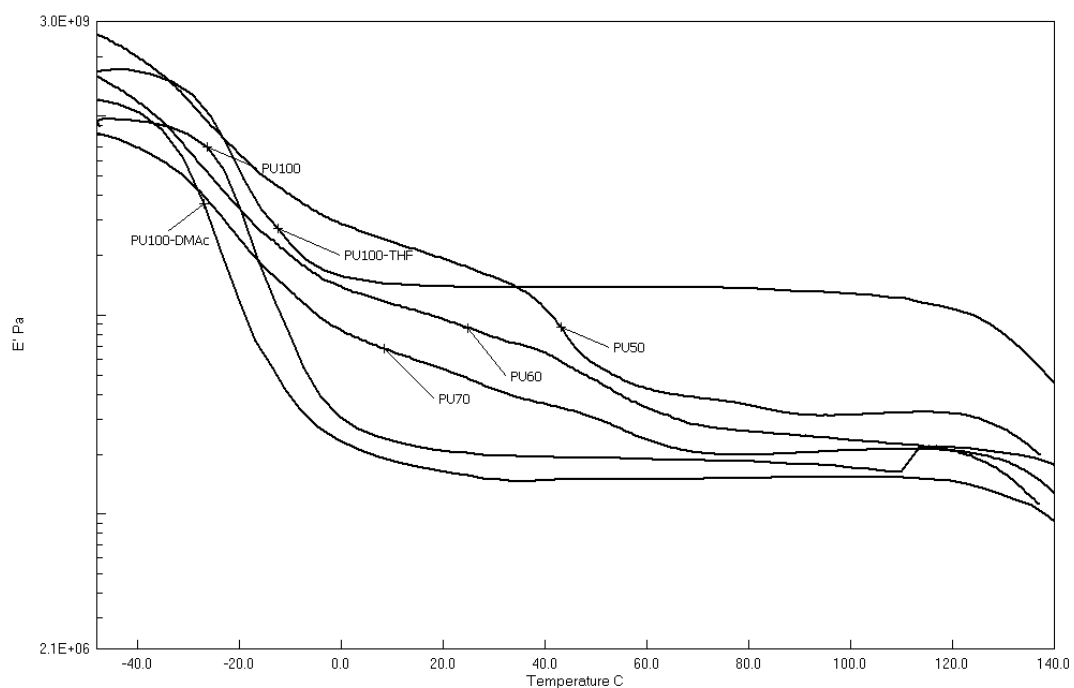
Table 6.3: DMA results of samples.

Code	$h_{\tan\delta}$	T_g (°C)
PU50	0.20	-23.9
PU60	0.27	-23.0
PU70	0.29	-24.9
PU100	0.51	-12.9
PU100-THF	0.34	-19.2
PU100-DMAc	0.54	-20.3

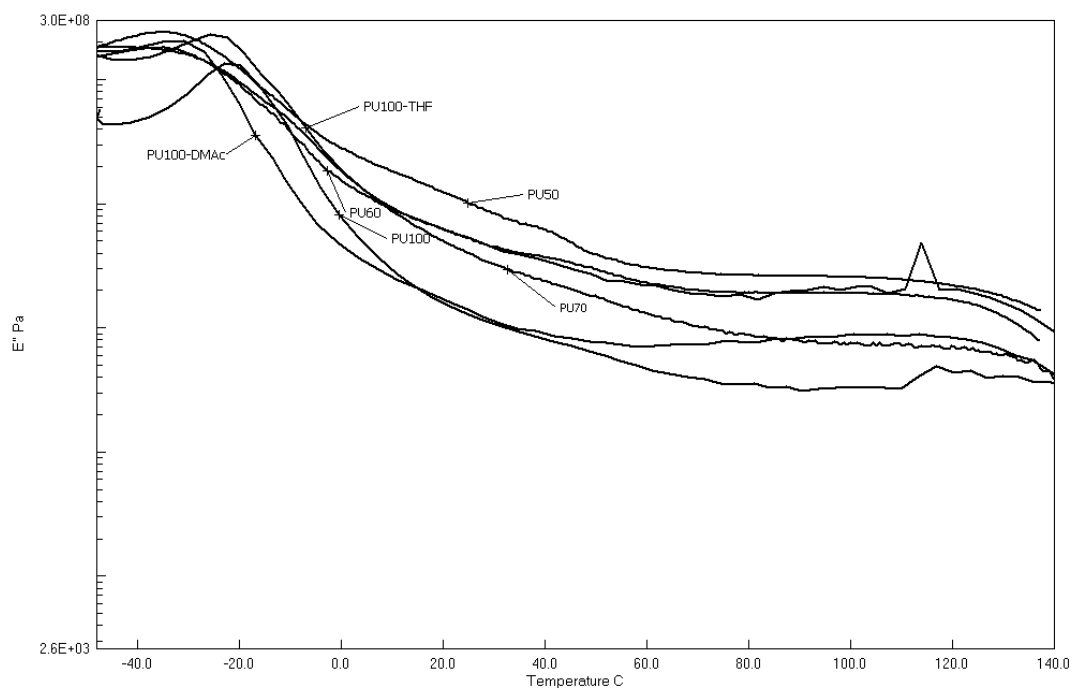
The height of the $\tan\delta$ peak ($h_{\tan\delta}$) is an indicator of chain mobility in a polymer system. Contrary to expectations, an increase of CO in polymer structure increased the height of the $\tan\delta$ peak. This can be explained by the presence of alkyl groups in the CO structure. In fact, CO ensured a crosslinked polymer structure due to its higher functionality, which makes chains difficultly move across the applied force. However, alkyl groups in the CO structure act as a lubricant and facilitate the movement of the polymer chain. There are similar explanations in literature[36].

T_g values of the PEG-free polymers were relatively greater than the others. Increasing CO amount in polymer increased sample T_g value and also height of the

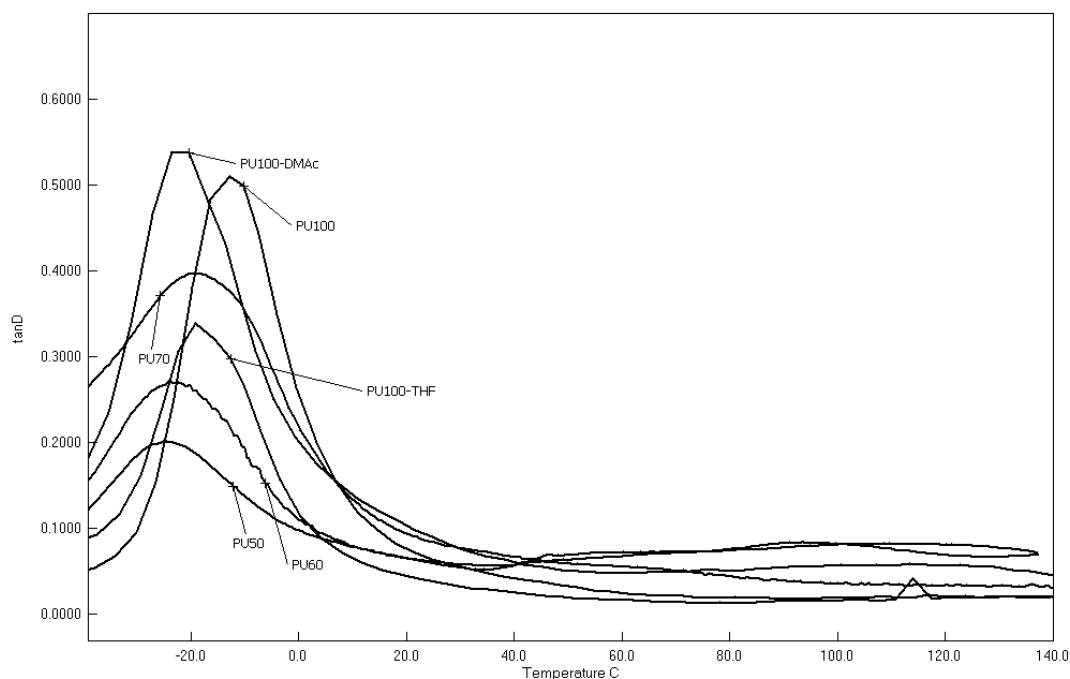
Tan δ peak. Comparing with DSC results, difference of T_g values for each samples can be explained by different measurement principles of devices. In DMA, sinusoidal force was applied to the sample while DSC measured thermal analysis without applying any force to the sample.



(a) Storage Modulus



(b) Loss Modulus

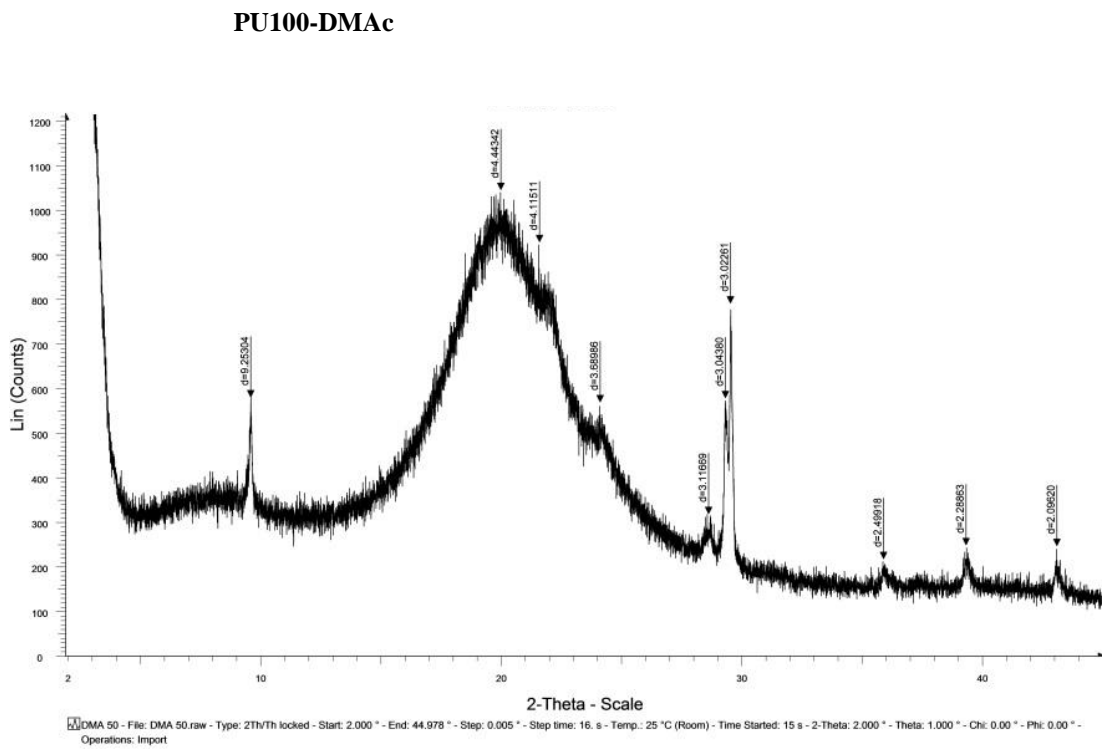
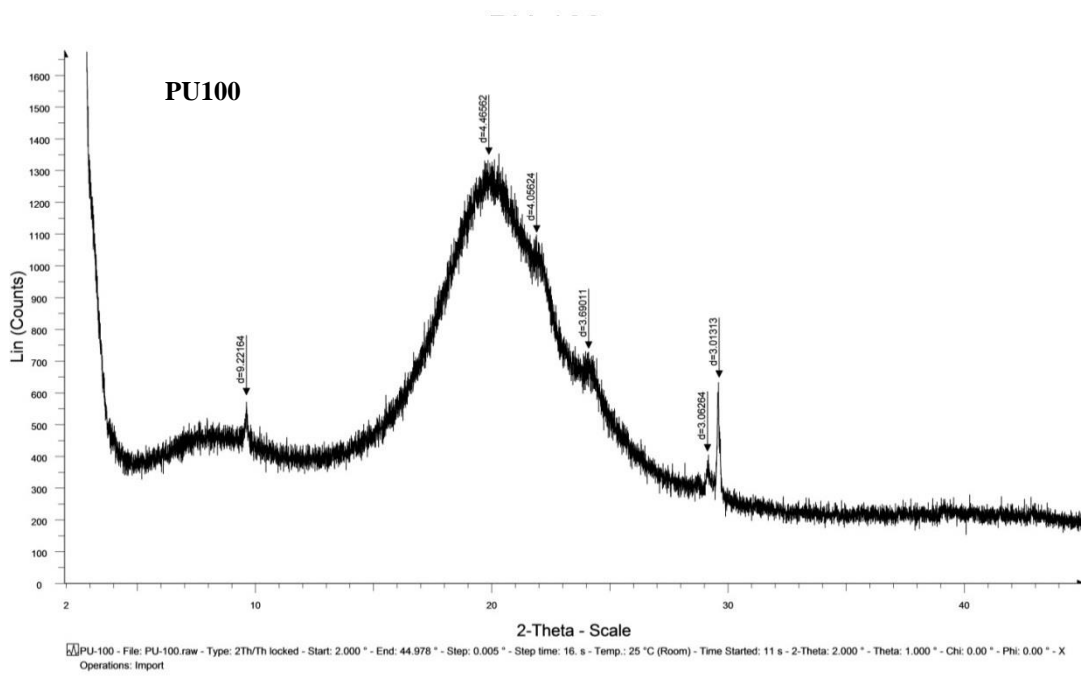


(c) $\tan\delta$

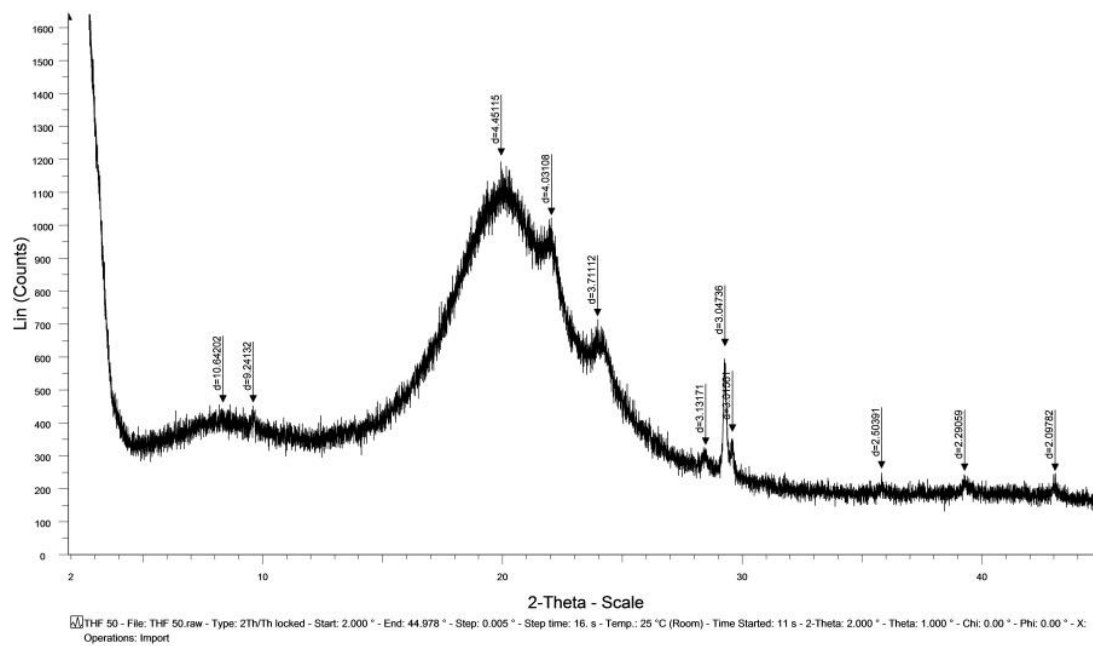
Figure 6.4:(a) Storage modulus, (b) loss modulus and (c) $\tan\delta$ of all samples.

X-Ray Diffraction

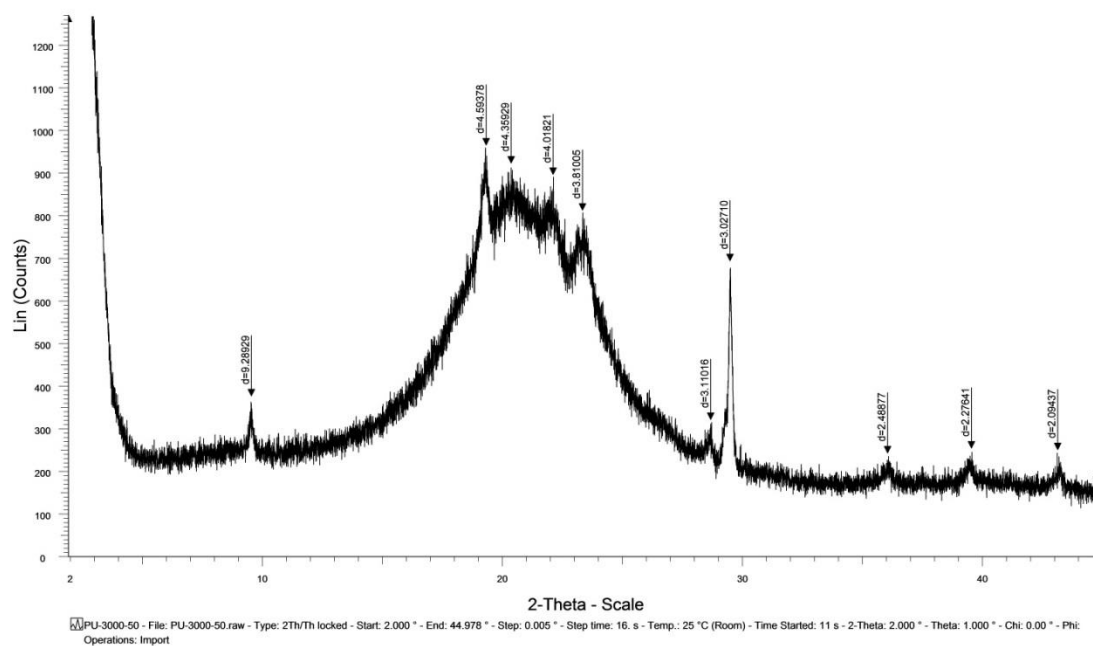
X-ray diffraction patterns for the samples PU50 and PU100 are given in the Figure 6.5. Between $2\theta=18-24^\circ$ sharp PEG peaks were observed for PEG based polymers. According to the XRD patterns, CO based polymers are amorphous in structure, on the other hand, for $2\theta=10$ and between $20-30^\circ$, regional crystalline peaks were detected. Crystallinity (%) of the samples were calculated under the area of the XRD peaks. Crystallinity percentage ($X_c\%$) of all samples is shown in the Table 6.4.



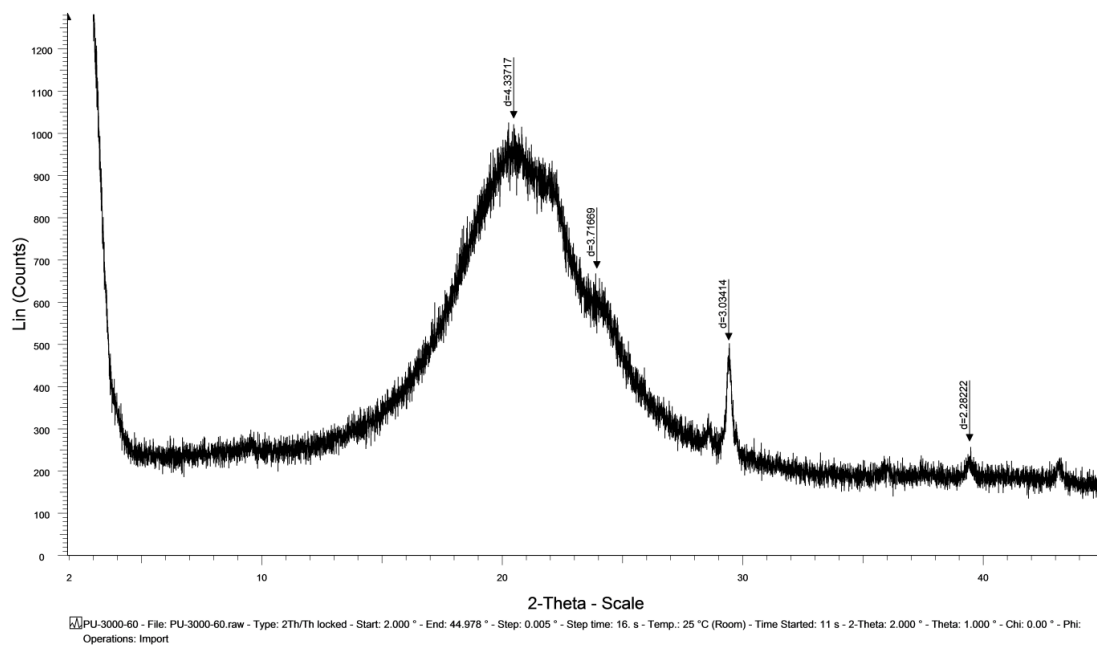
PU100-THF



PU50



PU60



PU70

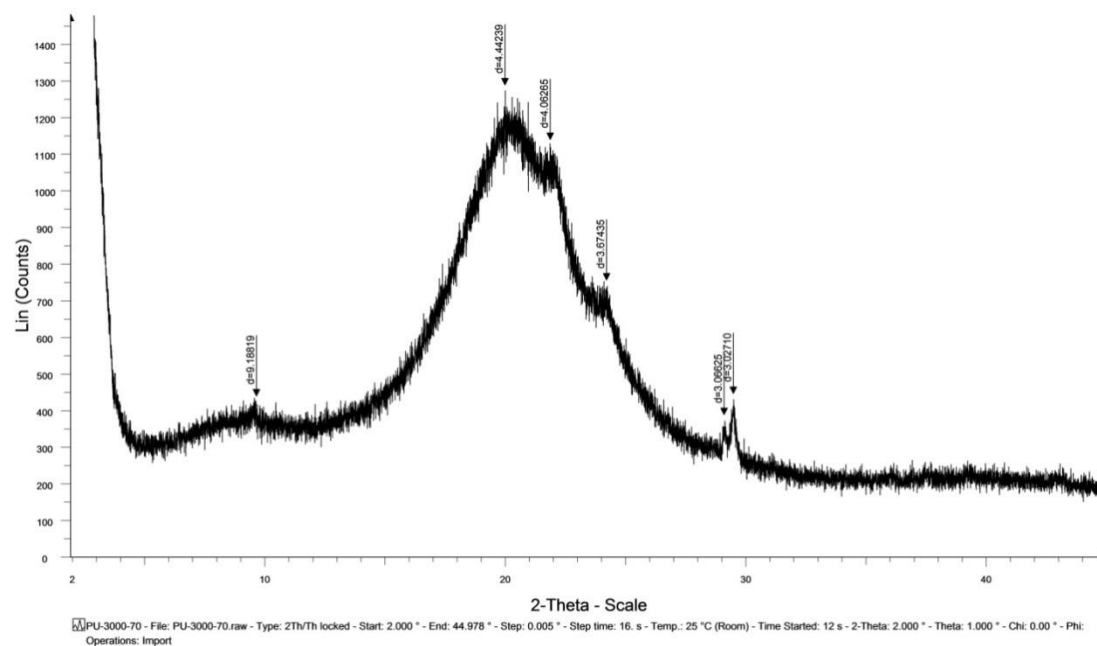


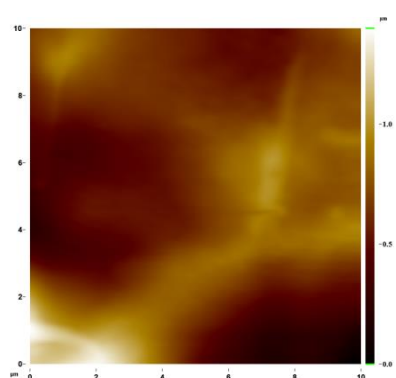
Figure 6.5:XRD patterns of the samples.

Table 6.4:Crystallinity percentage of the samples.

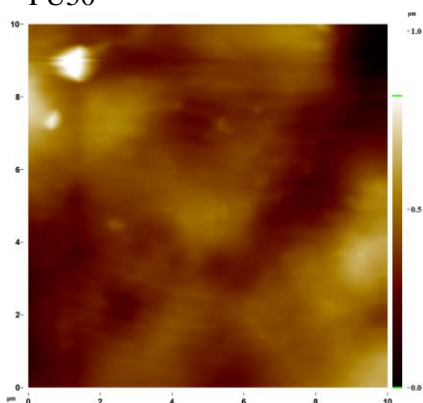
Code	$X_c\%$
PU50	42.3
PU60	38.5
PU70	37.9
PU100	35.1
PU100-THF	37.1
PU100-DMAc	36.3

Atomic Force Microscopy

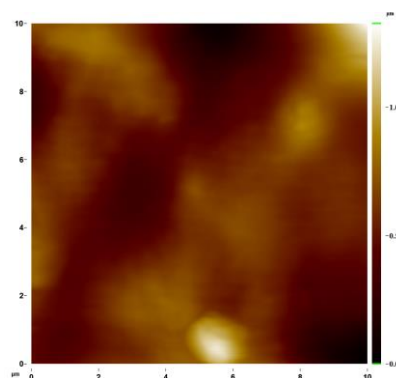
Surface topography and phase images of samples can be seen in Figure 6.6 and 6.7 respectively. Surface roughness are given in Table 6.5.



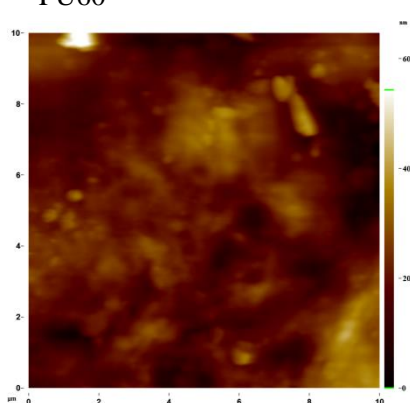
PU50



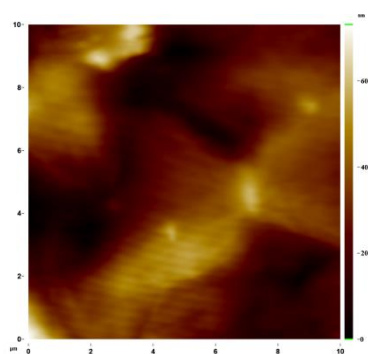
PU70



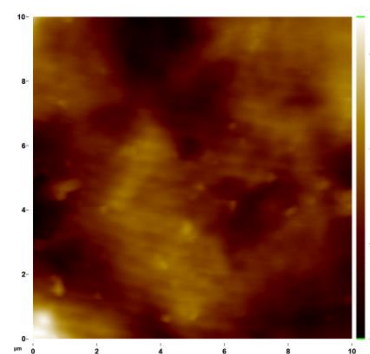
PU60



PU100



PU100-THF



PU100-DMA

Figure 6.6: Topography images of samples.

Table 6.5:Surface roughness of samples

Code	Roughness Values (nm)
PU50	164.85
PU60	128.91
PU70	84.45
PU100	50.54
PU100-THF	113.28
PU100-DMAc	76.79

According to the topology images, increasing PEG content in polymer structure increased surface roughness as was expected. For PEG free samples, addition of solvent in the reaction medium increased surface roughness in various degrees due to the difference in boiling point of solvents. Since boiling point of THF is lower than DMAc, polymer coded PU100-THF had the roughest surface among PEG free samples.

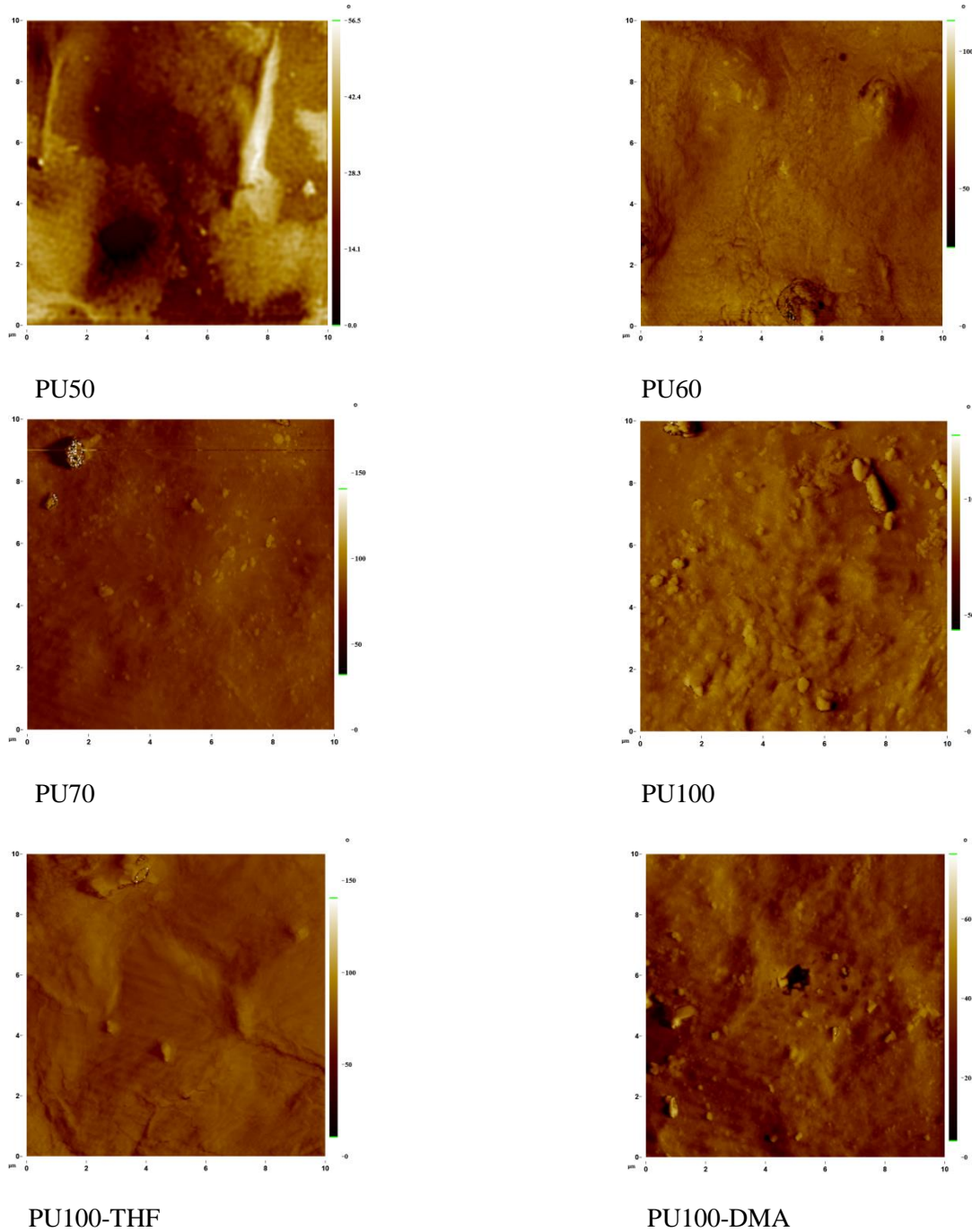


Figure 6.7: Phase images of samples.

A contrast in phase images given in Figure 6.7, is due to the variation of the energy dissipation of the vibrating cantilever, which is related to the presence of different phases and differences in surface adherence near the surface of the scanned material. Highly dissipating domains are expected to give dark contrast in the phase imaging, while more crystalline, less dissipating phases appear as bright areas [73].

In phase images, hard segments appeared as small fragments like filaments packed in thin structures. The main reason may be due to hydrogen bonding that is formed by hard segments of PUs [74].

Contact Angle Measurements

Contact angle (θ) and surface free energy (γ) of all samples are given in the Table 6.7. Due to the hydrophilic nature of PEG, decrease of PEG content increased contact angle and decreased surface free energy of the sample.

Table 6.6: Contact angle and surface free energy results of samples.

Code	θ ($^{\circ}$)	γ (mN/m)
PU50	63 \pm 2	49 \pm 1
PU60	65 \pm 0.5	46 \pm 2
PU70	68 \pm 1	42 \pm 0.5
PU100	96 \pm 1	32 \pm 1
PU100-THF	95 \pm 2	30 \pm 1
PU100-DMAc	93 \pm 1	31 \pm 1

6.1.3 Protein adsorption results

Amounts of adsorbed bovine serum albumin (BSA) on PU surfaces after immersion into protein solution are displayed in Figure 6.8. Concentration of adsorbed protein for all samples reached a maximum level in 10 minutes. Initial rate for protein adsorption was calculated from the slope of the linear part of the graph plotted amount of adsorped protein versus adsorption time.

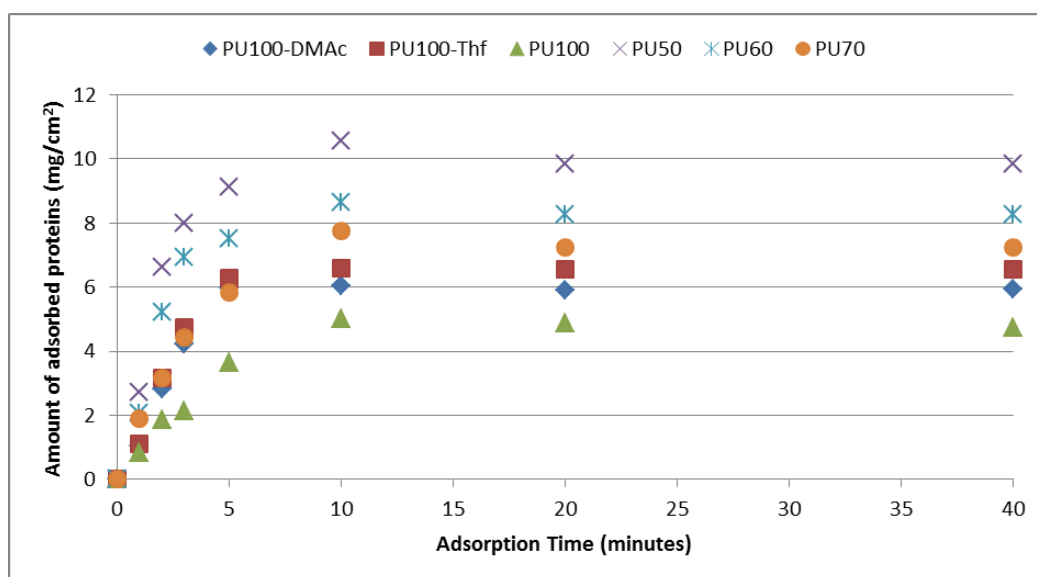


Figure 6.8: Amount of BSA adsorption.

It would be better to evaluate the rate of protein adsorption ($\text{mg}/\text{cm}^2 \cdot \text{min}$), surface hydrophilicity, roughness and crystallinity together, since the protein adsorption does not depend only on one parameter. In Table 6.7, crystallinity percentage (from Table 6.4), roughness (from Table 6.5), hydrophilicity (from Table 6.6) and the rate of protein adsorption for all samples is summarized.

Table 6.7: Crystallinity percentage, roughness, hydrophilicity and the rate of protein adsorption for all samples.

Code	Cryastallinity (%)	Surface Roughness (nm)	Water Contact Angle (°)	Protein Adsorption Rate (mg/cm ² .min)
PU50	42.3	164.85	63±2	2.86
PU60	38.5	128.91	65±0.5	2.38
PU70	37.9	84.45	68±1	1.30
PU100	35.1	50.54	96±1	0.75
PU100-THF	37.1	113.28	95±2	1.36
PU100-DMAc	36.3	76.79	93±1	1.26

It is well known that a decrease in crystallinity, surface roughness and contact angle decrease protein adsorption [7,14]. As seen from Table 6.8, the same correlation was observed between crystallinity, roughness and protein adsorption for PEG-based PUs. On the other hand, PU50 which was the most hydrophilic sample showed higher protein adsorption than PU60 and PU70. This can be explained by the effectiveness of crystallinity and roughness than hydrophilicity for PU films and also by the nature of the protein albumin. Figure 6.8 shows surface properties (hydrophilic residues, hydrophobic residues and polar residues) of the albumin. Since in native form, albumin thought as a ‘hard protein’ with low tendency for structural alterations, dominance of hydrophilic residues at the outer shell can explain its tendency to bind more on hydrophilic surfaces, while overcoming the water barrier on the hydrophilic polymeric surface (Figure 6.8). Moreover, a previous molecular dynamics simulation [37] on PEG-based and CO-based PUs indicated similar results, where water molecules were entrapped on the rough surface, which may be the case for the current observation for increased protein adsorption on hydrophilic PU samples.

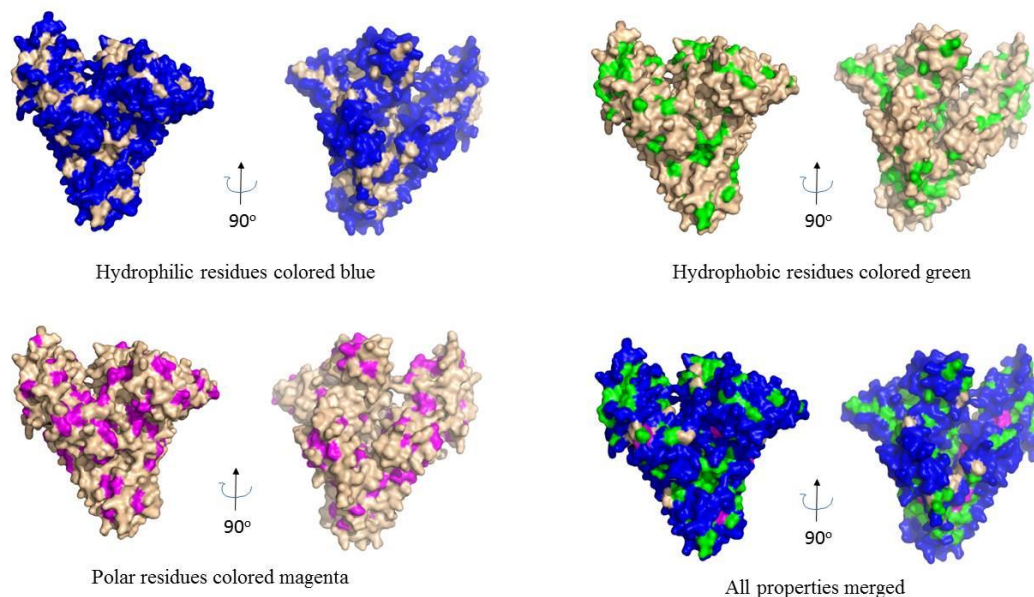


Figure 6.8: Surface properties of albumin protein.

In order to determine which parameter, crystallinity or roughness, is more effective in protein adsorption, samples with same hydrophilicity (PU100, PU100-THF, PU100-DMAc) were synthesized. The lowest level for protein adsorption and surface roughness were observed for the sample coded PU100. On the other hand, using different types of solvent in the reaction medium enabled to synthesize surfaces with same hydrophilicity but different in surface roughness. In Figure 6.10, results are presented for each parameter. These data showed that for protein adsorption on synthesized PUs, crystallinity was a more effective parameter, since sensitivity for protein adsorption, i.e. slope of the equations, was highest, as compared to other parameters, namely roughness and hydrophilicity. In Figure 6.11, all results are also presented as the percentage variance of each parameter taking PU100 as reference, since it displayed the lowest protein adsorption. Especially, for the water contact angle clusters (Figure 6.10), a linear trend was obtained when the percentage differences were calculated as shown in Figure 6.11.

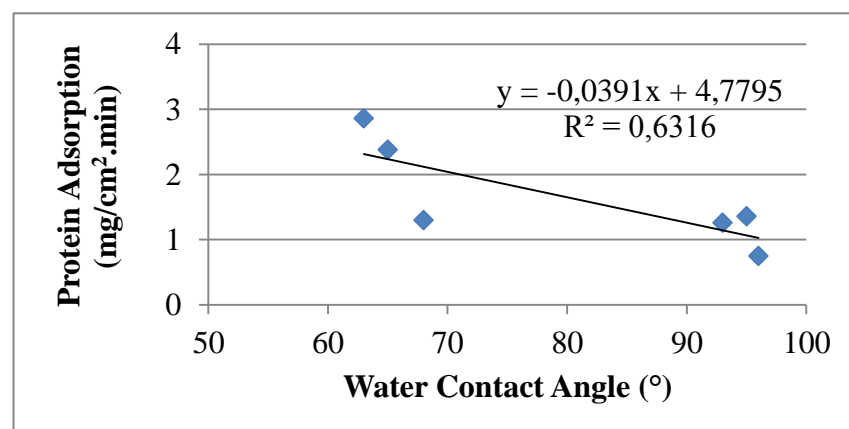
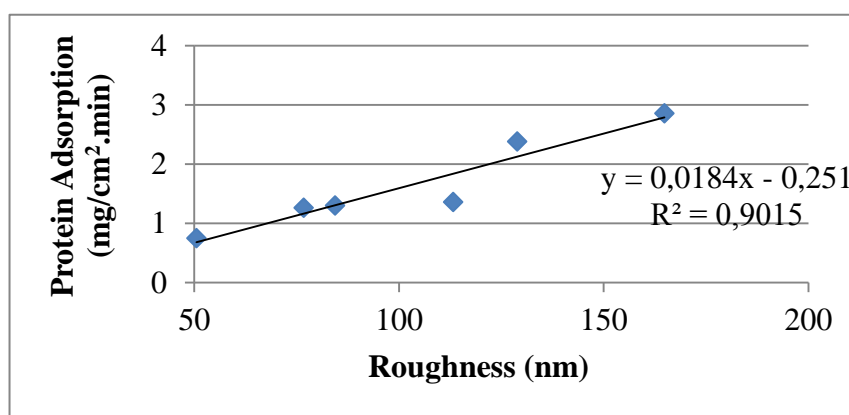
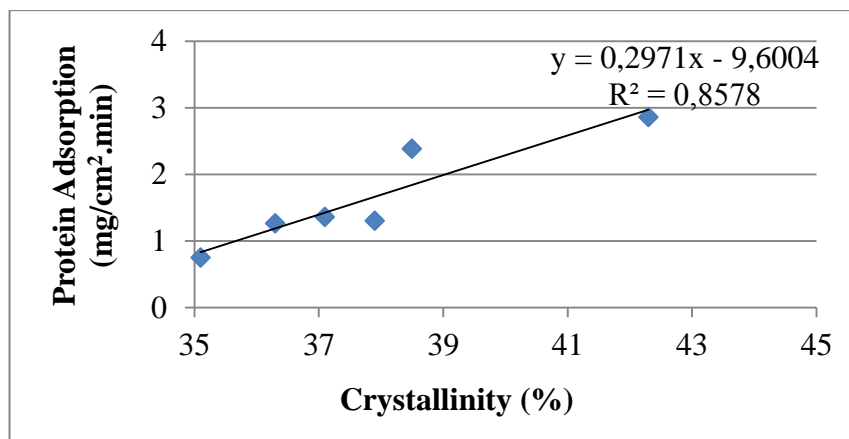


Figure 6.10: The effect of each parameter on protein adsorption on PU films.

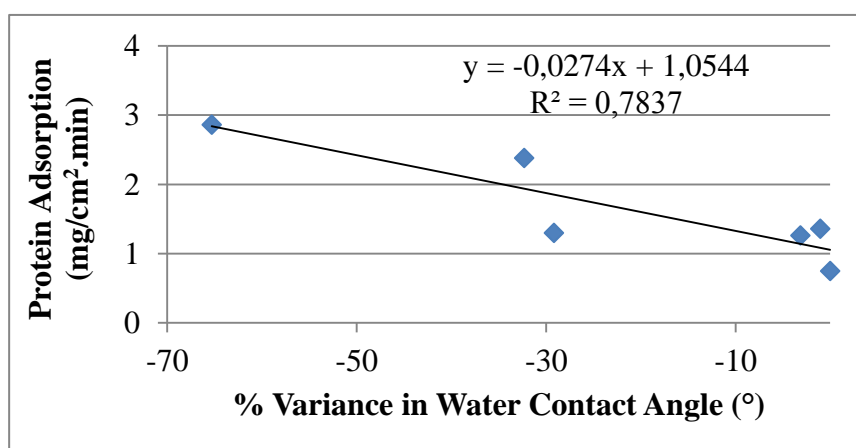
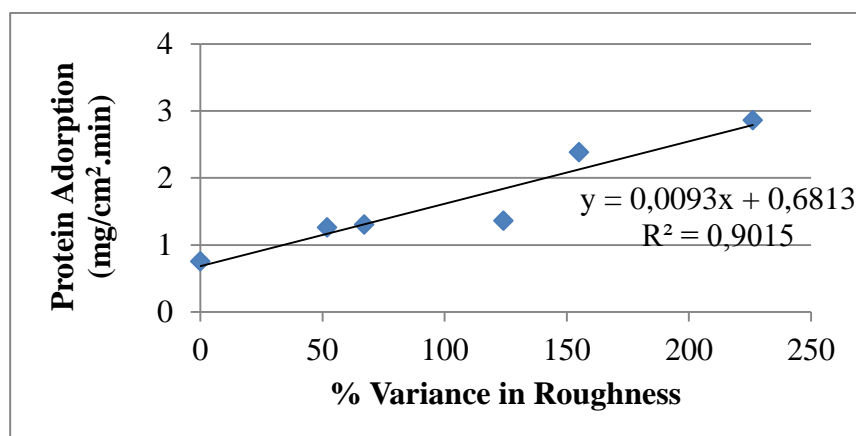
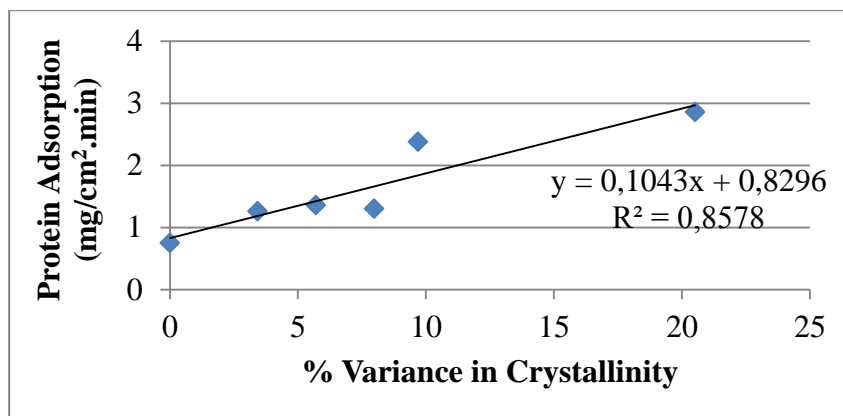


Figure 6.11: Percentage variance of each parameter according to the PU100.

6.2 Computational Results

The adsorption of bovine serum albumin on the PU surface was modeled by using a coarse-grained Brownian Dynamics simulation, as explained in the Methods section. Proteins were represented as uniform spheres and the polyurethane surface modeled as a lattice composed of binding and non-binding regions for proteins on smooth and rough surfaces. (Figure 6.12). Effect of crystallinity percentage, surface roughness and crowding on protein adsorption are presented in the following sections.

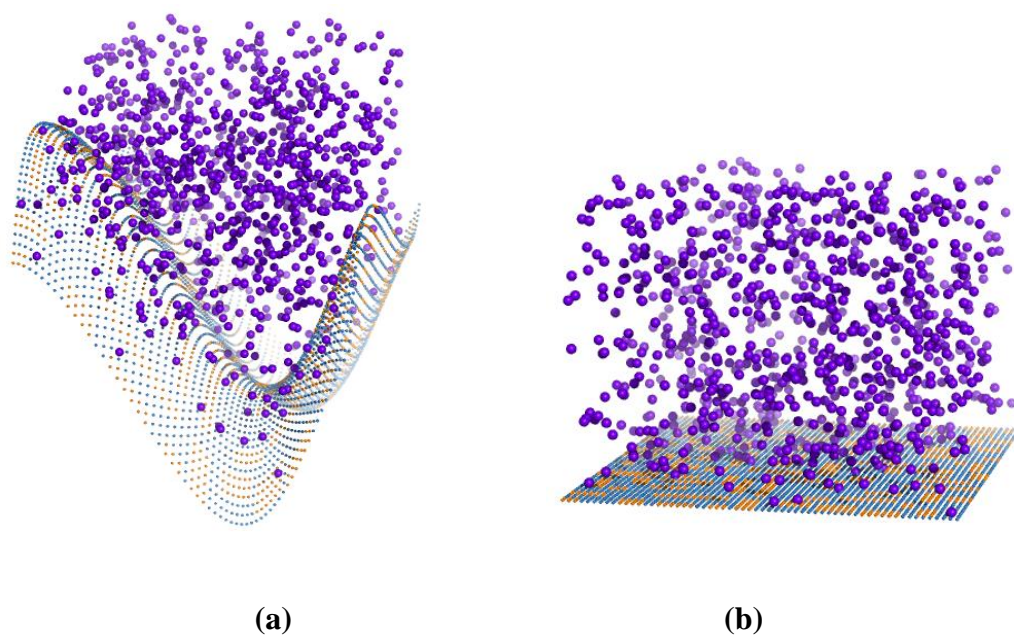


Figure 6.12: Protein adsorption on (a) rough and (b) smooth surfaces. Proteins are purple color spheres, amorphous non-protein binding regions are blue and crystalline protein binding regions are orange.

6.2.1 Effect of surface crystallinity on protein adsorption

It is recognized that crystallinity promotes protein adsorption [35], and increase in crystallinity percentage on the polymer surface is expected to effect adsorption kinetics. To investigate this property, surfaces with different degree of crystallinity, i.e. low and high, were modeled (Figure 5.4, bottom panel). In order to have a clear picture of the adsorption process with respect to time, concentration of adsorped proteins, C_{ads} ; surface coverage, calculated by taking the ratio of number of adsorbed sites over total number of adsorption sites; and ratio of concentration of adsorbed proteins over freely diffusing proteins in solution, C_{ads}/C_{sol} were calculated and plotted. In Figure 6.13, results are presented for the smooth surface. As the number of binding or adsorption regions increased for a constant number of proteins, more proteins had chance to be adsorbed. However, surface coverage rate was higher for low number of binding regions available, i.e. when we compared $b=800$ and $b=1300$ for both number of proteins $N=1000$ and 2000 , meaning that surface saturation was faster.

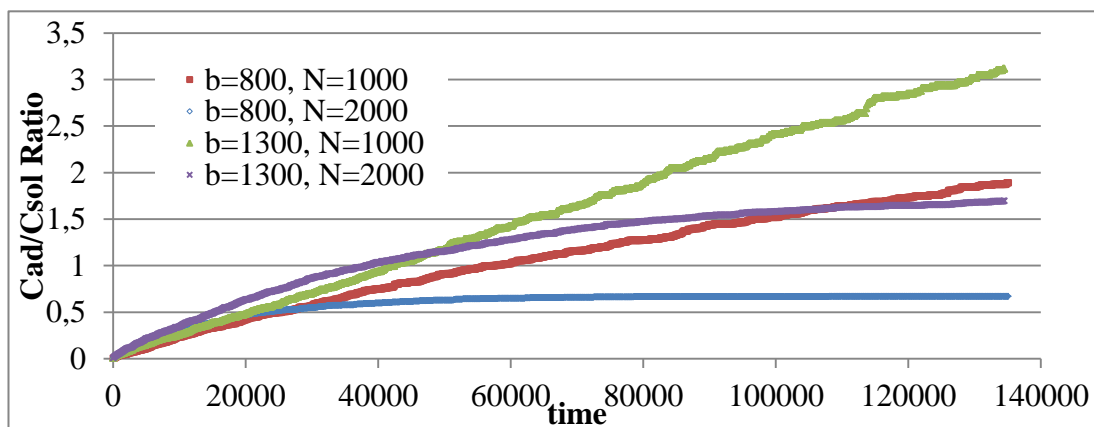
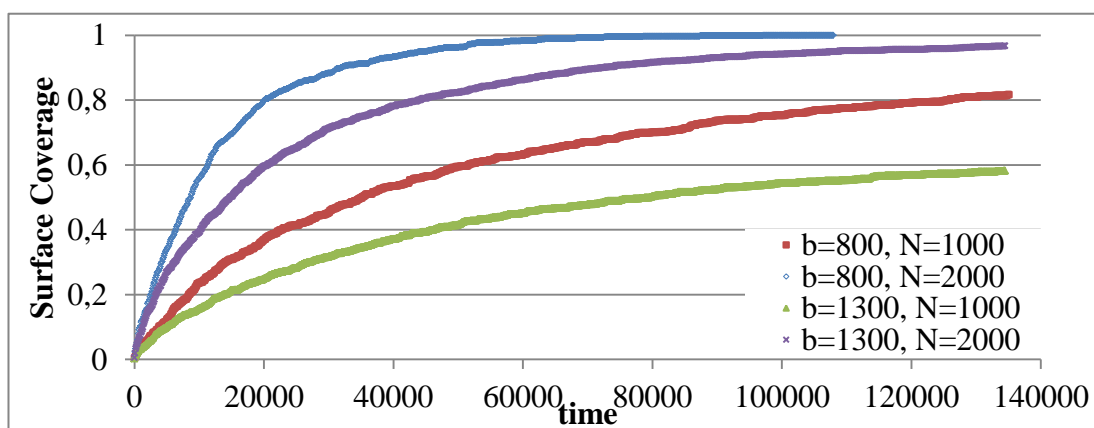
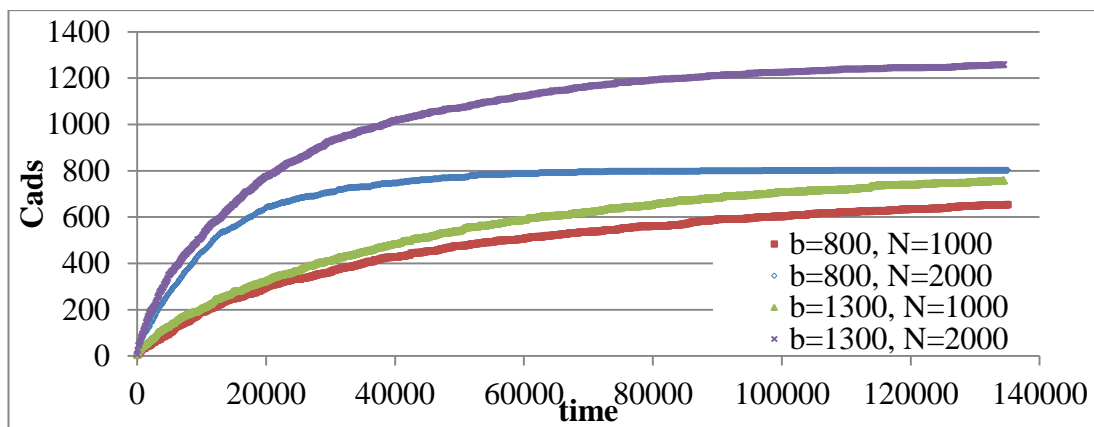


Figure 6.13: Protein adsorption on flat surface. b : amount of binding regions, N : amount of protein particles

This phenomenon was observed for the rough surfaces with different crystallinities (binding regions) as well, as displayed in Figure 6.14.

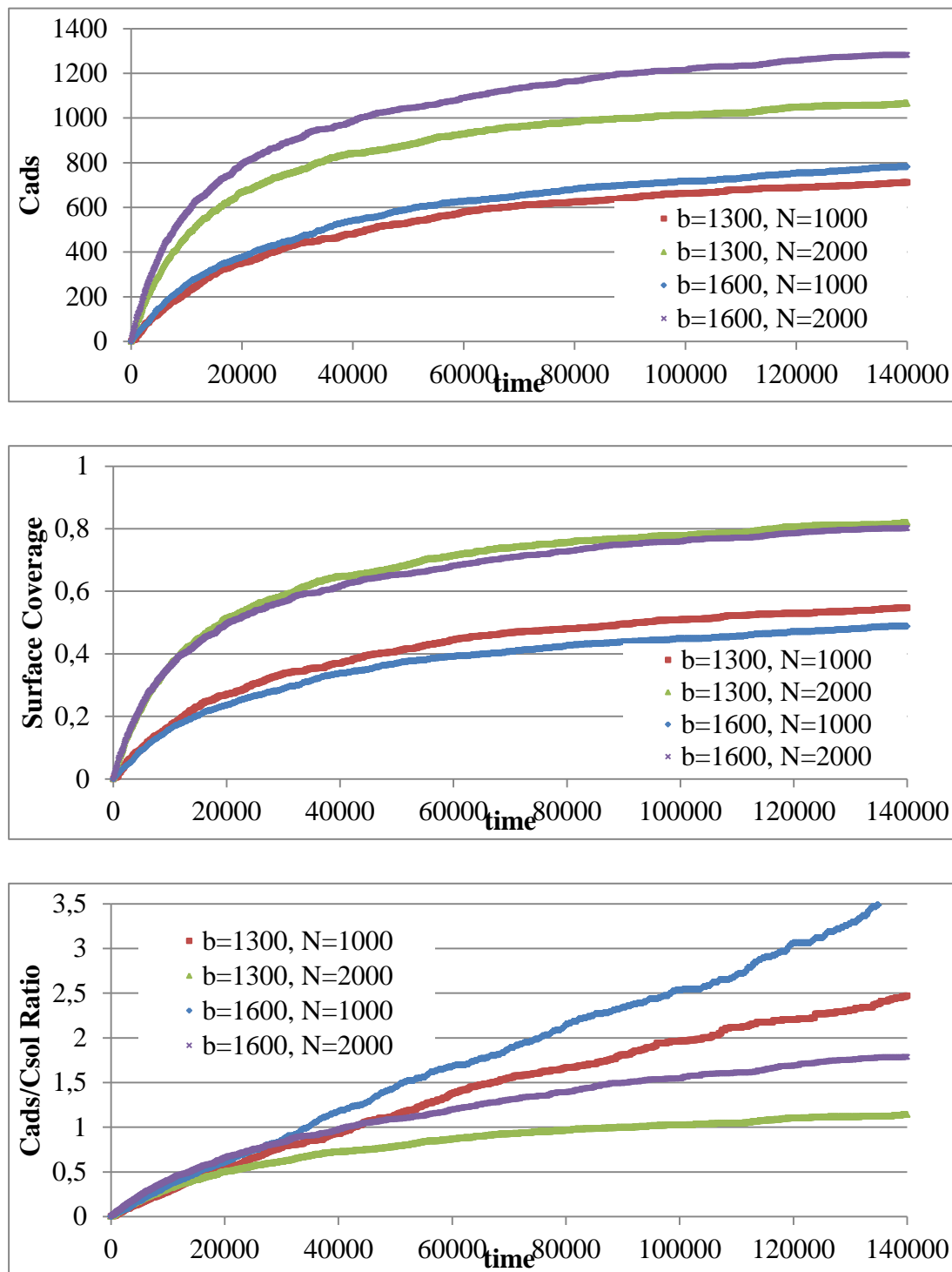


Figure 6.14:Protein adsorption on rough surface. b : amount of binding regions, N : amount of protein particle.

6.2.2 Effect of roughness on protein adsorption

Roughness in polymeric surfaces increases surface area when compared to smooth surfaces. The surface increase may promote an increase in crystalline regions, where proteins can be adsorbed, leading to a higher concentration of proteins adsorbed on the surface. Adsorption kinetics for smooth and rough surfaces, with different crystallinities were investigated for a constant number of protein particles in the system. Results are presented in Figure 6.15 for number of particles $N=1000$.

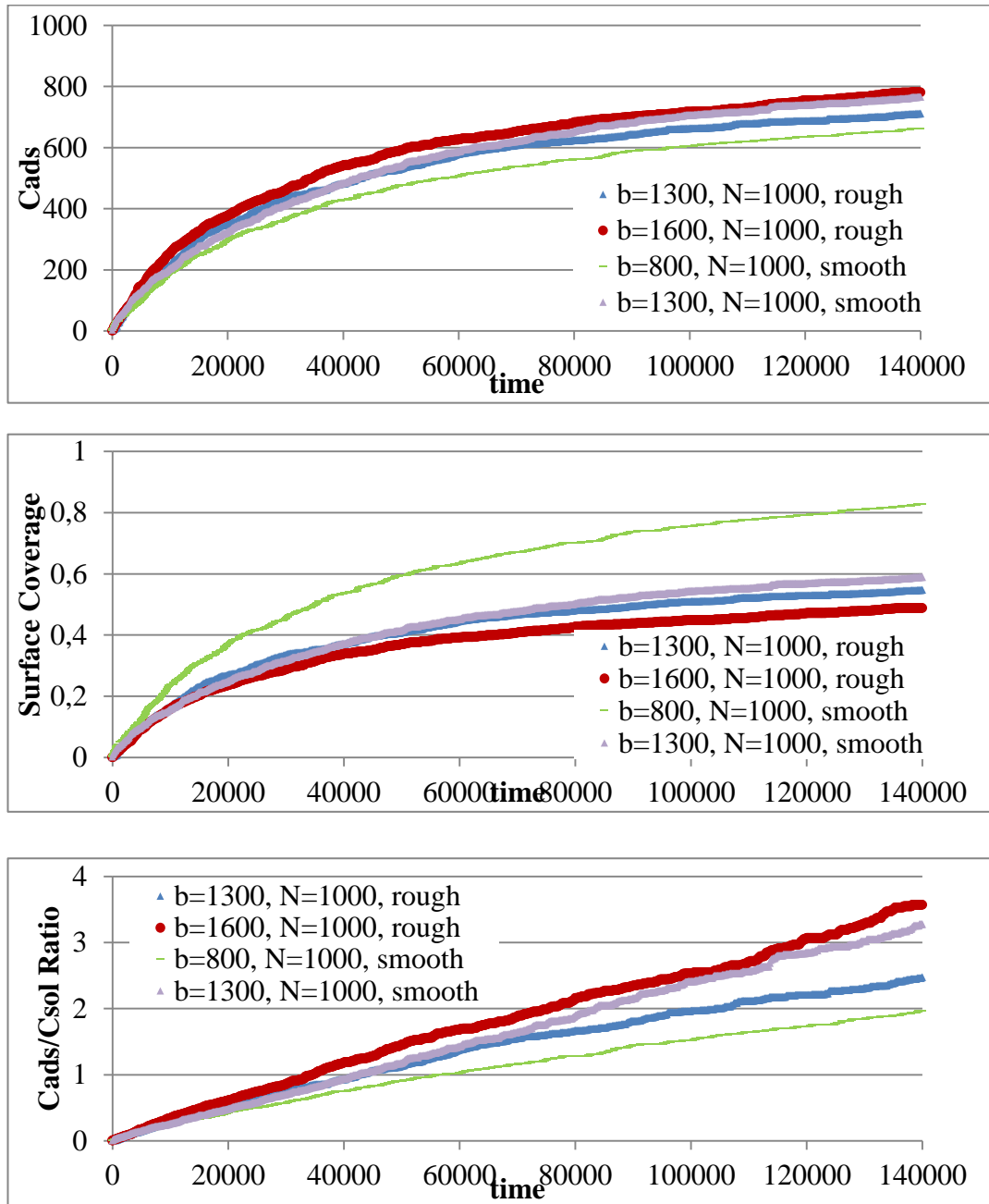


Figure 6.15:Effect of roughness on protein adsorption for $N=1000$

Adsorption rates were very similar for all studied cases, namely smooth and rough surfaces with different crystallinities. Eventually, all surfaces attained a saturation sooner or later; however, smooth surface with a smaller number of binding sites (low crystallinity, $b=800$) reached the saturation first, as expected. When the smooth and rough surfaces with the same crystallinity were compared (Figure 6.15, curves with $b=1300$), adsorption rates and surface coverage rates were very close to each other. If two extreme cases, smooth surface with number of binding regions $b=800$ and rough surface with $b=1600$ were compared, surface coverage rate was smallest for the rough surface. The main reason behind this was the crowding effect promoting protein adsorption.

In the adsorption process, protein molecules occupy an excluded volume when they diffuse freely in the solution. Their adsorption on a surface is thermodynamically favorable as they occupy less volume in the system. When the amount of proteins was increased, the rate of association with the binding surface was also increased, as seen from Figures 6.13 and 6.14 C_{ads}/C_{sol} plots. As the simple diffusion experiment presented here indicated, higher number of freely diffusing protein particles shifted the reversible adsorption reaction $A+P \leftrightarrow AP$ more to the right, where A was adsorption sites, P proteins and AP adsorbed proteins. As the difference between the number of adsorption sites and the protein concentration in solution got higher, such as for $b=800$ and $N=2000$ (smooth surface, Figure 6.13 and Figure 6.15), the adsorption and surface coverage rates were higher, when compared to $b=1300$ and $N=1000$ (rough surface, Figure 6.14 and Figure 6.15).

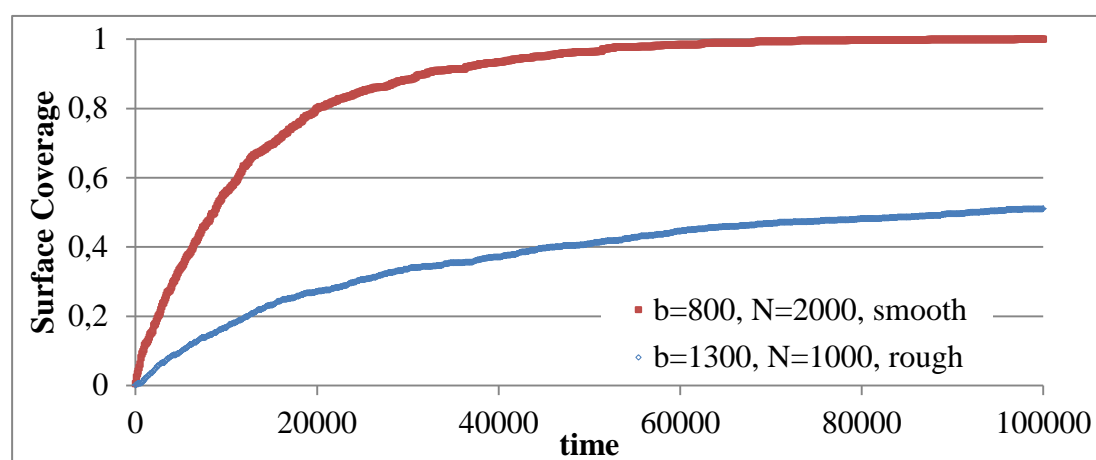


Figure 6.16:Macromolecular crowding effect on protein adsorption.

7. CONCLUSION

This thesis consisted of two parts, including both experimental and computational. In the experimental part the effect of surface crystallinity, roughness and hydrophilicity on protein adsorption of polyurethane films were investigated. In the computational part, the effect of crystallinity percentage, protein concentration and surface roughness on protein adsorption were determined and the results were compared with experimental results.

In the experimental part, CO and/or PEG based polyurethanes were synthesized in various hydrophilicity, roughness and crystallinity and they were characterized by FT-IR, DSC, TGA, DMA, XRD and AFM.

According to XRD results, sample that had a maximum PEG content was found as the highest crystalline one. Crystallinity of PEG-free polyurethanes was determined to be very close to each other and relatively lower amount than those containing PEG, which was expected and desired.

Based on DSC results, melting temperatures had been determined only for polyurethanes containing PEG. Glass transition temperature of PEG-free polyurethanes, were higher than those with CO and PEG based polyurethanes. DMA results also confirm the relationship between the glass transition temperature and the polymer structure even if they are not obtained with the same value from DSC.

TGA results showed that, an increase in the amount of CO resulted in a reduce of polymer heat resistance.

According to the water contact angle measurements, hydrophilicity of PEG-free polyurethanes found to be very close to each other. They have higher contact angle than the polyurethanes prepared from PEG and CO.

AFM results indicated that, increasing PEG content in polymer structure increases surface roughness as expected. For PEG free samples, addition of solvent in the reaction medium increases surface roughness in various degrees due to the difference in boiling point of solvents. In phase images, hard segments appear as small fragments like filaments packed in thin structures. This is thought to be due to hydrogen bonding which is formed by hard segments of polyurethanes.

Protein adsorption experiments show that crystallinity is distinctly more effective parameter on protein adsorption than roughness and hydrophilicity.

Considering the effect of surface roughness, hydrophilicity, crystallinity and protein adsorption results together, computational results indicated that the molecular crowding, i.e. high concentrations had the biggest impact on protein adsorption, then degree of surface crystallinity and finally roughness. Observation from simulations suggested the roughness had an implicit effect on protein adsorption by providing higher surface area compared to smooth surfaces. In other words, if high surface area revealed more crystalline regions, more proteins adsorbed on the surface. In contrary, if high surface area revealed more amorphous regions, protein adsorption rate diminished.

In future, the effect of flexibility of proteins on protein adsorption can be studied both by experimental and computational techniques for a more clear understanding of protein adsorption phenomena on polyurethane surfaces. Another parameter to include to these experiments would be considering the competition of small and large proteins in adsorption, as well as stable and flexible proteins present in the same solution.

REFERENCES

- [1] **Patel NR, Gohil PP.**(2012).A review on biomaterials: scope, applications & human anatomy significance,*International Journal of Emerging Technology and Advanced Engineering*2(4), 91-101.
- [2] **Adamczyk Z.** (2012).Modeling adsorption of colloids and proteins.*Curr.Opin. Colloid Interface Sci.* 17, 173–186.
- [3] **Norde W.** (2008).My voyage of discovery to proteins in flatland and beyond.*Colloids and Surfaces B: Biointerfaces*61, 1–9.
- [4] **Liu SX, Kim JT, Kim S.**(2008).Effect of polymer surface modification on polymer–protein interaction via hydrophilicpolymer grafting.*J. Food Sci.*73 (3), E143–E150.
- [5] **Hoven VP, Tangpasuthadol V, Angkitpaiboon Y, Vallapa N, Kiatkamjornwong S.**(2007). Surface-charged chitosan: preparation and protein adsorption. *Carbohydr.Polym.*68, 44–53.
- [6] **Adamczyk Z, Barbasz J, Ciesla M.**(2011).Mechanisms of fibrinogen adsorption at solid substrates.*Langmuir*27, 6868–6878.
- [7] **Vogler EA.**(2012).Protein adsorption in three dimensions.*Biomater.*33, 1201-1237.
- [8] **Kurkcuoglu O, Güner FS.**(In press).Focusing on protein adsorption at polyurethane surfaces.*Biomedical Polymers and Polymeric Biomaterials*.
- [9] **White F M.** (2011).Fluid Mechanics, *McGraw-Hill*, New York.
- [10] **Chinnam J, Das D, Vajjha R, Satti J.** (2015). Measurements of the contact angle of nanofluids and development of a new correlation.*International Communication in Heat and Mass Transfer*62, 1-12.
- [11] **Tsonos C, Apekis L, Zois C, Tsonos G.** (2004).Microphase separation in ion-containing polyurethanes studied by dielectric measurements, *Acta Materialia*52, 1319-1326.
- [12] **Yilgor I, Yilgor E, Guclu Guler I, Ward CT, Wilkes GL.** (2006). FTIR investigation of the influence of diisocyanate symmetry on the morphology development in model segmented polyurethanes.*Polymer*47, 4105-4114.
- [13] **Aneja A, Wilkes GL.** (2003). A systematic series of model PTMO based segmented polyurethanes reinvestigated using atomic force microscopy.*Polymer* 44, 7221-7228.

- [14] **Rabe M, Verdes D, Seeger S.** (2011). Understanding protein adsorption phenomena at solid surfaces. *Advances in Colloid and Interface Science* 162, 87-106.
- [15] **Carusi A, Burrage K, Rodriguez B.** (2012). Bridging experiments, models and simulations: An integrative approach to validation in computational cardiac electrophysiology. *AJP-Heart* 303, H144-H155.
- [16] **Ermak DL, McCammon A.** (1978). Brownian dynamics with hydrodynamic interactions. *J. Chem. Phys* 69, 1352-1360.
- [17] **Hsieh C, Li L, Larson R.** (2003). Modeling hydrodynamic interaction in Brownian Dynamics: simulations of extensional flows of dilute solutions of DNA and polystyrene. *J. Non-Newtonian Fluid Mech* 113, 147-191.
- [18] **Raffaini G, Ganazzoli F.** (2007). Understanding the performance of biomaterials through molecular modeling: crossing the bridge between their intrinsic properties and the surface adsorption of proteins. *Macromol. Biosci.* 7, 552-566.
- [19] **Ramsden JJ.** (1993). Concentration scaling of protein deposition kinetics. *Phys. Rev. Lett.* 71(2), 295-298.
- [20] **Andrade JD, Hlady V, Wei AP.** (1992). Adsorption of complex proteins at interfaces. *Pure Appl Chem.* 64, 1777-1781.
- [21] **Andrade JD, Hlady V.** (1987). Plasma protein adsorption: the big twelve. *Ann NY Acad Sci* 516, 158-172.
- [22] **Liu SM, Haynes CA.** (2004). Mesoscopic analysis of conformational and entropic contributions to nonspecific adsorption of HP copolymer chains using dynamic Monte Carlo simulations. *Journal of Colloid and Interface Science* 275, 458-469.
- [23] **Ma C, Zhou G, Zhang G.** (2010). Protein resistance of polyurethane with hydrophilic and hydrophobic soft segments. *J. Polym. Sci. Part B: Polym. Phys.* 48(18), 1987-1993.
- [24] **Jones KL, O'Melia CR.** (2000). Protein and humic acid adsorption onto hydrophilic membrane surfaces: Effects of pH and ionic strength. *J. Membr. Sci.* 165 (1), 31-46.
- [25] **Privman V, Nielaba P.** (1992). Diffusional relaxation in dimer deposition. *Europhys. Lett.* 15, 673-678.
- [26] **Zheng J, Song W, Huang H, Chen H.** (2010). Protein adsorption and cell adhesion on polyurethane/pluronic surface with lotus leaf-like topography. *Colloids Surf. B: Biointerfaces* 77, 234-239.
- [27] **Chen H, Hu X, Zhang Y, Li D, Wu Z, Zhang T.** (2008). Effect of chain density and conformation on protein adsorption at PEG-grafted polyurethane surfaces. *Colloids and Surfaces B: Biointerfaces* 61, 237-243.

- [28] **Wu Y, Simonovsky FI, Rather BD, Horbett TA.** (2005).The role of adsorbed fibrinogen in platelet adhesion to polyurethane surfaces: A comparison of surface hydrophobicity, protein adsorption, monoclonal antibody binding, and platelet adhesion. *J. Biomed. Mater. Res. A*.74(4), 722-38.
- [29] **Bauer S, Schmuki P, von der Mark K, Park J.** (2013). Engineering biocompatible implant surfaces Part I: Materials and surfaces.*Progress in Materials Science*58, 261-326.
- [30] **Clarotti G, Schue F, Sledz J, Ait Ben Aoumar A, Geckeler KE, Orsetti A, Paleirac G.**(1992). Modification of the biocompatible and haemocompatible properties of polymer substrates by plasma-deposited fluorocarbon coatings.*Biomaterials*.13(12), 832-40.
- [31] **Campbell CE, Von Recum AF.**(1989).Micro-topography and soft tissue response.*J.Invest.Surg.*2, 51-75.
- [32] **Korbelar P, Dylevsky I.** (1988).Experimental implantation of hydrogel into bone.*J.Biomed.Mater.Res.*22,751-762l.
- [33] **Pangman WJ.** (1958). Compound prosthesis device. USA.
- [34] **Yang JM, Lin HT.** (2001).Wettability and protein adsorption on HTPB-based polyurethane films.*J. Membr. Sci.*187, 159–169.
- [35] **Nagaoka S, Takiuchi H.** (1992). Interactions between blood components and hydrogels with poly(oxyethylene) chain of various chain length. *Kobunshi Ronbunshu*.39, 165-171.
- [36] **Akkas T, Citak C, Sirkecioglu A, Güner FS.** (2013).Which is more effective for protein adsorption: surface roughness, surface wettability or swelling? Case study of polyurethane films prepared from castor oil and poly(ethylene glycol). *Polym. Int.* 62(8), 1202-1209.
- [37] **Panos M, Sen TZ, Ahunbay MG.** (2012).Molecular simulation of fibronectin adsorption onto polyurethane surfaces.*Langmuir*28, 12619-12628.
- [38] **Norde W.** (1994). Protein adsorption at solid surfaces: A thermodynamic approach. *Pure & Appl. Chem.*66(3), 491-496.
- [39] **Norde W, Haynes, CA.** (1995).Reversibility and the mechanism of protein adsorption.*In proteins at interfacev II: Fundamentals and Applications.*
- [40] **Zheng J, Li L, Chen S, Jiang S.** (2004). Molecular simulation study of water interactions with oligo (ethylene glycol)-terminated alkanethiol self-assembled monolayers. *Langmuir*20 (20), 8931–8938.
- [41] **Zheng J, Li L, Tsao HK, Sheng YJ, Chen S, Jiang S.** (2005). Strong repulsive forces between protein and oligo (ethylene glycol) self-assembled monolayers: A molecular simulation study. *Biophys. J.*89(1), 158–166.

- [42] **He Y, Chang Y, Hower JC, Zheng J, Chen S, Jiang S.** (2008). Origin of repulsive force and structure/dynamics of interfacial water in OEG–protein interactions: A molecular simulation study. *Phys. Chem. Chem. Phys.* 10(36), 5539–5544.
- [43] **Rex S, Zuckermann MJ, Lafleur M, Silvius JR.** (1998). Experimental and Monte Carlo simulation studies of the thermodynamics of polyethyleneglycol chains grafted to lipid bilayers. *Biophys. J.* 75(6), 2900–2914
- [44] **Langmuir I.** (1932). Vapor pressures, evaporation, condensation and Adsorption. *J. Am. Chem. Soc.* 54(7), 2798–2832.
- [45] **Talbot J, Tarjus G, Van Tassel PR, Viot P.** (2000). From car parking to protein adsorption: an overview of sequential adsorption processes. *Colloids Surf. A: Physicochemical Eng. Asp.* 165, 287–324.
- [46] **Schaaf P, Talbot J, Rabeony HM, Reiss H.** (1988). Random sequential adsorption of squares on a lattice. *J. Phys. Chem.* 92, 4826–4829.
- [47] **Tarjus G, Schaaf P, Talbot J.** (1990). Generalized random sequential adsorption. *J. Chem. Phys.* 93, 8352–8360.
- [48] **McGuire J, Wahlgren MC, Arnebrant T.** (1995). Structural stability effects on the adsorption and dodecyltrimethylammonium bromide-mediated elutability of bacteriophage t4 lysozyme at silica surfaces. *J. Colloid Interface Sci.* 170, 182–192.
- [49] **McGuire J, Krisdhasima V, Wahlgren MC, Arnebrant T.** (1995). Comparative adsorption studies with synthetic, structural stability and charge mutants of bacteriophage T4 lysozyme. In: *Proteins at Interfaces II: Fundamentals and Applications*; Horbett, T. A., Brash, J. L. Ed.s.; American Chemical Society: Washington, DC, 52–65.
- [50] **Wahlgren M, Elofsson U.** (1997). Simple models for adsorption kinetics and their correlation to the adsorption of β -lactoglobulin A and B. *J. Colloid Interface Sci.* 188, 121–129.
- [51] **Wertz C, Santore M.** (2002). Adsorption and reorientation of lysozyme on hydrophobic surfaces. *Langmuir* 18, 1190–1199.
- [52] **Minton AP.** (2001). Effects of excluded surface area and adsorbate clustering on surface adsorption of proteins II. Kinetic models. *Biophys J.* 80, 1641–1648.
- [53] **Costa D, Tougeriti A, Tielens F, Gervais C, Stievano L, Lambert JF.** (2008). DFT study of the adsorption of microsolvated glycine on a hydrophilic amorphous silica surface. *Phys Chem Chem Phys* 10(42), 6360–6368.
- [54] **Rimola A, Civalleri B, Ugliengo P.** (2008). Neutral vs zwitterionic glycine forms at the water/silica interface: structure, energies, and vibrational features from B3LYP periodic simulations. *Langmuir* 24(24), 14027–14034.

- [55] **Gambino GL, Grassi A, Marletta G.** (2006). Molecular modeling of interactions between L-lysine and functionalised quartz surfaces. *J Phys Chem B* 110, 4836-4845.
- [56] **Latour RA.** (2008). Molecular simulation of protein-surface interactions: Benefits, problems, solutions, and future directions. *Biointerphases* 3(3), FC2–FC12.
- [57] **Agashe M, Raut V, Stuart SJ, Latour Ra.** (2005). Molecular simulation to characterize the adsorption behavior of fibrinogen γ -chain fragment. *Langmuir* 21, 1103-1117.
- [58] **Raffaini G, Ganazzoli F.** (2006). Protein adsorption on the hydrophilic surface of a glassy polymer: a computer simulation study. *Phys Chem Chem Phys* 8, 2765-72.
- [59] **Raffaini G, Ganazzoli F.** (2010). Protein adsorption on a hydrophobic surface: a molecular dynamics study of lysozyme on graphite. *Langmuir* 26, 5679-5689.
- [60] **Ravichandran S, Talbot J.** (2000). Mobility of adsorbed proteins: A Brownian Dynamics study. *Biophysical Journal* 78, 110-120.
- [61] **Bernardi M, Ricci S, Zaccherini G.** (2014). Role of human albumin in the management of complications of liver cirrhosis. *J Clin Exp Hepatol* 4, 302-311.
- [62] **Merchant B, Madura J.** (2011). A review of coarse-grained molecular dynamics techniques to access extended spatial and temporal scales in biomolecular simulations. *Annual Reports in Computational Chemistry* 7.
- [63] **Shi Q, Izvekov S, Voth G.** (2006). Mixed atomistic and coarse-grained molecular dynamics: Simulation of a membrane-bound ion channel. *The Journal of Physical Chemistry B* 110, 15045-15048.
- [64] **Miyahara M, Watanabe S, Higashitani K.** (2006). Modeling adsorption and order formation by colloidal particles on a solid surface: A Brownian dynamics study. *Chemical Engineering Science* 61, 2142 – 2149.
- [65] **Mereghetti P, Gabdoulhine RR, Wade RC.** (2010). Brownian Dynamics simulation of protein solutions: structural and dynamical properties. *Biophysical Journal* 99, 3782–3791.
- [66] **Lee P, Helms V, Geyer T.** (2012). Coarse-grained Brownian dynamics simulations of protein translocation through nanopores. *J.Chem.Phys* 137, 145105-145110.
- [67] **Sinitskiy A, Volth G.** (2013). Coarse-graining of proteins based on elastic network models. *Chemical Physics* 422, 165-174.
- [68] **Garnier T, Nastar M.** (2013) Coarse-grained kinetic Monte Carlo simulation of diffusion in alloys. *Phys.Rev.B* 88, 134207-13412.
- [69] **Flory PJ.** (1953). Principles of Polymer Chemistry. *Cornell University Press*, Ithaca, NY, 1953.
- [70] **Marrink SJ, Risselada HJ, Yefimov S, Tielman DP, De Vries AH.** (2007). The MARTINI force field: Coarse grained model for biomolecular simulations. *J. Phys. Chem. B* 111, 7812-7824.

- [71] **Ayton GS, Voth GA.** (2007). Multiscale simulation of transmembrane proteins. *J. Struct. Biol.* 157, 570-578.
- [72] **Muller-Plathe F.** (2002). Coarse-graining in polymer simulation: From the atomistic to the mesoscopic scale and back. *Chem. Phys. Chem.* 3, 755-769.
- [73] **Schön P, Bagdi K, Molnár K, Markus P, Pukánszky B, Vancso J.** (2011). Quantitative mapping of elastic moduli at the nanoscale in phase separated polyurethanes by AFM. *European Polymer Journal* 47, 692–698.
- [74] **Corcuera MA, Rueda L, d'Arlas FB, Arbelaiz A, Marieta C, Mondragon I, Eceiza A.** (2010). Microstructure and properties of polyurethanes derived from castor oil. *Polymer Degradation and Stability* 95, 2175-2184.

APPENDICES

APPENDIX A: FT-IR spectrums.

APPENDIX B: DSC spectrums.

APPENDIX C: TGA spectrums.

APPENDIX D: DMA spectrums.

APPENDIX E: Calibration curve that is used to calculate protein adsorption

APPENDIX A

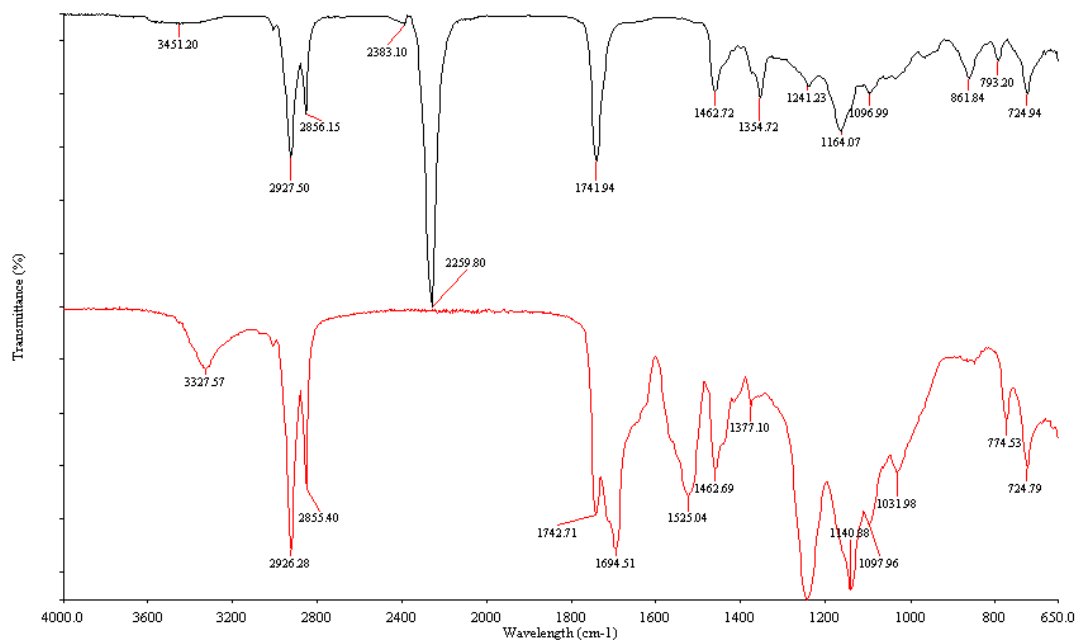


Figure A.1 : FT-IR spectrum of PU100-THF

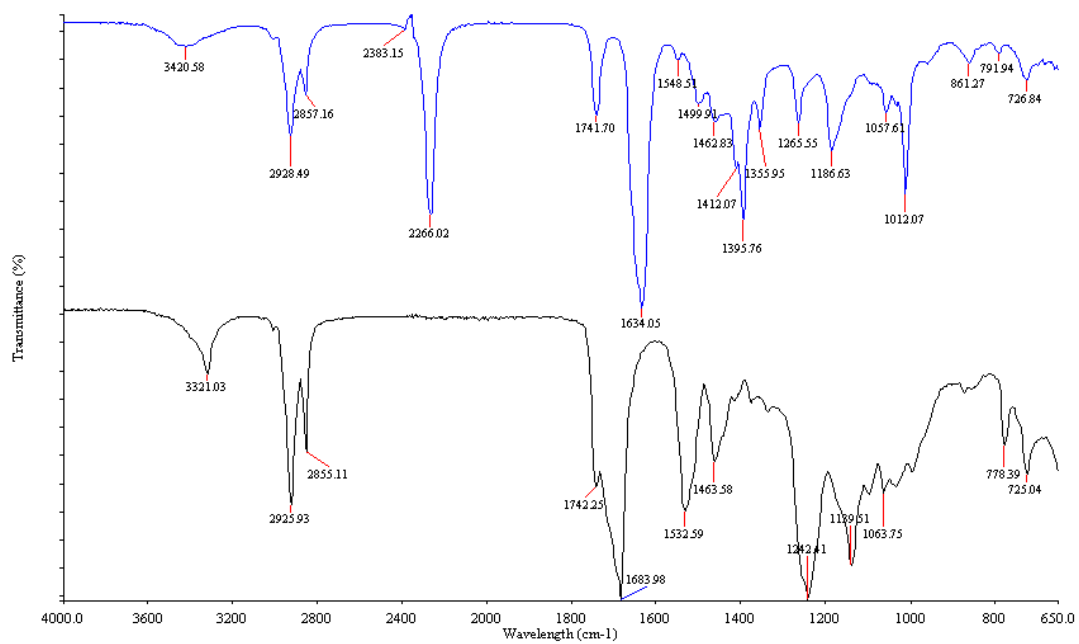


Figure A.2 : FT-IR spectrum of PU100-DMAc

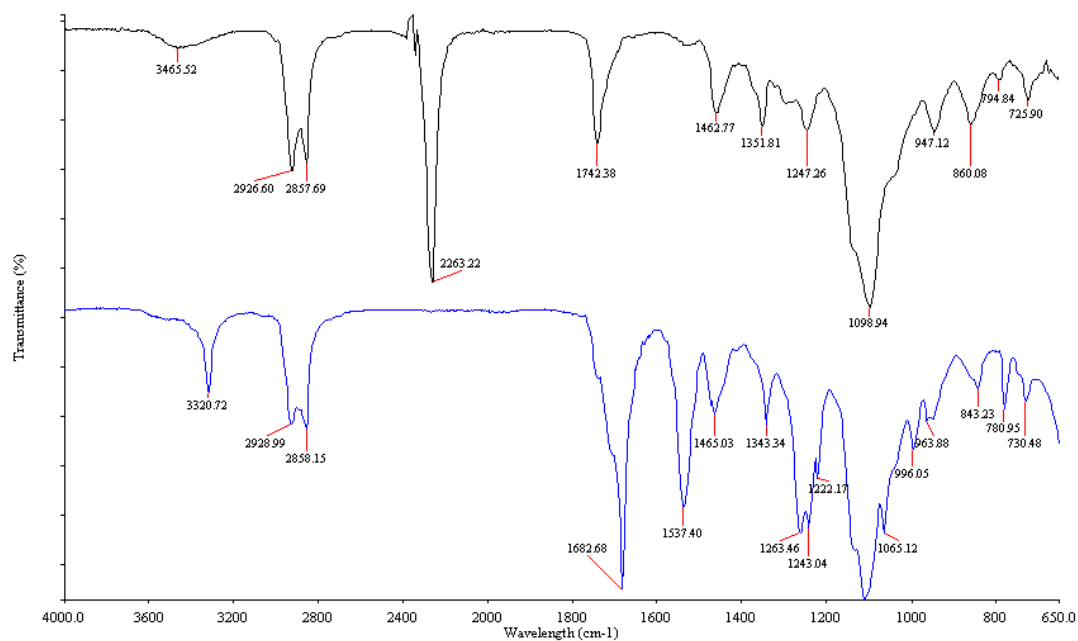


Figure A.3 : FT-IR spectrum of PU50

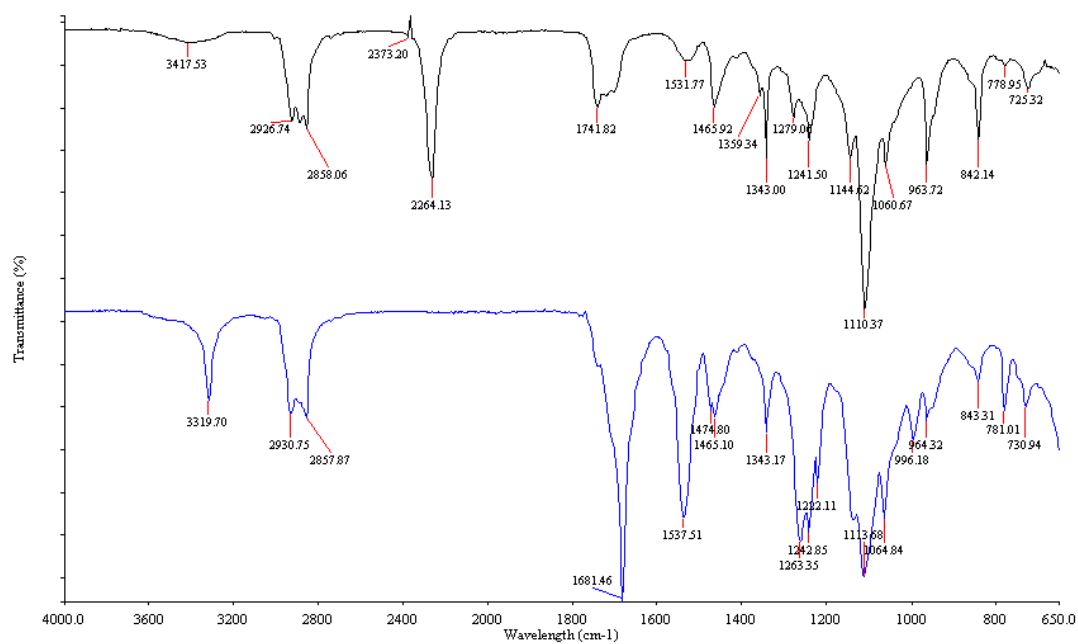


Figure A.4 : FT-IR spectrum of PU60

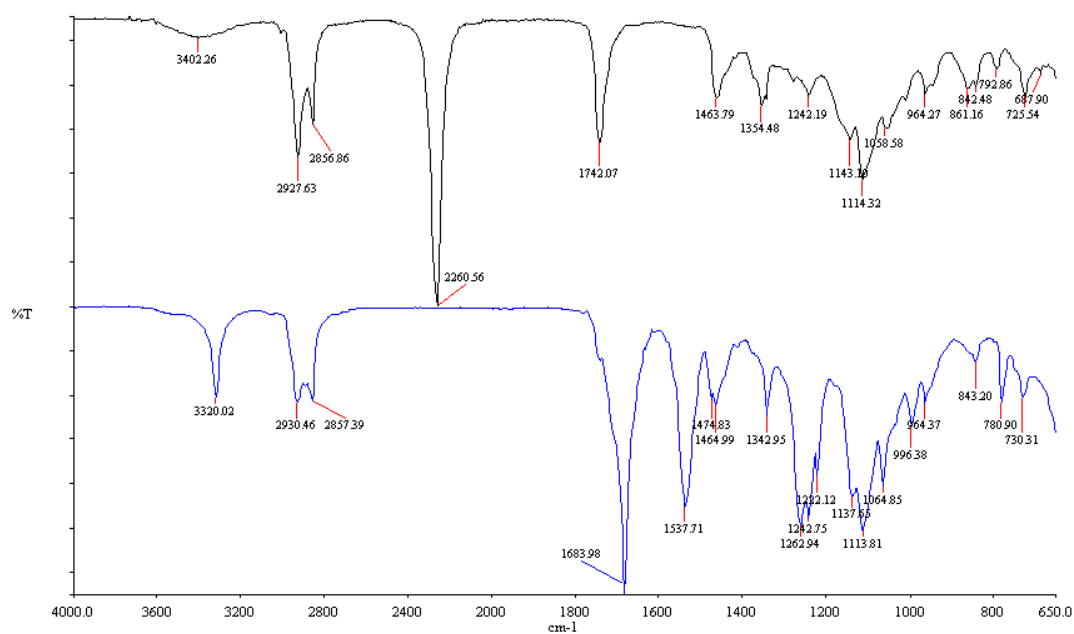


Figure A.5 : FT-IR spectrum of PU70

APPENDIX B

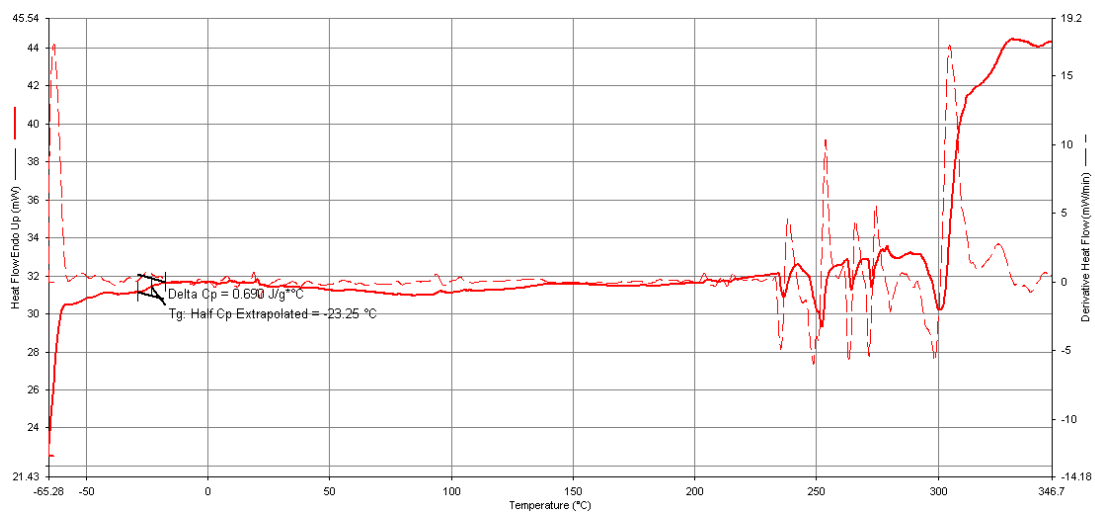


Figure B.1: DSC spectrum of PU100-THF

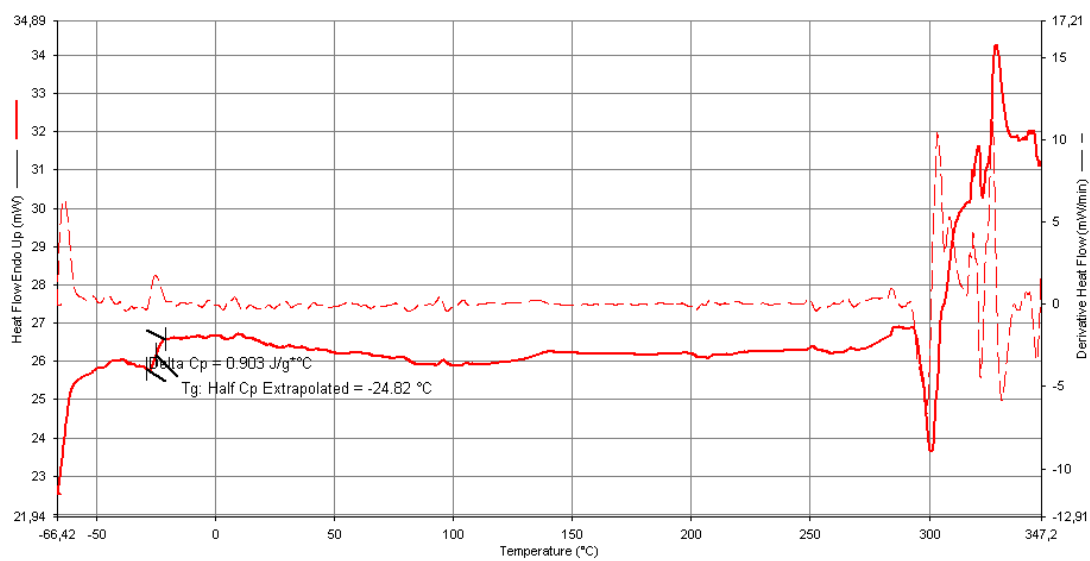


Figure B.2: DSC spectrum of PU100-DMAc

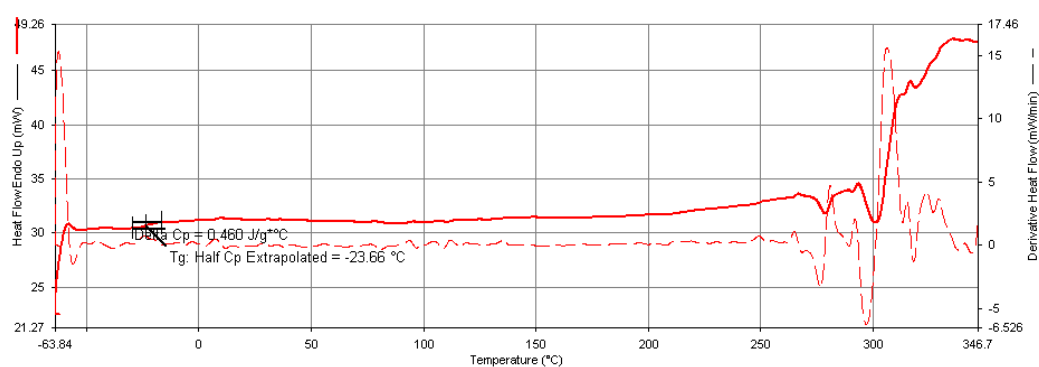


Figure B.3: DSC spectrum of PU100

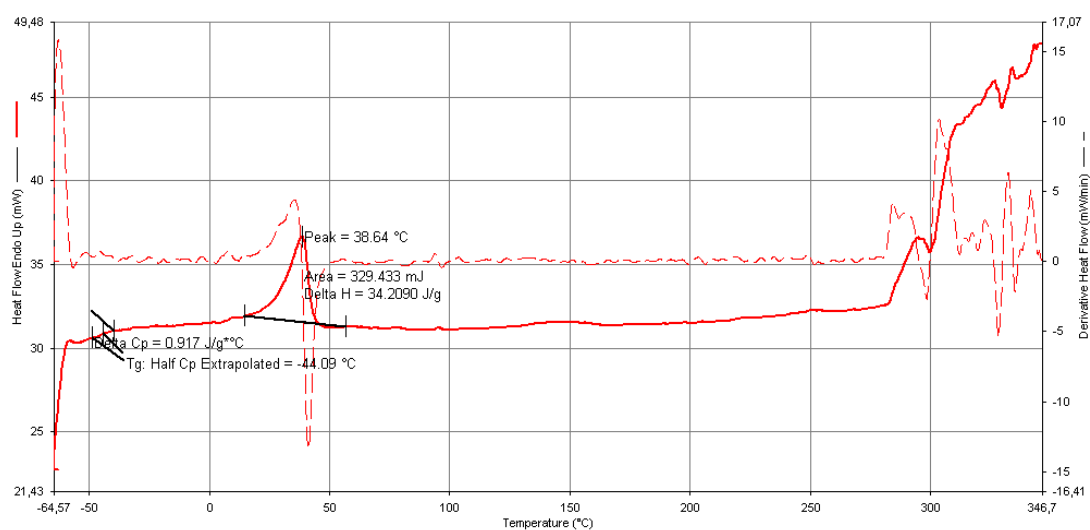


Figure B.4: DSC spectrum of PU50

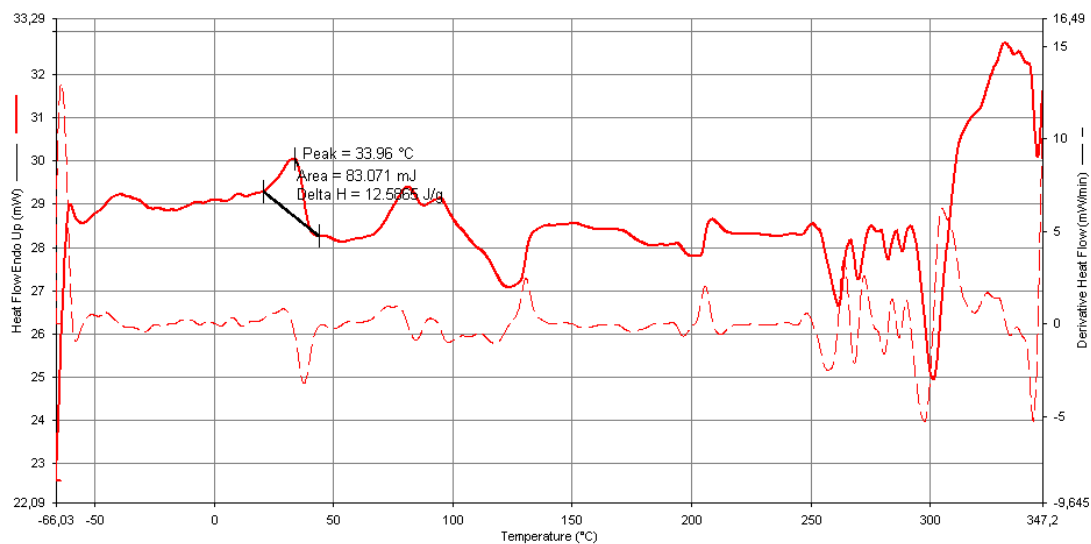


Figure B.5: DSC spectrum of PU60

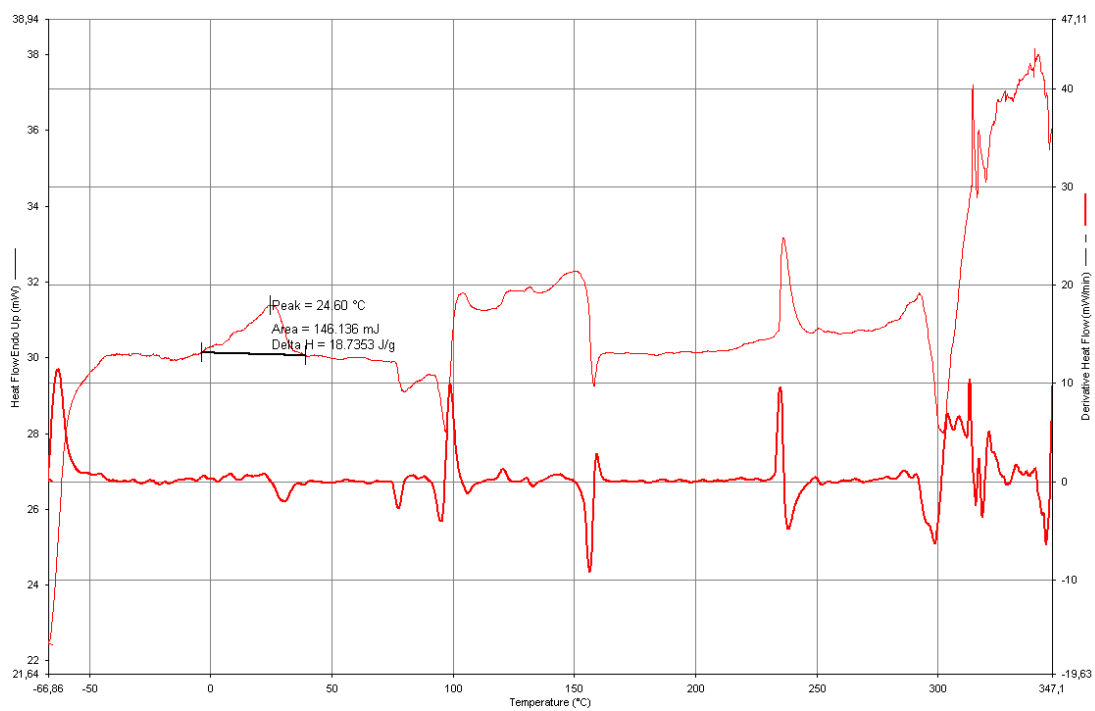


Figure B.6: DSC spectrum of PU70

APPENDIX C

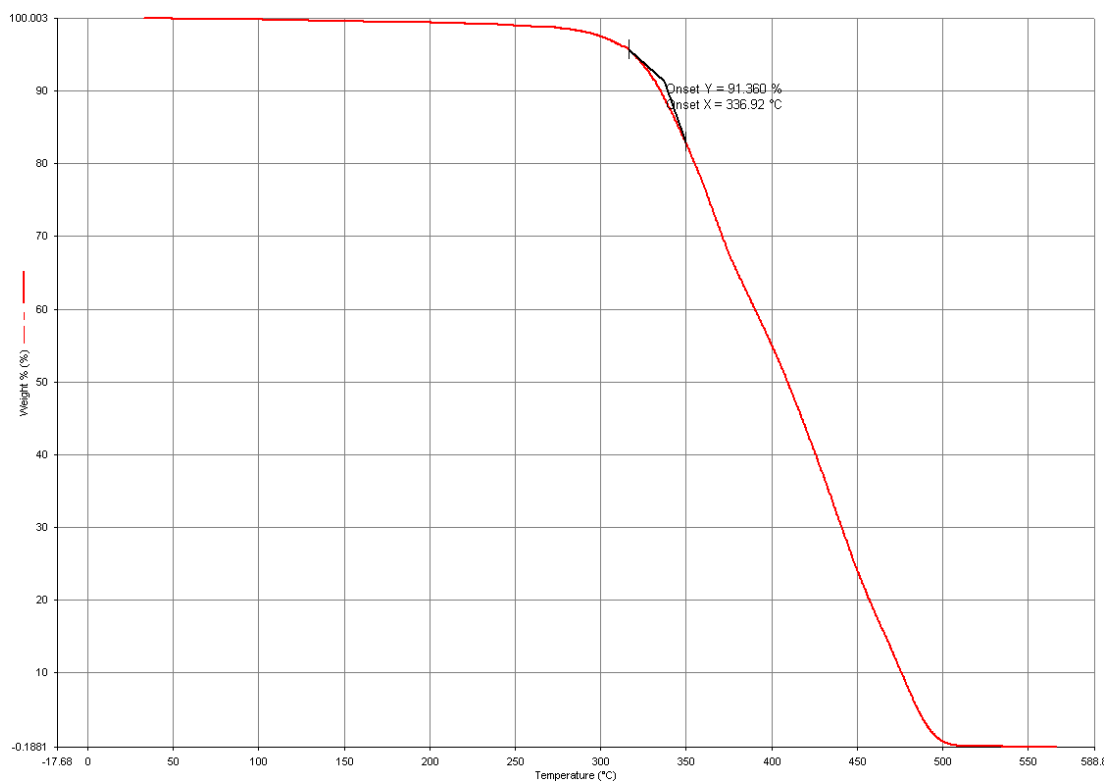


Figure C.1: TGA spectrum of PU100-DMAc

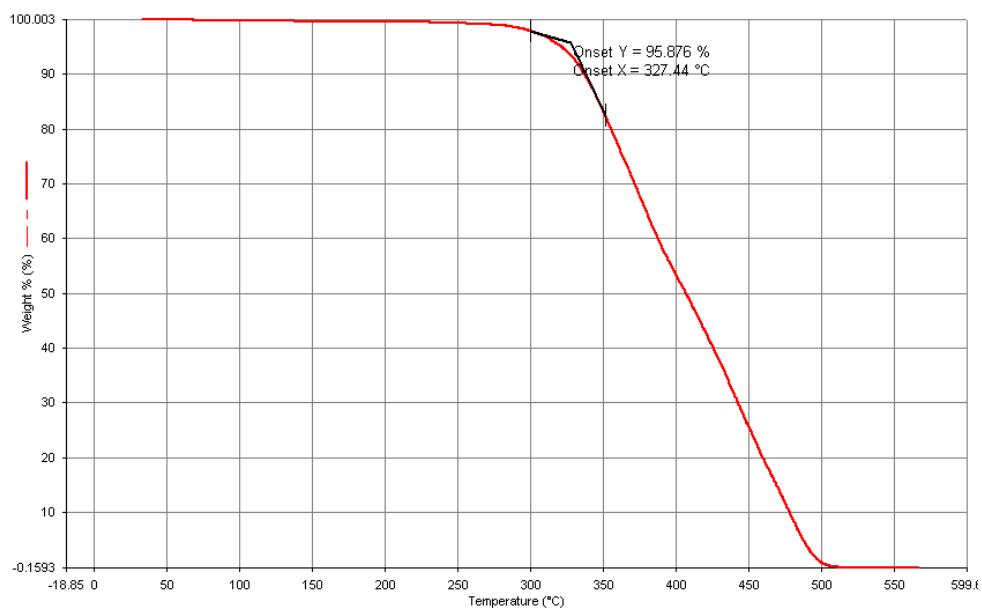


Figure C.2: TGA spectrum of PU100-THF

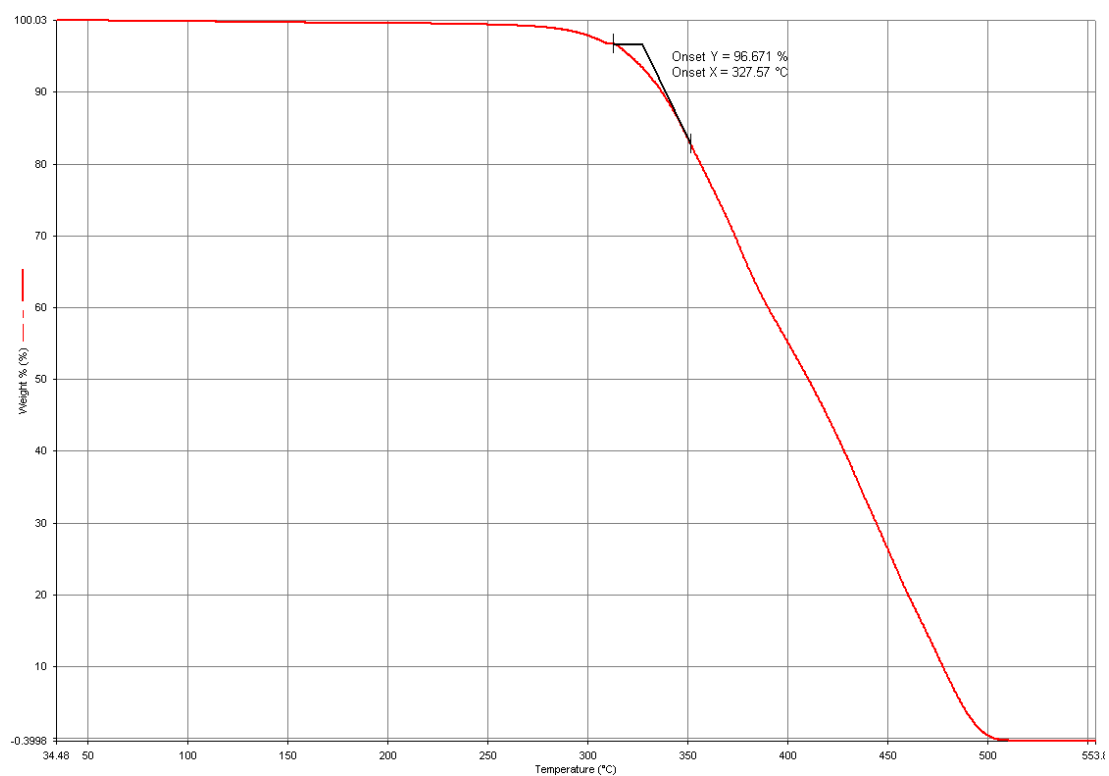


Figure C.3: TGA spectrum of PU100

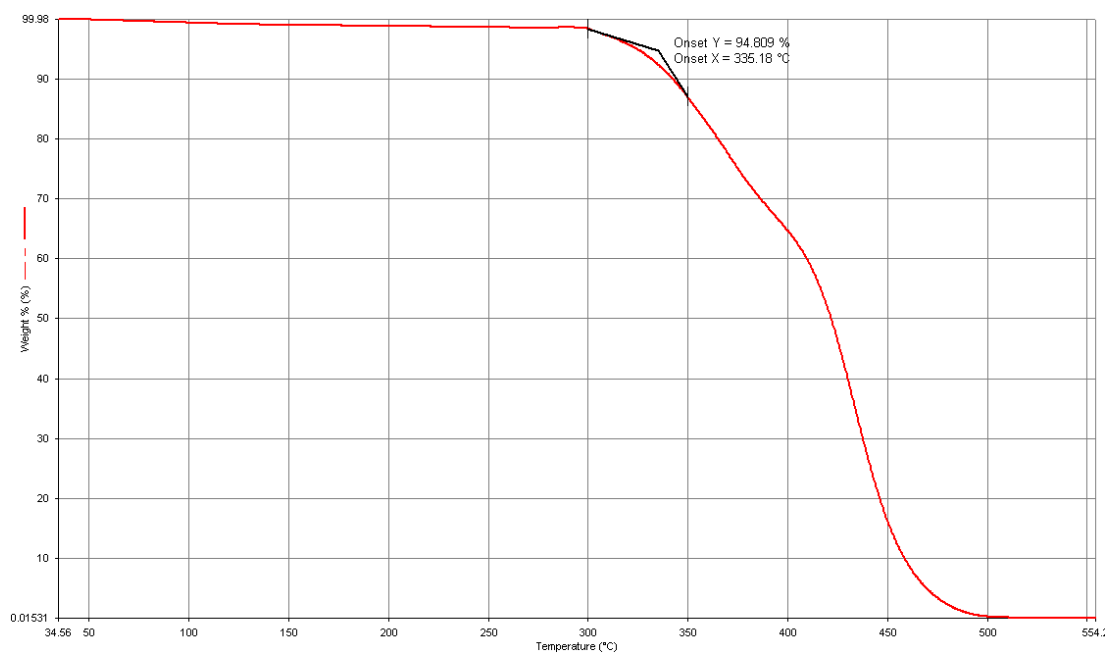


Figure C.4: TGA spectrum of PU50

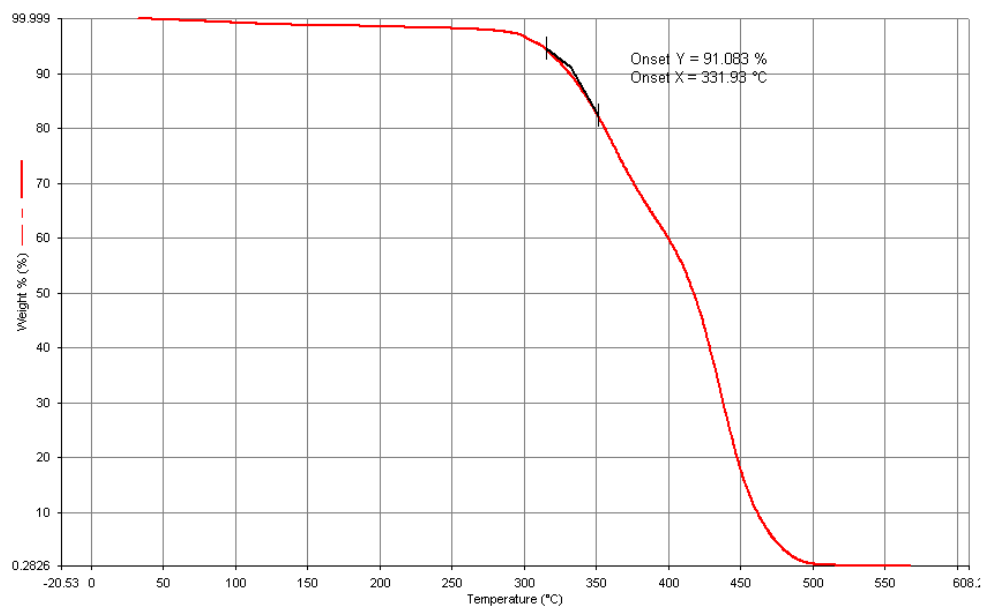


Figure C.5: TGA spectrum of PU60

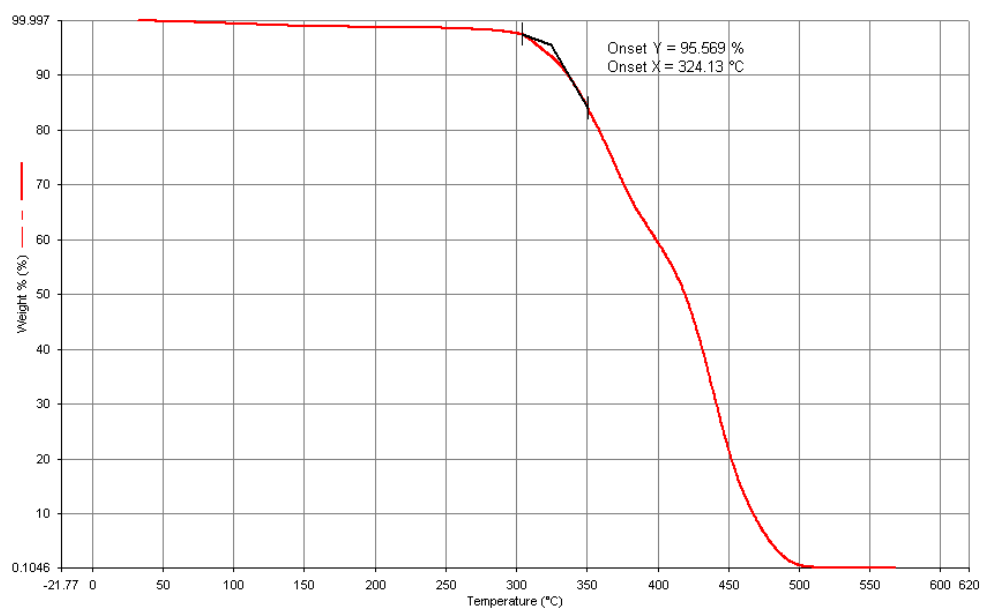


Figure C.6: TGA spectrum of PU70

APPENDIX D

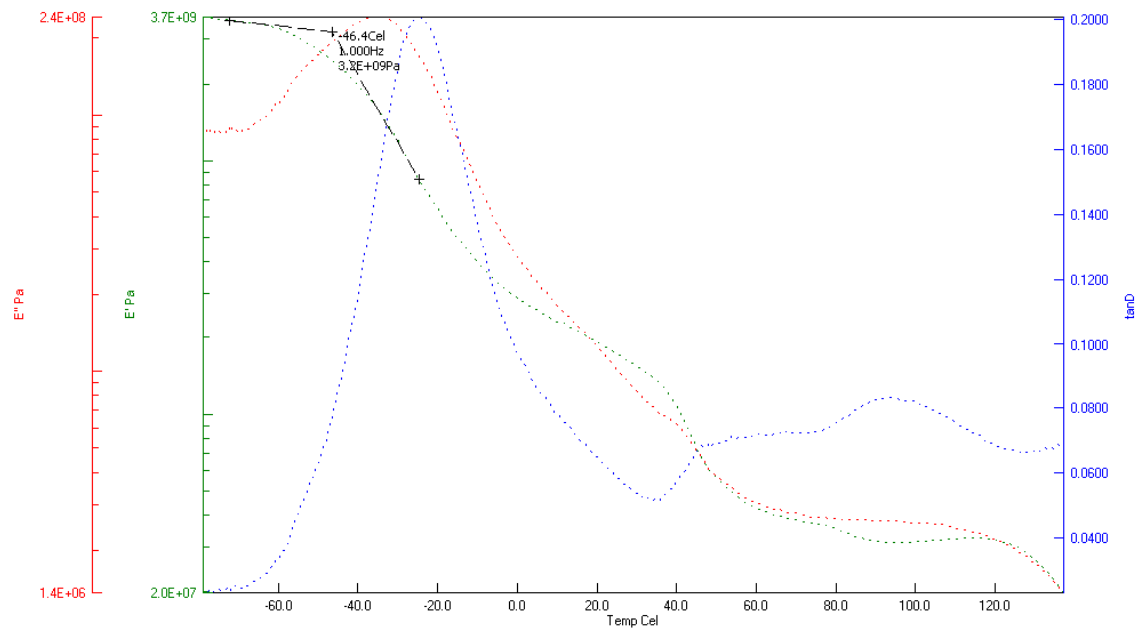


Figure D.1: DMA spectrum of PU50

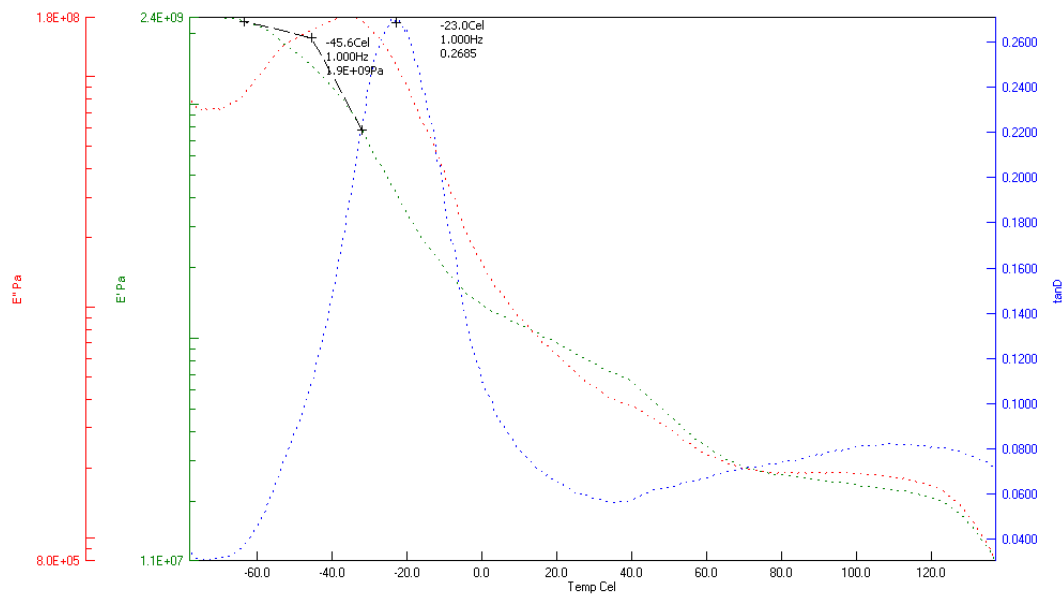


Figure D.2: DMA spectrum of PU60

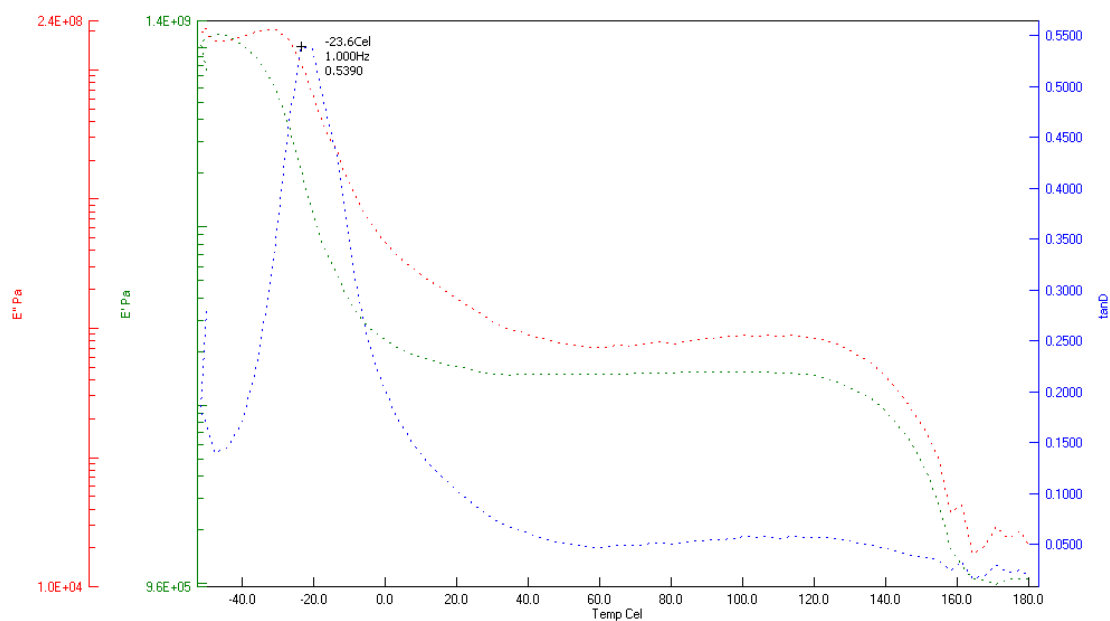


Figure D.3: DMA spectrum of PU100-DMAc

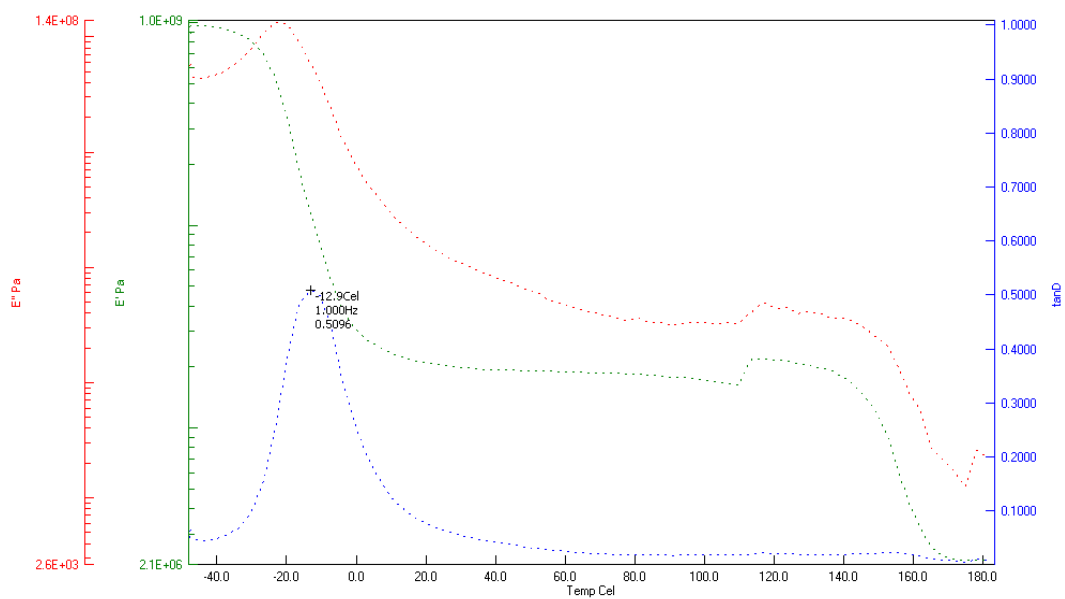


Figure D.4: DMA spectrum of PU100-THF

APPENDIX E

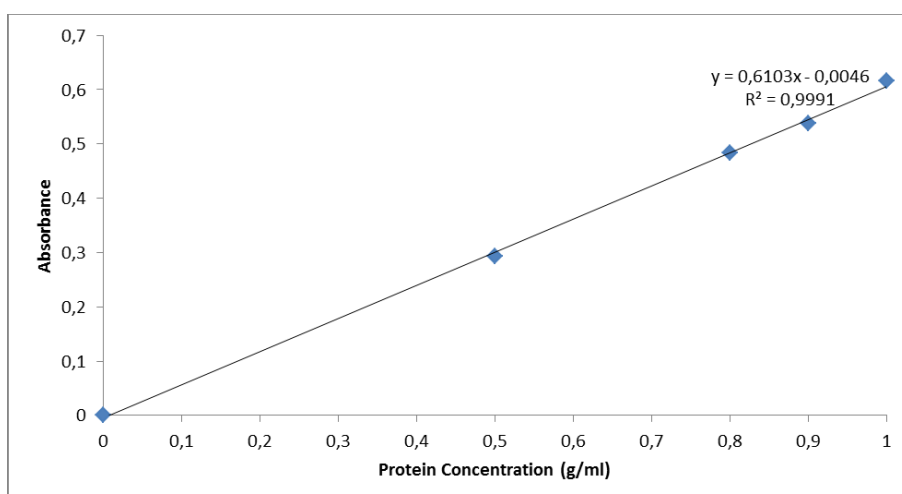


Figure E.1: Calibration curve for protein adsorption

CURRICULUM VITAE

Name Surname: Selin Sofi KÜRKÇÜOĞLU

Place and Date of Birth: 23.03.1988

Address: Kadıköy/İstanbul

E-Mail: hilkat@itu.edu.tr

B.Sc.: Physics, Isık University

PUBLICATIONS/PRESENTATIONS ON THE THESIS

- Hilkat S., Kurkcuoglu O., Guner F.S., Modeling protein adsorption on polyurethane films: A Brownian Dynamics Study. *World Polymer Congress*. June 2012, USA.
- Hilkat S., Kurkcuoglu O., Guner F.S., Poliüretan Filmlere Protein Adsorpsiyonunun Brownian Dinamiği İle Modellenmesi. *UKMK-10*. September 2012, Turkey
- Hilkat S., Kurkcuoglu O., Guner F.S. Brownian Dynamics Simulations of Protein Adsorption on Polyurethane films. *Chemical physics Congress X*. October 2012, Turkey.
- Hilkat S., Kurkcuoglu O., Guner F.S., Modelling Protein Adsorption on Polyurethane Surfaces: The Effect of Surface Properties. *APME2013*. July 2013, UK.